UNIVERSITÀ DEGLI STUDI DI MILANO

DEPARTMENT OF BIOMEDICAL SCIENCES FOR HEALTH

Ph.D. Program in Integrative Biomedical Research (R-23)

Thesis

Combined study of segmental motions and the motion of the body centre of mass during walking: normative data and applications to functional diagnosis and treatment in Rehabilitation Medicine

Ph.D. candidate:

Luigi Catino, M Sci
R11874

XXXIII cycle

Tutor:
Prof. Luigi Tesio, MD

Co-tutor:
Chiara Diletta Malloggi, Ph.D.

The academic year 2019-2020

Summary

Glossary

CoM	Centre of Mass
DST	Double Stance Time. The period in which both ground reaction forces are ≥ 30N.
Ekf (Ef)	Kinetic Forward Energy.
Ekl	Kinetic Lateral Energy.
Ekv	Kinetic vertical Energy.
Ep	Potential Energy.
Etot	Total Energy given by the sum of Ekf + Ekl+ Ev.
Ev	Vertical Energy, given by the sum of Ekv+Ep.
Froude Number	A dimensionless number used to normalize the speed with the different sizes of subjects. $Fr = \frac{{V_f}^2}{gh}$, where V_f=forward velocity, g=gravity acceleration, h=subject's stature
GRF	Ground Reaction Force.
ICC	Intraclass Correlation Coefficient.
POA	Point of Application.
$R_{\%}$ (R)	Percent Recovery. The Percent recovery is summarized by the following question: $R_{\%} = \frac{\lvert W_f\rvert + \lvert W_l\rvert + \lvert W_v\rvert - \lvert W_{tot}\rvert}{\lvert W_f\rvert + \lvert W_l\rvert + \lvert W_v\rvert}$. See below in the glossary the meaning of each component of the equation.
Side of the double-stance phase	The side of the posterior foot.

SL	Step Length. The sagittal distance between the reflective markers placed on the lateral malleolus of the posterior and the anterior foot at the ground strike of the anterior foot.
SST	Single Stance Time referred to each lower limb. It is the period in which that limb is the only one to determine a ground reaction force ≥ 30N.
Step	The ensemble of kinematic, dynamic, and electrophysiological events taking place between two subsequent foot-ground contacts. Foot ground contacts were determined from vertical ground forces ≥ 30N.
Stride length in split modality	The sum of the length of two subsequent steps, or the average length between the unilateral strides of the left and right side.
Stride length, unilateral	The sagittal distance is covered by the external malleolus of one side between the two subsequent steps, or the average length between the unilateral strides of the left and the right side.
Swing Time	Referred to each lower limb, it is the time in which the lower limb does not generate a ground reaction force ≥ of 30N.
t_{fast}	Time [s] of the fast belt. The time interval during which the POA originates from the slower belt.
Total Stance Time	The period in which the vertical ground reaction force determined by feet is ≥ 30N.
t_{slow}	Time [s] of the slow belt. The time interval during which the POA originates from the slower belt.
tS_{tride}	Time [s] of stride. It represents the whole stride duration.

$\bar{V}CoM_{split}$	The velocity of the CoM during split walking [m s^{-1}] is the weighted mean forward velocity of the CoM during a single stride in split-belt walking.
$\bar{V}CoM_{split,6strides}$	Mean Velocity [m s^{-1}] of the CoM during split across 6 strides in a single participant.
$\bar{V}CoM_{split,all}$	Mean Velocity [m s^{-1}] of the CoM during split across 6 strides per 12 participants (n=72).
V_{fast}	Known and constant velocity [m s^{-1}] of the fast belt of the treadmill.
$\bar{V}^{MED}CoM_{split,6strides}$	Median Velocity [m s^{-1}] of the CoM during split across 6 strides in a single participant.
$\bar{V}^{MED}CoM_{split,all}$	Median Velocity [m s^{-1}] of the CoM during split across 6 strides per 12 participants (n=72).
V_{slow}	Known and constant velocity [m s^{-1}] of the slow belt of the treadmill.
W_{ext}	External work, i.e. the work provided by the muscles.
W_f	Forward Work.
W_l	Lateral Work.
W_v	Vertical Work.
$\dot{W}$	Power, computed as the first derivative of work.

PREFACE

The guiding thread. Different experimental studies were nested within a wider context

The present Ph.D. program was nested in the broader research line on walking, seen as the translation of the body system as a whole. In the history of science, the birth date of ideas is always hard to locate. One can reasonably say that modern experimentation on this topic began around 1930 with the pioneering works of the physiologist Wallace O. Fenn[1], and then exploited (mostly in Italy) by the physiologists Rodolfo Margaria and Giovanni A. Cavagna. This robust, profound, and unifying vision then branched into various cultural streams, one of which is searching for the clinical potential of research on the Centre of Mass (CoM) motion. This dates back approximately to 1980. This line of research was triggered by G.A. Cavagna and was mostly exploited by a physiatrist, Luigi Tesio, who supervised the present Thesis. The guiding thread of this "clinically oriented" research branch is the relationship between altered segmental motion and the motion of the CoM. No surprise, therefore, that experiments were, are, and will be conducted in the future, both on "classic" analysis of lower limb movements, and CoM trajectories, either with distinct or combined analyses.

The rationale of the running experimental campaign (to which the Ph.D. program gave a partial contribution) can be articulated in 4 main reasons:

Reason 1. The motion of the lower limbs: describing is not equivalent to interpreting

Despite its remarkable technical progress, Clinical Gait Analysis (CGA) has not yet found satisfying clinical applications, thus maintaining its prevalent status of research technique. A recent consensus conference highlighted that the information obtained by CGA, unless for the case of very few pathological conditions, substantially remains descriptive and redundant. In particular, results do not seem to contribute meaningfully to clinical decisions, either diagnostic or therapeutic.

Reason 2. The motion of the Centre of Mass may help to interpret segmental alterations.

The main hypothesis subtending this Ph.D. research project is that the missed clinical translation of CGA relies upon the lack of an interpretative key of segmental alterations. The motion of the CoM

may provide such a key. Which segmental motions' alterations are primitive, and which of these represent a result of a "convenient" adaptation? Is motor learning in sports training and rehabilitation driven by the optimization of the CoM motion rather than by the optimization of segmental motions?

Reason 3. The motion of the Centre of Mass may be efficient in asymmetric gaits. Does this paradox prevent recovery?

Impaired walking, therefore, seems to represent at least in part an active adaptive mechanism that tends to maintain the work per unit distance within normal limits and that, paradoxically, could demotivate any attempt to restore symmetry. Therefore, attempts to "force" a more symmetric motion between the lower limbs should be compared with their impact on the CoM motion.

Reason 4. Optimizing balance, not only work, may constraint the CoM motion in health and disease.

The motion of the body CoM is usually studied in the sagittal plane. Ergometric (i.e., work-related) aspects of its pendular motion have already been described in detail. However, the movement of the CoM is inevitably deployed along a three-dimensional (3D) path, inclusive of lateral excursions. Knowledge of this topic is minimal. It looks likely that excessively approaching the "no-return" point of the lateral trajectory leads to an increased risk of falling. At least from the perspective of balance, it seems essential to study the 3D trajectory of the body CoM, and not only the energetic cost of its forward translation.

It is hoped that the variety of studies exploited during the Ph.D. program will not evoke a feeling of fragmentation and inconsistency within the program itself. Efforts will be made to link individual experiments' findings to the picture of overall knowledge in the field. Possibly, the many-faceted findings arising from this Ph.D. program raised more questions than answers: but, hopefully, results seem to converge in making more understandable the puzzle of the relationships between segmental and body system motions, thus fostering a more comprehensive appraisal of walking impairments.

Luigi Catino

1. Introduction

Walking is usually studied both in physiology and clinical medicine from the perspective of segmental motions, highlighting the kinematic, dynamic, and neurophysiological aspects of the cyclic lower limb's oscillations. The impact of focal impairments, however, can be better interpreted if these are correlated to the mechanical translation of the entire body system, represented by its centre of mass (CoM). Many segmental characteristics of gait (step frequency, angular excursions, sequences of muscular output) can be explained as the minimization of the work done to translate the body CoM thanks to an efficient and inverted pendulum-like exchange, at each step, between potential and kinetic energies.

The laboratories able to provide a simultaneous, combined and synchronized analysis between segmental movements and motion of the centre of mass are rare. In recent years a combined analysis has become possible in clinical contexts. In the Lab where this Thesis was realized, a treadmill mounted on force sensors (GAFT, Gait Analysis on Force Treadmill)[2], with two independent belts, was adopted (split-GAFT method). Walking on a treadmill has kinematic and dynamic characteristics very similar to those of overground gait[2]. Kinematic and electromyographic (EMG) analyses adopted the same methods used in overground Gait analysis (i.e., optoelectronic systems and wireless surface EMG [sEMG] transducers).

The experimental setup allowed to measure synchronously the dynamic and kinematic parameters of the motion of the CoM and of the lower limbs, and the EMG from several muscles. The effect of split-belt walking could also be observed.

The present project aims at the clinical translation of GAFT and split-GAFT. Five different goals will be achieved:

1. Completing the data related to the 3D motion of the body CoM during walking, already available for healthy adults, for pediatric age (5-13 years old).
2. Study of the curvature peaks of the 3D trajectory of the body CoM during walking in healthy adults.
3. Description of the effect of split-walking in terms of segmental motion in healthy adults.
4. Study of the velocity of the CoM during split-gait.
5. A paradigmatic clinical case.

In the present Thesis, Appendixes cover historical or methodological aspects that widen the experimental studies' cultural context. The Appendixes are conceived as corollaries of the main text. The reader can ignore them with no detriment for the continuity of the scientific presentation.

State of the art

The motion of the segments: describing is not equivalent to interpreting

The cyclic motion of lower limbs during walking is analyzable with great precision. Kinematic (angular excursions), dynamic-ergometric (forces, torques, joint powers), and neurophysiologic aspects (muscular activation profiles using electromyography, EMG) can be registered synchronously in dedicated laboratories and can offer measures of the effectiveness of therapeutic interventions. Despite its remarkable technical progress, Clinical Gait Analysis (CGA) has not yet found satisfying clinical applications, thus maintaining its prevalent status of research technique. A recent consensus conference highlighted that the information obtained by CGA, unless for the case of very few pathological conditions, substantially remains descriptive and redundant. Mostly, it does not significantly contribute to the clinical decision, either diagnostic or therapeutic[3].

The motion of the body Centre of Mass (CoM) during walking: an interpretative key

The hypothesis subtending this project is that the failure of the clinical translation of CGA relies upon the lack of an interpretative key of segmental alterations: which of them are primitive and unavoidable and which of them represent the result of a convenient adaptation?

Gait analysis: segmental approach versus systemic approach

The primary purpose of the cyclic motion of lower limbs is the forward translation of the body system[4]. This allows studying walking from two complementary standpoints: the segmental and the systemic approach. The former emphasizes the sequence of cyclic movements of body segments (mostly, the lower limb joints)[5], while the latter refers to the motion of the body system as a whole with respect to the ground. The scientific literature usually focused on the segmental approach. However, the systemic approach provides critical information and a key to interpret the results of segmental studies. The development of the systemic approach dates from the 19th century thanks to the studies of J.E. Marey. Jules Etienne Marey (1830-1904) provided the first graphic representation

of a method to estimate the motion of the centre of gravity during walking in his work entitled "La Machine Animale: locomotion Terrestre et aérienne" published in 1874. The subject wore a tool able to detect and transduce the vertical accelerations of the head during walking (see Fig. A1.1 in the *Appendix 1*). Marey argued that the head's vertical displacements could represent the ones of the body centre of gravity, as far as the human body is considered as a rigid body. The gold standard in the CoM motion analysis nowadays is represented by the so-called Newtonian method, implemented by G.A. Cavagna[6] and then clinically developed by L. Tesio[7–9]. The method allows a direct measure of the 3D CoM motion. It requires the subject to perform at least two consecutive steps on sensorized force platforms.

Changes of mechanical energy of the CoM: the inverted pendulum model

During walking, the oscillation of the CoM on the supporting lower limb can be assimilated to the CoM motion in an inverted pendulum[10]. At each step, the CoM is lifted while decelerating forward and then is lowered while accelerating forward. Familiar examples of the inverted pendulum are given by the pole-vault jump and the mechanic metronome. A useful metaphor is that of a sphere rolling along a bumpy path (Fig. 1.1)[5,11].

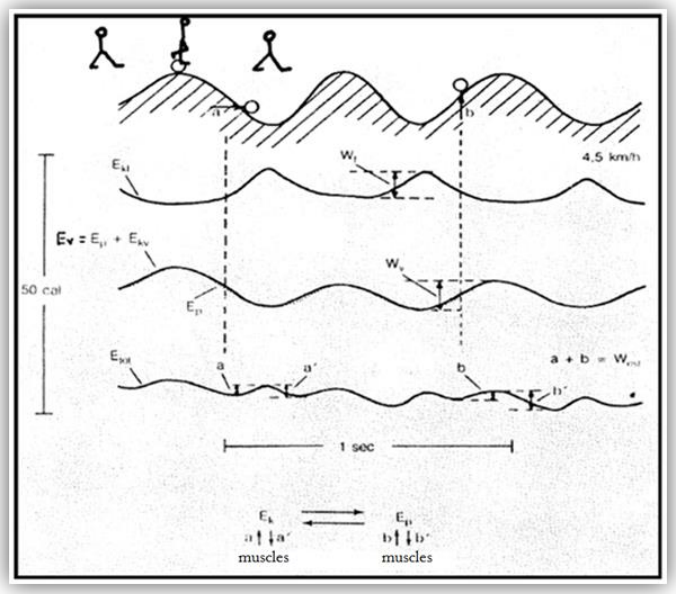

Fig. 1.1. Mechanical energetic variations of the body CoM (represented by a sphere rolling on bumps-dashed areas) during various strides at 1.25 m s^{-1}, in an adult man (78 kg, 1.77 m, 23 y.o.). In the first curve under the shaded areas, the kinetic forward Energy (Ekf=1/2 MV^2, where M is the body mass, and V the velocity) is reported. The intermediate curve shows Ev variations, the sum of potential Energy (Ep = weight for vertical displacement, dotted line), and kinetic vertical Energy. The curve below represents Etot, the sum of Ekf and Ev (Cavagna, GA[11] and Tesio L[5]).

A formal notation needs to be adopted. During forward deceleration and contemporaneous lift of the CoM an increase of Potential gravitational energy (E_P) and a decrease of kinetic energy due to the forward velocity (E_{kf}) is observed. The opposite occurs during the acceleration of the CoM. In a pendulum, Ep and Ekf are in opposition of phase and of similar amplitude: this allows the transformation of one energy into another and vice-versa. In an ideal pendulum, the sum of Ep and Ekf should be constant.

Consequently, there would be no need for an energy input from outside the body system (in practice, here, no need for muscle work). This exchange is not perfect as E_{tot} is not constant so that the CoM motion with respect to the ground requires muscular work ("external" work). The greater the energy exchange, the greater the muscular work "recovered" (see below).

Each increment of E_{tot} occurs, by definition, at the cost of external work[12]. It can be noted that two increments of E_{tot} occur during one stride (Fig 1.4). During the double stance phase, an increment in E_{tot} occurs to complete the forward acceleration of CoM (*a* increment in Fig. 1.1)[13,14]. At the beginning of the single stance phase, another increment of E_{tot} occurs to complete the vertical lift of the CoM (*b* increment in Fig. 1.1).

It is worth noting that another type of work is needed to sustain the cyclic motion of the limbs with respect to the CoM ("internal" work[5,11]). As a rule, the sagittal CoM motion during one step is virtually identical to the motion during the next step. This symmetry is also highlighted by analyzing the ratio between ergometric variables such as power, work, and "recovery" of muscular work (see below), referred to each limb. Their ratio, equal to 1, demonstrates complete symmetry of the CoM motion in physiological gait[5,15]. The motions in the lateral direction, of course, are not identical, but they are a mirror image of each other. Hence they are also symmetrical (more on this later on).

Mechanical efficiency of the CoM motion

During the stride (see Fig.1.1), W_{ext} is lower than the sum of the work underlying the increments of the kinetic and potential energy of the CoM (W_f and W_v, respectively): this is caused by the aforementioned pendulum mechanism[5].

The percentage of spared or "recovered" muscular work along a walking cycle can be summarized by the so-called "percent recovery" or, simply, R, given by the simple formula:

$$R_{\%} = \frac{|W_f| + |W_l| + |W_v| - |W_{tot}|}{|W_f| + |W_l| + |W_v|} * 100 \qquad [1.1]$$

In a perfect pendulum, during each stride $R_{\%}$ would be 100%. During walking at self-selected speed (in adults, about 1.3 m s^{-1}), $R_{\%}$ can trespass 60% and declines at higher or lower speeds[16]. It would be noted that the efficiency of the pendulum-like mechanism, hence the percent recovery (dubbed R_{inst}), undergo relevant instantaneous changes during the stride. However, here they will not be considered[17,18].

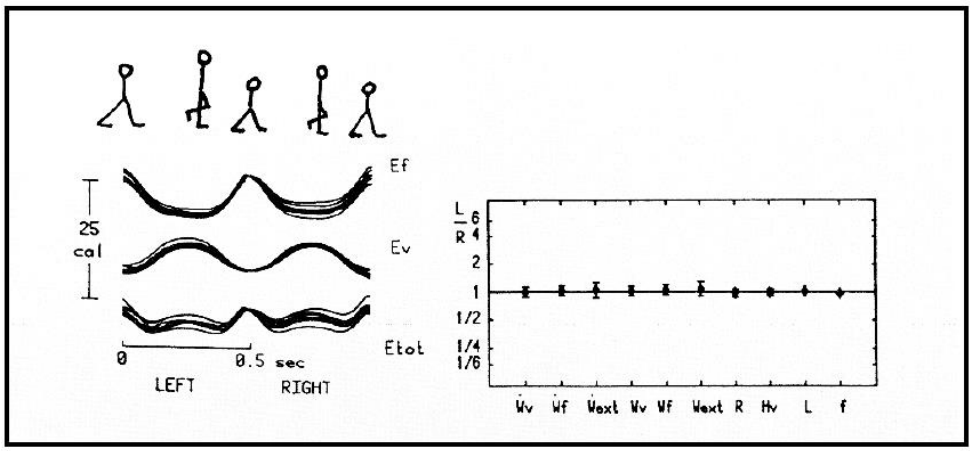

Fig. 1.2. The curves on the left represent Kinetic Energy (Ekf), vertical Energy (Ev), and total Energy (Etot) of the Centre of Mass (CoM) during two consecutive steps at the subject's self-selected speed. Tracks of successive strides are graphically overlapped. The double stance duration has been normalized. The track starts with the left step. The track on the right shows the ratio between values of different variables (abscissa) measured during the left and the right step (on the ordinate in the logarithmic scale). Values greater than 1 indicate greater values on the left step. The measured variables are the power necessary to the lift (Ẇv), and to the forward (Ẇf) acceleration of the CoM, the muscular power required to maintain the body in motion with respect to the ground (Ẇext), the related variables of work (Wv, Wf, Wext), the recovery of muscular "external" work due to the exchange between Ep and Ekf (R, or %R) the maximum height reached from the CoM with respect to the minimum level reached during the two steps (Hv), length and frequency of the steps (L, f). The whole picture gives an "index of asymmetry" of the locomotor mechanics. In a normal subject, there is complete symmetry[5].

CoM in pathologic claudication

G.A. Cavagna and L. Tesio studied for the first time the CoM motion in claudication, e.g. in hemiplegia and unilateral coxarthrosis[5,7,15]. Variables related to the CoM motion as external work, power, R, and maximum height reached by CoM have been studied. They evidenced that, whatever the underlying pathology, patients with unilateral lower-limb impairments provided W_{ext} 3 to 5 times lower during the step performed on the affected limb, compared to the next step.

Fig. 1.3 gives an example of patients with unilateral hip arthritis (upper panels) and modest hemiparesis (lower panels). In the hemiplegic patient, a higher CoM lift during the step on the healthy limb can be noted. At the clinical inspection, the paretic limb was flaccid. Moreover, a foot drop prevented a normal clearing off the ground was it not for an elevation of the pelvis on the paretic side (non si capisce). This mechanism entailed a lift of the lower limb *en bloc*, hence a substantial raise of the CoM. It is worth noting that in both patients, the exchange between Ef and Ev is higher during the step made while "pole-vaulting" over the affected limb, thus minor increments of Etot are registered.

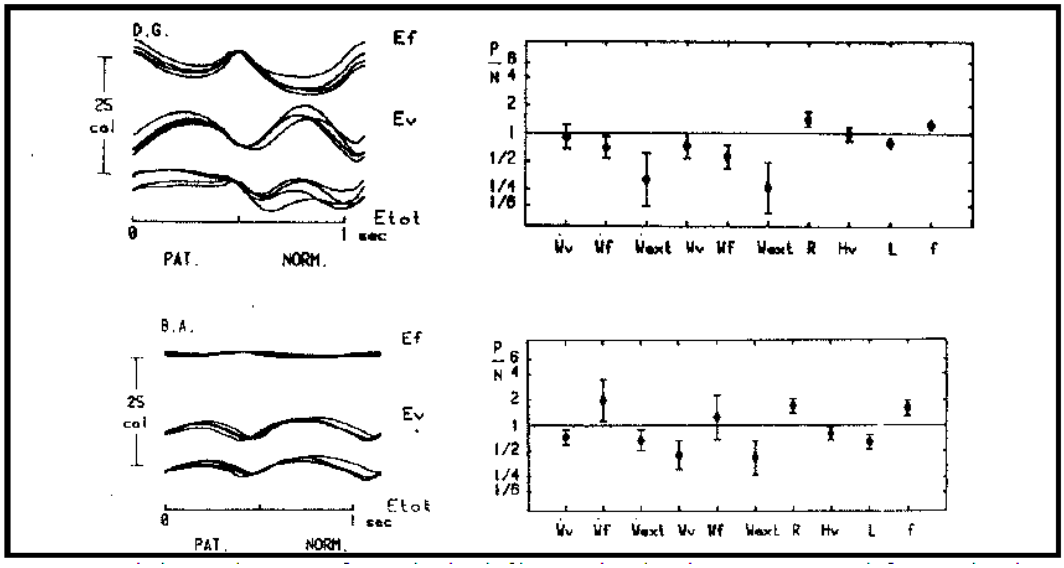

Fig. 1.3. The figure replies the same information reported in Fig 1.2 for two representative patients. The upper panels refer to a subject (man, 55 yrs, , 95 kg, 180 cm height, average forward speed 1.16 m s^{-1}) with mono-lateral coxarthritis and quadriceps hypotrophy; the lower panels refer to a patient with hypotonic hemiparesis (man, 23 yrs, 66 kg, 170 cm height, average forward speed 0.64 m s^{-1}). Curves on the left represent the variation of Kinetic Energy (Ef), Potential Energy (Ev) and Total Energy (Etot) of the CoM during two consecutive strides at a self-selected speed. Tracings initiate with the affected limb (PAT). Each step starts when E_{kf} reaches the maximum as per Cavagna's method convention (as a rule, during the double stance phase,). The step is then named (right or left) after the side of the lower limb entering a single stance phase. Tracings on the right report, on the ordinate (log scale), the ratio between the values of different variables (abscissa) measured during each of the two subsequent steps (see Fig. 1.2). Values above 1 indicate values higher during the step mainly performed on the affected side (taken from Tesio L, 1991[5]).

The CoM: morpho-functional aspects of its trajectory

The CoM motion is usually studied in the sagittal plane. However, its movement unavoidably happens along a 3D path, comprehensive of modest lateral excursions. Knowledge of this topic is minimal. Indeed, the path[19] and the dynamic characteristics of the trajectory of the CoM[18] have been

described at different walking velocities in healthy adult subjects. It is an elegant "figure-of-eight" - called "bow tie". The shape and the perimeter of the *bow tie* considerably change as a function of the walking velocity[18,19] and also in various pathologic alterations of walking (unpublished results). Therefore, it seems relevant to investigate not only the energetic cost of the forward translation of the CoM but also its 3D trajectory.

Matching the systemic and segmental views of walking: segmental and CoM power production

A primary constraint of the CoM motion is minimizing the energy expenditure per unit distance. For this reason, the neural control of gait is likely to be designed accordingly. Research questions have mostly focused on segmental or CoM motion rather than on their interaction. However, in recent years some studies endorsed an integrated perspective. A recent review[4] traces back the study of the motion of the CoM oriented to clinical application and, in particular, a research line that highlighted the correlations between the E_{tot} changes and the temporal step phases. Neptune et al.[20] identified four temporal phases dubbed "Regions". These were based on the zero-crossing on the external power applied to the CoM during one step: Region 1, the step-to-step transition of the leading leg as it absorbs the mechanical energy of impact; Region 2, the raising of the CoM in early single-limb support; Region 3, the lowering of the CoM in late single-limb support, and Region 4, the step-to-step transition of the trailing leg as it propels the body (Fig.1.4).

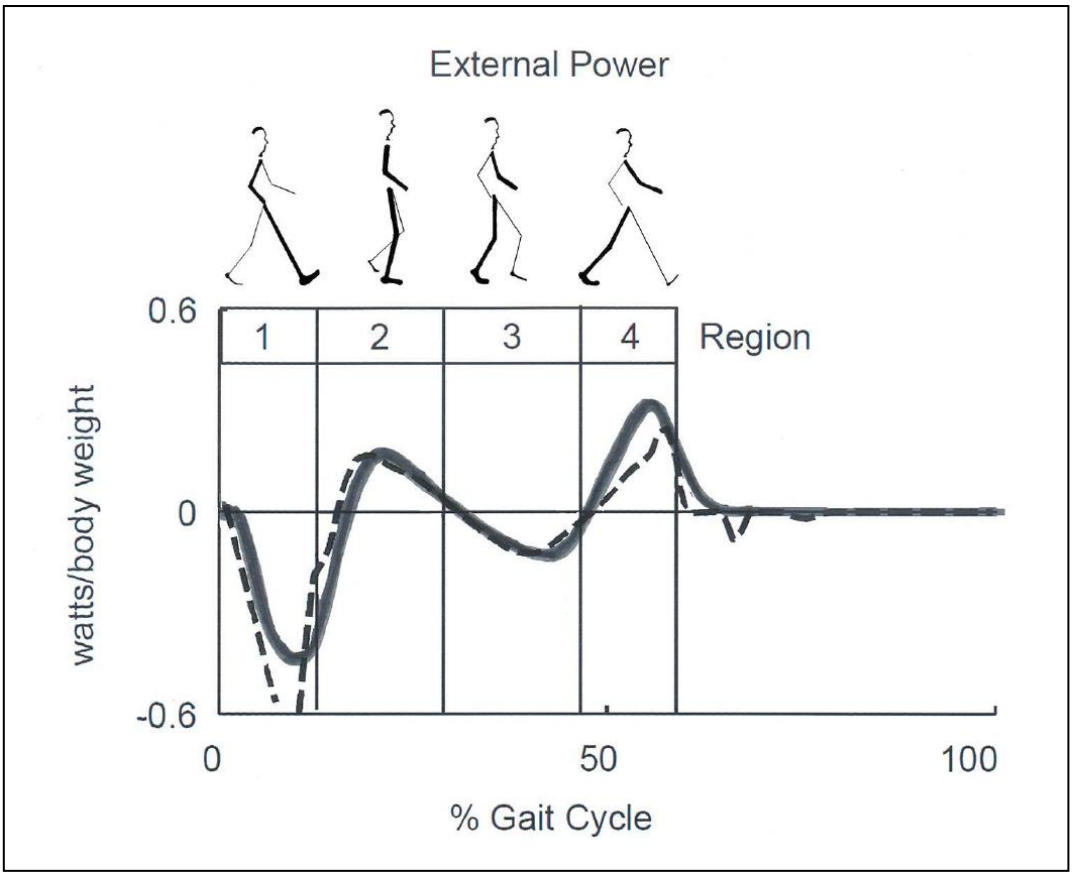

Fig 1.4. Sketch of Neptune's Regions of the step. Regions are defined by the zero crossings of the external power curve, which corresponds approximately to double support in Regions 1 and 4, and to the rise and fall of the centre of mass (CoM) during single stance in Regions 2 and 3, respectively. Late Regions 3 and 4 correspond to the push-off phase, according to other authors. Continuous and dashed lines correspond to experimental and model-simulated data. The figure is taken from Tesio et al.[4] adapted from Neptune et al.[20], used with permission.

Clinical application of knowledge on the CoM motion requires inferences on the underlying role of segmental impairments. In this view, the observation of synchronous E_{tot} changes and muscle recruitment looks essential.

The sequence of activation of lower limb muscles can be recorded using sEMG or fine-wire implanted electrodes. Several different studies demonstrated the sequence of activation of lower-limb muscles both in adults [21,22] and children [23]. These studies provided evidence that the plantar flexors are active, both mechanically and electrically, from midstance to mid-push-off (Neptune's Region 3 and 4, respectively, see Fig. 1.4), while the ankle dorsal flexors are active during early stance and late push-off (Regions 1, 2 and 4, respectively). The mechanical role of the plantar flexors seems crucial: their power is nowadays considered the main responsible of the body CoM propulsion. [24,25,26,27]

Active stretching of the plantar flexors occurs at midstance, thus facilitating the power production during push-off. Simultaneously, the lengthening contraction (hence the negative work) of the plantar flexors group[28,29] or the Soleus[30] is primarily responsible for the braking action concerning the CoM fall in late stance.

Gait studies on split-belt treadmills

The classic Gait Analysis uses platforms embedded in the floor to record ground reaction forces (GRF) during foot contact. Less frequently, force-sensorized treadmills and, even more rarely, force treadmills composed of two independent belts that can run at different speeds are used (split-belt treadmill).

Walking on a split-belt treadmill can induce kinematic and dynamic asymmetries between the two consecutive steps.

In the case of split-belt treadmill studies, the protocol typically includes three successive phases:

a. *Tied* phase. The belts rotate at the same velocities,
b. *Split* or *adaptation* phase. The velocity of one belt is increased for almost 5-15 minutes
c. *Post-adaptation* phase in which belts return at the previous tied velocity [31].

The split-belt paradigm was first introduced by Dietz et al.[32] in 1994 in a study on the capacities for early adaptation of the (supposed) spinal circuitries that underlie human walking. More recently, Reisman et al.[33] demonstrated that parameters related to a single step (intralimb parameters), i.e., *stance time*, *swing time,* and *stride length,* are modified in 3-5 strides during the split phase (*effect*).

At the beginning of this phase, the limb placed on the faster belt (for simplicity defined from now on as "fast limb") has a net reduction of *stance time* and an increase of *swing time* with respect to the contralateral limb, in close analogy with the "escape" limp seen in pathologic claudication. No further changes occur during the remaining split phase[34–37]. During the *post-adaptation* phase, the same parameters return quickly to the basal condition (Fig. 1.5).

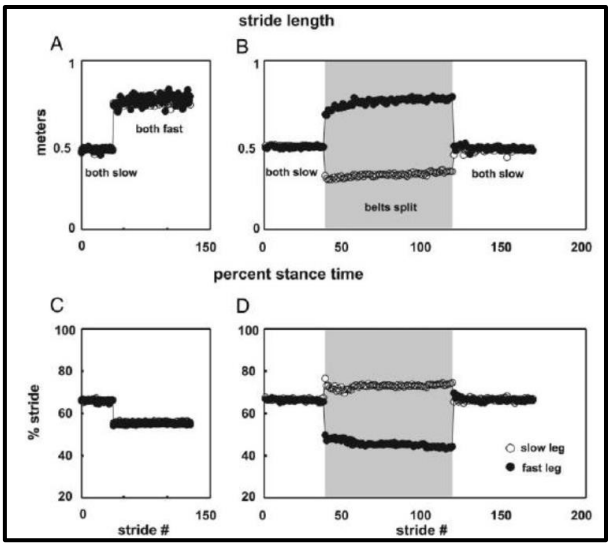

Fig. 1.5. Variation of the intralimb parameters (stride length, upper panels, and percent stance time, lower panels) during the tied condition (A,C), split (gray area of panels B and D), and post-adaptation (white area of the graphs B and D) obtained in the study of Reisman et al.[33].

Interlimb parameters, i.e., s*tep length* and *double stance time,* change slowly during adaptation. At the beginning of the split-phase, the *step length* (here, the "anterior" step, named after the anterior limb) and the *double stance time* of the slow limb (anterior limb) increase, while those referred to fast limb decrease. In *post-adaptation,* an opposite asymmetry occurs until symmetry is restored in a few minutes (Fig. 1.6).

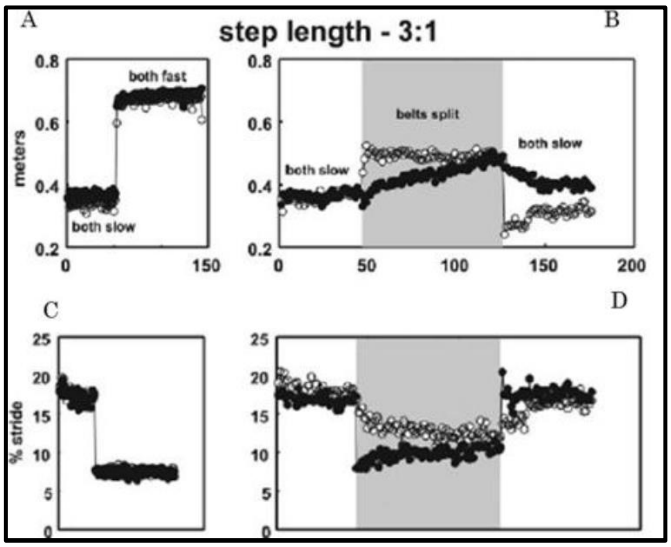

Fig. 1.6. Variation of the interlimb parameters (step length, upper panels, and percent double stance time, lower panels) during tied conditions (A, C), split (velocity ratio between the belts 3:1) (gray area of panels B and D), and post-adaptation (white area of B and D graphs) obtained in the study of Reisman et al.[33].

This phenomenon is called *after-effect*, and it is the result of motor adaptation. Adaptation consists of the Central Nervous System's capacity to modify and provide a stable adjustment of motor commands based on the mechanical context[35,38]. Retention of the acquired patterns when the mechanical context does not require them any longer (after-effect) is considered a learning marker.

Overview of experimental goals and potential relevance of the results

The research's primary goal presented in this Thesis is contributing to the clinical translation of GAFT and split-GAFT. The study has no pretense about reaching a full integration of the analysis of the CoM into routine clinical practice. In this endeavor, five different partial goals were pursued:

1. Completing the data on the 3D motion of the body CoM during walking, already available for healthy adults, concerning pediatric age (5-13 y.o).
2. Study of the curvature peaks of the 3D trajectory of the body CoM during walking in healthy adults.
3. Investigation of the effect of split-walking in terms of segmental motion in healthy adults.
4. Study of the real velocity of the CoM during split-gait.
5. A paradigmatic clinical case.

Although sharing the same common purpose, each of these studies required independent studies, described in separate Chapters.

The first and second goal of the present Thesis is discussed in Chapters 3 and 4, adding new information on the motion of the CoM. In Chapter 3, the 3D path of the CoM in a pediatric population (5-13 years) is described. In Chapter 4, the 3D trajectory of the CoM is investigated in terms of its peak curvature, taken as an index of balance during walking.

The third and fourth goals of the present Thesis are discussed in Chapter 5 and 6, respectively, focusing on split-walking (split-gait). In particular, in Chapter 5, the split-walking is investigated from the segmental standpoint, focusing on the dynamic aspects. In Chapter 6, the velocity of the body CoM during split-walking is computed.

The fifth goal is discussed in Chapter 7. The adaptation of one limping patient to split-walking is evaluated to test the potential role of split-walking as a therapeutic exercise. This study

(in progress) is nested in a clinical trial in which split-walking is applied to patients with unilateral impairments coming from various pathologic conditions. In the present Thesis, a case report of a patient with unilateral impairment due to hemispheric neurosurgery is discussed.

2. General methods

This section summarizes the general methods used in the research described in the present Thesis. Further details, specific for the different studies, will be provided in the next Chapters.

A Gait Analysis on Force Treadmill (GAFT) method has been adopted. The GAFT consists of a split-belt force treadmill integrated with commercially available systems for optoelectronic kinematics and telemetric sEMG registration. This instrumentation has been validated in Tesio et al.[2].

Fig 2.1. In the figure, the GAFT method is shown. The apparatus is composed of 8 near-infrared cameras (4 shown in the figure marked in red), wireless EMG (marked in white), a video registration system (marked in blue), and a split-belt treadmill, composed of two half treadmills, mounted on force sensors (white arrows indicate the two half treadmills). The picture was taken from the gait analysis laboratory of the neuro-motor rehabilitation unit of Istituto Auxologico Italiano, IRCCS, Milan.

General experimental procedure

Ethics

Written informed consent was provided from all the participants enrolled in the studies. The experiments were conducted according to the Declaration of Helsinki of the World Medical Association. These studies were approved by the ethic committee of Istituto Auxologico Italiano. The exam procedure here described was the same adopted for all of the different studies.

Lower limb dominance: Waterloo footedness questionnaire-revised

Participants were tested for their foot dominance by means of the Waterloo footedness questionnaire revised [39]. The participant had to indicate which limb he/she would prefer in various motor activities.

Preparation of the participant

An undershirt, short trousers, socks, and ballet-flat shoes were provided to each participant. These clothes allowed appropriate markers' positioning, freedom of movement and correct detection of markers' displacement. Markers were positioned as per the Davis protocol[40]. Force, belt speed, and markers' displacement signals were sampled at 250 Hz. The participant's height and weight were measured precisely.

Walking trial

Different walking trials are requested. The modalities of each trial and the whole sessions were specific for the study goals (see below).

Computations

Segmental motion

Joint kinematics was recorded through an optoelectronic system. The markers' 3D displacement was captured using ten near-infrared stroboscopic cameras (Smart-D optoelectronic system; BTS Bioengineering Spa, Milan, Italy), thus enabling the estimation of the ankle, knee, and hip 3D excursions.

The joint moment and power were computed through the spatiotemporal synchronization of the ground reaction force vectors and the joint centres of rotation. In this work, kinematic and dynamic variables were analyzed only along the sagittal plane.

The motion of the CoM

Basic algorithms

The length of the 3D path of the CoM was computed through the algorithms proposed by Cavagna (1975) and Cavagna et al. [15,41]. Briefly, force signals provided the accelerations of the body CoM in the anterior-posterior (AP), the vertical (V), and the lateral (L) directions. From the V forces, the offset provided by the participant's weight was subtracted. Double integration of accelerations provided the CoM displacements in a 3D space, representing changes with respect to an unknown initial state. The method assumes that the average displacements of the CoM are nil in the vertical, lateral and (provided the treadmill velocity is subtracted) in the forward direction, with respect to the force sensors (of course cyclic changes occur around the average position) over the sequence of strides analyzed (six of them in the present Thesis). This implies that, on average, the CoM is not displaced laterally, upward or downward, and that walking occurs at the same average velocity of treadmill (it is said that the CoM does not *"drift"*). This may not be exactly the case, however. A "drift" is conventionally considered as acceptable when the sum of the increments of velocity along the selected strides does not differ from the sum of the decrements by more than 5%.

Data analysis

All signals were synchronized and off-line analyzed. The protocol to compute spatiotemporal parameters, joint sagittal power, joint sagittal range of motion, muscle lengthening was provided by BTS Bioengineering Spa, Milan, on Smart Analyzer programming language. On the same protocol, the computation of energy changes and the displacements of the CoM during the stride was implemented by a bioengineer, who works in the laboratory where the Thesis was realized. Stride time was normalized to 100-time points. Results were averaged across six subsequent strides (unless specified otherwise) for each participant and then grand-averaged across participants. Further computations, statistics, and graphic representation were performed using MATLAB (version 8; MathWorks Inc., Natick, Massachusetts, USA), STATA (version 14.0; STATA Corp., College Station, Texas, USA), and SigmaPlot software (version 12.0; Systat Software Inc., San Jose, California, USA).

Statistics

The Shapiro-Wilk test was used to assess the normality of the distribution of variables. Continuous variables were expressed as means and standard deviations (SD) in case of normality distribution and as medians and interquartile (IQ) ranges in case of non-normality distribution. Categorical

variables were given as absolute numbers and percentages. In case of normality distribution, all variables were compared using a paired Student's *t*-test or a repeated analysis of variance (ANOVA). In the case of non-normality distribution, non-parametric Wilcoxon signed-rank or Friedman ANOVA were used. In the case of significant ANOVA models, Tukey's (or the Wilcoxon signed-rank test in case of non-normality) post-hoc tests were run on contrasts between pairs of conditions. Significance was set at $P < 0.05$. The Benjamini-Hochberg "false discovery rate" correction for multiplicity[42] was adopted whenever appropriate.

Further details will be provided in distinct Chapters.

3. Experimental study: the three-dimensional path of the body centre of mass (CoM) during walking in children: an index of neural maturation[43]

Gait analysis was performed on 24 children, 5-13 years of age. The participants were divided into 4 age groups (5-6, 7-8, 9-10, 11-13 years, respectively). They were requested to walk at selected velocities, within a range of velocities perceived as very slow and very fast. The data were acquired during a previous experimental campaign. Results inherent to the segmental motion analysis have already been published [44], demonstrating the applicability of GAFT to children. The goal of the present study is to describe the 3D trajectory of the CoM, so far described only in adults. If the average forward velocity is subtracted to the CoM velocity, in adults, its 3D trajectory has a figure-of-eight shape, upward concave, about 18 cm long. Given its shape, it has been dubbed the "bow tie" [18,19].

Goals of the study:

a. Providing normative data on the morphology of the CoM "bow tie" for pediatric age.
b. Investigating the relationship between the bow tie's morphology and the walking speed as a function of age after controlling for body size (here, participant's stature). The total length and maximal lateral, vertical, and forward displacements of the CoM path were calculated with the direct-Newtonian method from the GRF during complete strides.

Any age-related differences in the bow tie parameters can be considered as candidate indexes of locomotor maturation.

Introduction

The motion of the body centre of mass (CoM) during locomotion represents a summary indicator of the motion of the whole body system[45]. In recent decades, a study of the CoM motion has provided information on the mechanics of walking, both in humans and other animals, in terms of energy expenditure, mechanical efficiency, and symmetry between subsequent steps [8]. An 'inverted pendulum'-like mechanism, allowing a remarkable saving of muscular work, has been demonstrated in human adults[8], children[41], and biped and quadruped animals[45], as well as in adults[13] and children[46] with various gait impairments.

Several studies have investigated energy changes associated with the CoM motion, but much less attention has been paid to kinematic aspects, that is, its three-dimensional (3D) path during strides. This has only been investigated in two studies of healthy adults[18,19] and in one study of children[47]. A key issue, still poorly understood, is the change in the 3D path of the CoM with a child's development. The development of mature walking reflects not only changes in body size and mass distribution[48] but also maturation of the central nervous system. However, the staging of this usual process of development remains controversial.

Adult-like motion patterns are gradually observed between 4 and 13 years of age, with differences observed among papers and on the gait parameters considered. This holds for lower limb joint rotations[49], lower limb electromyography patterns[23], and the power at the lower limb joints [50], etc. In contrast, the efficiency of the pendulum-like mechanical energy transfer of the CoM appears to be matured by age 5 years[41,47] . However, whether this also holds for the 3D path of the CoM during a stride is unknown. In adults, once the forward average speed is controlled for, the 3D path appears to reflect a closed figure-of-eight shape that is upward concave on the frontal plane, which has been named the "bow tie"[19], with an overall length in the order of 16–20 cm. Moreover, the path length and shape changes as a function of walking speed.

In the present study, the 3D path of the CoM during walking was analyzed in healthy children 5–13 years of age. The study aims were to disentangle the effect of age from that of absolute forward speed and body size and to define preliminary pediatric normative values. If these goals are met, the 3D path of the CoM during walking might present a possible index of the maturation of neural control of gait.

Specific methods

The three-dimensional path of the CoM during walking was compared across healthy children 5–6 years (n = 6), 7–8 years (n = 6), 9–10 years (n = 5), and 11–13 years of age (n = 5) and healthy adults (23–48 years, n = 6). Participants walked on a force-sensorised treadmill at various velocities, normalized to body size through the adimensional Froude number [51], given by Eq. 2.1 (see general methods section)

$$Fr = \frac{{V_f}^2}{gh} \quad [3.1]$$

Where V_f is the average treadmill velocity, g the gravity acceleration, and h the participant's height. The 3D motion of the body CoM was computed from the GRF (see the general methods section).

Graphic representation of the CoM path

Force and force-derived signals were synchronized and analyzed offline with algorithms available within the SMART Software Suite (BTS Bioengineering Spa, Milan, Italy). The stride period (one stride equals two consecutive steps) was defined as the time interval between three subsequent peaks of the forward speed of the CoM following the heel strike. For a graphic representation of the CoM path, results were averaged across six subsequent strides within each participant and then grand-averaged across each age group. Given that vertical, lateral, and forward (net of the treadmill) velocities are nil, the CoM path can be represented as cyclic and virtually closed 3D paths around an average position (Fig. 3.1).

The graphic representation of the CoM path was made according to Tesio et al. [19]. A summary of results in adult participants is reported below.

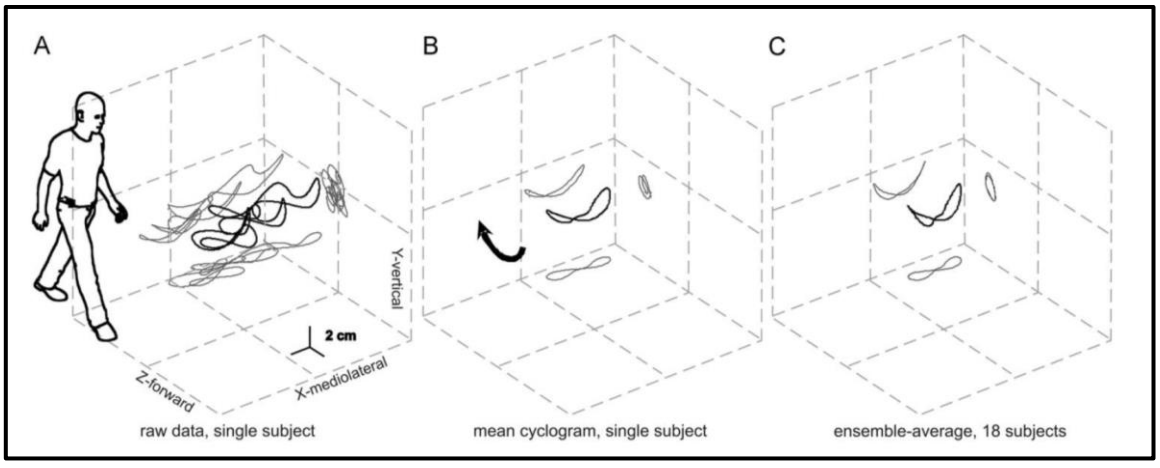

Fig 3.1. Three-dimensional path of the body CoM during walking at 1.0 m s^{-1} in healthy adults. In panel A, the outlined human form (arbitrary graphic scaling) highlights the orientation of the spatial coordinates with respect to the walking subject. The black curve represents the path over 6 subsequent strides made by a representative subject (man, 23 years, height 1.77 m, weight 74 kg, leg length 0.91 m). The gray curves give planar projections of the black one. Panel B shows the path averaged over the 6-stride sequence represented in panel A. The curved arrow shows the direction of rotation (from top, clockwise on the right step and counterclockwise on the left step). Panel C gives the CoM path grand-averaged across 18 subjects at the same speed. For averaging purposes, the curves were normalized to 100 points through spline

interpolation. The 1.0 m s^{-1} speed corresponds to 0.11 Froude units (see Methods) for subject B and to a 0.10–0.14 Fr units range across the whole sample (taken from Tesio et al.[19]).

For any given speed, the six subsequent cyclograms of 3D displacements of the CoM were plotted onto orthogonal axes (A–P, V, and L), thus giving rise to a 3D closed curve (a Lissajoux-like polar graph). The planar projections of this 3D object were also represented. Within the selected stride sequence, average speed may change from stride to stride, thus causing modest erratic drifts of the individual cyclograms, hence the fuzzy appearance of the series of subsequent tracings (see Fig. 3.1). This effect is neutralized by normalizing each curve to 100 points through spline interpolation and averaging coordinates across curves. Grand-averaging across subjects was also performed.

Statistics

The effect of age group and Fr on each spatial parameter was evaluated with linear regression models with repeated measures. In these models, the within-subjects effects were 'walking speed' and 'step number' [52], and the fixed effects were 'age group' and 'Fr.' Moreover, to allow for a nonlinear relationship between Fr and each spatial parameter, a flexible regression modeling approach based on first-order and second-order fractional polynomials was applied [53]. In brief, for a regression model involving a single continuous covariate x, first- and second-order fractional polynomial models can be written as follows:

$$\text{First-order: } B_0 + B_1 \times x^p \qquad [3.2]$$

$$\text{Second-order: } B_0 + B_1 \times x^p + B_2 \times x^q \qquad [3.3]$$

Values of p and q are typically restricted to the set $S \in \{-2, -1, -0.5, 0, 0.5, 1, 2, 3\}$, which provides practical flexibility. By convention, $x^0 = log(x)$ and when $p = q$ then x^q is set to $x^p \times log(x)$. The best functional form was selected based on Akaike's Information Criteria (AIC), with preference given to the model with the lowest AIC [54]. Some participants could not reach all of the imposed walking speeds. Therefore, selecting the best fractional polynomial was performed considering only complete data, and missing data were imputed from the selected fractional polynomial. In order to include random variability in different strides for each walking speed, a random number was added to the imputed value generated by a normal random variable with a mean equal to 0 and variance equal to the observed variance, that is, age group-specific between stride variance. The four fitting

models converged for walking speeds ranging from 0.3 to 1.1 $m \cdot s^{-1}$. Finally, pairwise comparisons among age groups were conducted using Tukey's post-hoc test to consider type I error (alpha). Statistical significance was set at 0.05, two-sided.

Results

Table 3.1 reports demographic and anthropometric data of all the participants, divided for each age group.

	5–6 years old	7–8 years old	9–10 years old	11–13 years old	23–48 years old
Number of participants	6	6	5	5	6
Sex, male/female	1/5	4/2	3/2	2/3	3/3
Age, years	5.86 (0.35)	7.85 (0.36)	9.61 (0.49)	11.80 (0.74)	32.39 (7.94)
Height, cm	115.88 (4.67)	135.34 (7.86)	143.18 (6.83)	148.49 (6.12)	173.39 (4.61)
Weight, kg	21.48 (3.23)	31.69 (7.37)	41.32 (5.67)	41.71 (6.11)	72.25 (19.63)
Lower limb length, cm	58.60 (3.36)	68.63 (8.86)	75.72 (5.10)	79.37 (4.96)	90.87 (2.81)
ASISd, cm	16.27 (0.57)	17.63 (0.67)	19.82 (0.81)	18.31 (0.87)	25.49 (1.66)

Table 3.1. The table reports the characteristics of the participants across age groups. Values for age, height, weight, lower limb length, and ASISd are represented as mean (sd).
ASISd: the distance between right and left anterior superior iliac spines.

Figure 3.2 shows the 3D path of the CoM and its projection on the three orthogonal planes for each age group. The 3D path representation is made for two different speeds, corresponding to the highest and lowest Fr speed reached by all participants, respectively. Between rows, a difference in shape, related to the different speeds, is observed: at all ages, the 3D path acquires a more bent, upward concave shape on the frontal plane at the higher (right column) compared with the lower (left column) speed range. Within rows, the absolute changes with age are far less evident. The participants' sizes are very different across age groups. Age-related differences emerge if the displacements of the 3D path are standardized to participants' heights, h.

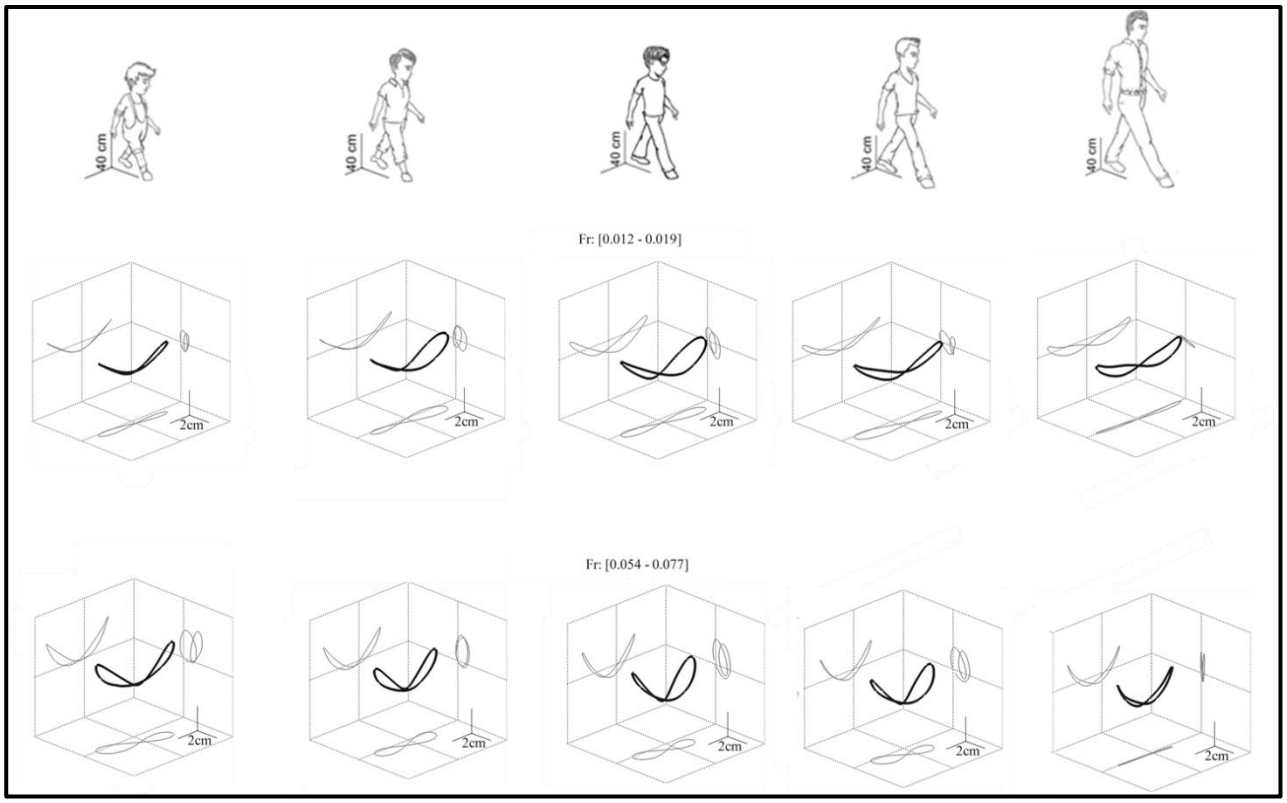

Fig 3.2. The figure shows the three-dimensional (3D) path of the centre of mass (CoM) during walking on a force-sensing treadmill averaged over six consecutive strides and grand-averaged across participants in each age group. The displacement due to the average forward speed is subtracted. From left to right, each column refers to separate age groups. Each row represents the mean value of trials obtained for the same range of Froude (Fr) speeds as indicated, i.e. 0.012-0.019 Fr (0.38-0.56 m s^{-1}) and 0.054-0.077 Fr (0.90–1.11 m s^{-1}). The black and gray curves represent the 3D path of the CoM and its planar projections, respectively. The human outline forms (scaled to the mean participant height across all age groups) highlight the spatial coordinates' orientation with respect to the walking direction.

Figure 3.3 illustrates the relationships between the CoM path parameters and the Fr speed for each age group. The relationships between the CoM path parameters and the Fr speed can be represented by a U-shaped curve for each age group. The CoM path parameters are lower at all speeds, as a rule, as participants get older. In particular, age-dependence holds for the lateral size of the path (x/h) and the total length (path length/h) (top and bottom panels, respectively). The corresponding fitting equation and the data model fit indices (AIC values) are reported. For each parameter, the selected second-order fractional polynomial followed this function:

$$Fr^2 + Fr^2 \times log\ (Fr) \qquad [3.4]$$

Moreover, for each parameter, the F test associated with the age group covariate had a P-value <0.001.

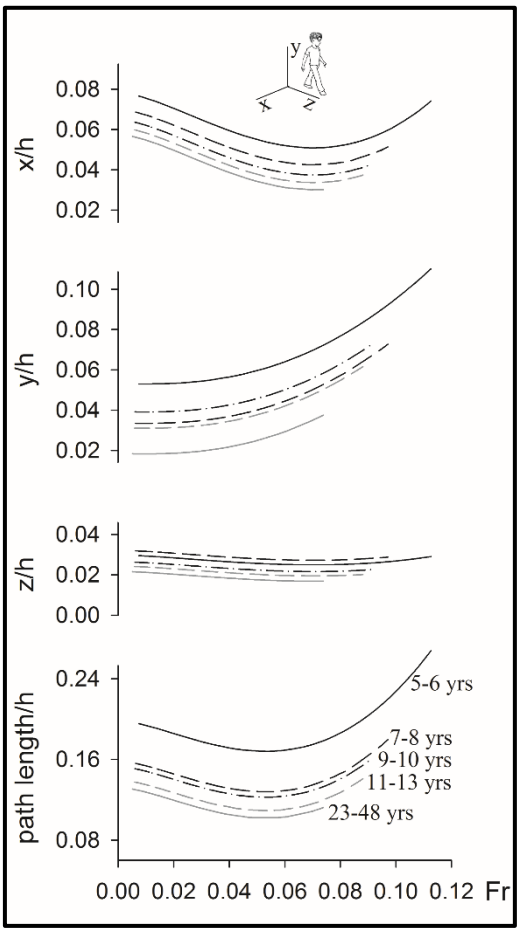

Fig.3.3. Spatial parameters of the centre of mass (CoM) path during one stride on the ordinate, as a function of walking speed (in Froude units, Fr), on the abscissa. From top to bottom, each panel refers to the displacements of the CoM, standardized to participant's height (h), in the lateral (x/h), vertical (y/h), and forward (z/h) directions, and to the total length of the path (path length/h). Note the different scales of path length/h with respect to other CoM parameters. Each panel represents the mean value of trials obtained for a range of walking speeds from 0.3 to 1.1 m s^{-1}. Curves from the different age groups are superimposed. They can be identified from their distinct tract and from the labels assigned in the bottom panel. The human outline form on the top highlights the orientation of the spatial coordinates with respect to the walking direction. Each of the four parameters of the CoM path was fitted as follows (subscripts to the group variable refer to the corresponding age group):

$$x/h = 0.078 + Group_{23\text{-}48} \times (-0.020) + Group_{11\text{-}13} \times (-0.017) + Group_{9\text{-}10} \times (-0.013) + Group_{7\text{-}8} \times (-0.008) + Fr^2 \times (23.769) + Fr^2 \times ln(Fr) \times (11.035)$$

$$y/h = 0.053 + Group_{23\text{-}48} \times (-0.035) + Group_{11\text{-}13} \times (-0.022) + Group_{9\text{-}10} \times (-0.014) + Group_{7\text{-}8} \times (-0.020) + Fr^2 \times (9.572) + Fr^2 \times ln(Fr) \times (2.328)$$

$$z/h = 0.030 + Group_{23\text{-}48} \times (-0.008) + Group_{11\text{-}13} \times (-0.005) + Group_{9\text{-}10} \times (-0.003) + Group_{7\text{-}8} \times (0.002) + Fr^2 \times (4.240) + Fr^2 \times ln(Fr) \times (1.969)$$

Path length/h= 0.199 + $Group_{23-48}$ × (-0.062) + $Group_{11-13}$ ×(-0.059)+ $Group_{9-10}$ × (-0.046) + $Group_{7-8}$ × (-0.040) +Fr^2 × (52.606) + Fr^2 × ln(Fr) × (21.587)

Table 3.2 presents the significance of the ten possible post-hoc contrasts between pairs of age groups. In general, contrasts were only significant between nonadjacent pairs of age groups and most frequently for the x/h parameter. In clinical practice, nomograms which can map individual parameters are needed.

		x/h		y/h		z/h		Path length/h	
Comparison between age groups (years)		Mean difference (CI 95%)	P-value	Mean difference (CI 95%)	P-value	Mean difference (CI 95%)	P-value	Mean difference (CI 95%)	P-value
23–48 (n=6)	11–13	-0.004 (-0.009 to 0.001)	0.636	-0.013 (-0.023 to -0.003)	0.104	-0.003 (-0.007 to 0.002)	0.720	-0.007 (-0.022 to 0.008)	0.869
	9–10	-0.007 (-0.012 to -0.002)	0.038*	-0.021 (-0.031 to -0.011)	0.001*	-0.005 (-0.009 to -0.001)	0.166	-0.021 (-0.036 to -0.006)	0.057
	7–8	-0.012 (-0.017 to -0.008)	<.0001*	-0.015 (-0.025 to -0.006)	0.022*	-0.010 (-0.014 to -0.006)	<.000*	-0.026 (-0.040 to -0.012)	0.004*
	5–6 (n=6)	-0.021 (-0.026 to -0.016)	<.0001*	-0.035 (-0.044 to -0.025)	<.0001*	-0.008 (-0.012 to -0.004)	0.002*	-0.066 (-0.081 to -0.051)	<.0001*
11–13 (n=5)	9–10	-0.004 (-0.009 to 0.001)	0.610	-0.008 (-0.019 to 0.002)	0.561	-0.002 (-0.007 to 0.002)	0.869	-0.013 (-0.029 to 0.002)	0.449
	7–8	-0.009 (-0.014 to -0.004)	0.006*	-0.002 (-0.012 to 0.008)	0.990	-0.008 (-0.012 to -0.004)	0.004*	-0.019 (-0.034 to -0.004)	0.106
	5–6	-0.017 (-0.022 to -0.012)	<.0001*	-0.022 (-0.032 to -0.012)	0.001*	-0.005 (-0.010 to -0.001)	0.096	-0.059 (-0.074 to -0.044)	<.0001*
9–10 (n=5)	7–8	-0.005 (-0.010 to 0.000)	0.270	0.006 (-0.004 to 0.016)	0.806	-0.006 (-0.010 to -0.001)	0.071	-0.005 (-0.020 to 0.010)	0.954
	5–6	-0.013 (-0.019 to -0.008)	<.0001*	-0.014 (-0.024 to -0.004)	0.064	-0.003 (-0.008 to 0.001)	0.548	-0.046 (-0.061 to -0.030)	<.0001*
7–8 (n=6)	5–6	-0.008 (-0.013 to -0.004)	0.008*	-0.020 (-0.029 to -0.010)	0.001*	0.002 (-0.002 to 0.006)	0.799	-0.040 (-0.055 to -0.026)	<.0001*

AIC	-8933.8	-7183.6	-8644.8	-7738.6

Table 3.2. The table illustrates the nonlinear regression model results for each spatial parameter over Froude (Fr) speed and age group (see Statistics paragraph for details). The upper row refers to the centre of mass (CoM) path parameters, normalized to participants' heights, i.e. lateral (x/h), vertical (y/h), and forward (z/h) displacements and the total length of the three dimensional (3D) path (path length/h). The mean difference between age groups and the 95% confidence limits are presented, with p-values juxtaposed. The leftmost column presents, in separate cells, the age groups and number of participants (n). The next column presents the other three age groups to be contrasted (Tukey's post-hoc). Data were obtained for absolute walking speeds ranging from 0.3 m s^{-1} to 1.1 m s^{-1}.

The preliminary nomograms of the relationship between the CoM path parameters and the Fr speed with the 95% confidence limits and 95% individual tolerance (prediction limits) are shown in Fig.3.4.

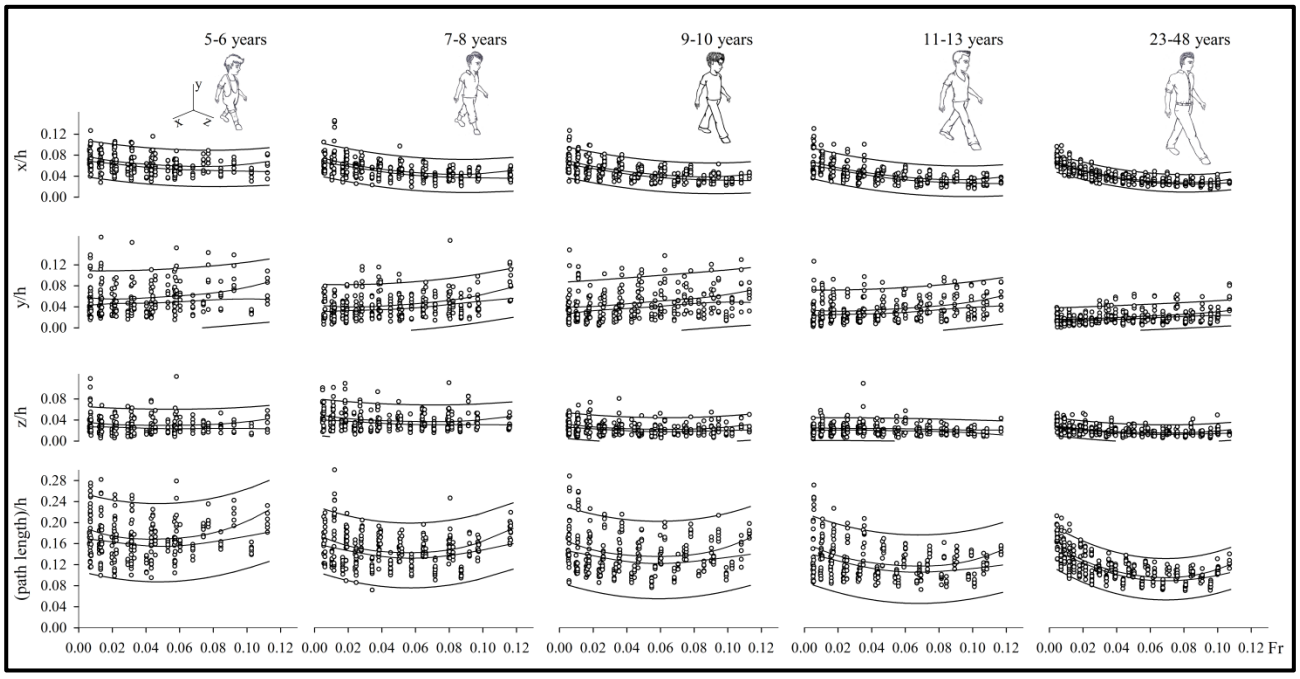

Fig. 3.4. Spatial parameters of the three-dimensional path of the centre of mass (CoM) during one stride as a function of walking speed in Froude (Fr) units. From top to bottom, each panel refers to displacements of the CoM in the lateral (x), vertical (y), and forward (z) directions and to the total length of the path, all normalized with respect to participants' heights. From left to right, each column represents different age groups. For all figures, each dot refers to a stride (six strides for each participant). Data were fitted with a second-order polynomial regression equation. Inner and continuous outer lines encase the 95% confidence and tolerance ('prediction') limits, respectively. The lower limits were not represented if negative (thus representing statistical artifacts). The outlined human forms at the top of each column are scaled with respect to the overall mean height and highlight the orientation of the spatial coordinates with respect to walking direction

Discussion

This is the first study that compares the 3D path of the CoM across different stages of child development to the author's knowledge.

The results suggest that the CoM path shape changes as a function of speed, mostly in its lateral size, in children 5–13 years of age. A decrease in the lateral oscillation of the CoM with increasing speed has previously been reported in adults walking over normal ground[55] and on a treadmill[19]. The present study demonstrates a shrinking of the CoM path laterally with increasing age in children, after accounting for the effects of height and absolute forward speed. In the literature, several age-related walking mechanics changes have been described[56,57], which reflect the maturation of motor control. After age 2, the pendulum-like energy-saving mechanism of the CoM[45] appears to be mature, although achieved through different joint mechanics, compared to adults[41]. The relevance of age-dependent changes in the CoM trajectory, particularly its lateral size, arises. After all, lateral oscillations of the CoM, following accelerations and displacements of small amplitude, require only a tiny fraction (around 5%) of the total 'external' work needed to keep the body in motion[6,58]. Our results suggest that balance control rather than energy expenditure is relevant in lateral CoM displacements. The classic ballistic model of the CoM motion assumes a bi-dimensional sagittal motion. A clear limitation of this model lies in the lateral redirection of the 'pendulum' (almost a U-turn) at each step. This happens during the single stance phase, and it requires a weak yet quick and precise injection of muscular work against the ground, lasting for about 50 ms. In this critical phase of the step, the curvature of the CoM trajectory peaks, and the ballistic efficiency of the pendulum drops to zero giving way to fully active, muscle-driven control[18]. This 'turning' phase of the stride has already been highlighted as being at risk for causing a fall sideways[59] , thus becoming a target for clinical observation[60] and possibly providing cues to fall prevention[58]. These suggestions were previously validated, demonstrating that when the CoM has a passive-ballistic, pendulum-like motion, a 'power law' links the tangential speed and the curvature of the CoM [18], like in many other human movements. However, both the ballistic mechanism and its "law" vanish during active forward acceleration (just before and during the double stance) and when the lateral direction of oscillation is inverted. This suggests that active control is suddenly re-established in these phases of the stride. Notably, the CoM turns actively during mid-stance on a single leg when the CoM is dangerously moving over the supporting foot's external limits. If so, why should the CoM oscillate

on the frontal plane, concerning body size, more in children than in adults at dynamically equivalent speeds? A tentative answer is that the lateral 'shrinking' of the CoM trajectory, relative to body height, reflects balance control's maturation. This is consistent with the results showing that the base of support's absolute width is invariant [61] or even decreasing as age increases [62]. Therefore, the narrowing of the CoM path makes oscillations over a support base safer as they become relatively narrower with body elongation.

The present study is subject to three significant limitations. First, the sample size was small. Second, the participants' age was not lower than five years. Third, treadmill walking presents some differences concerning walking over a solid ground [2,44]. For these reasons, results can only be generalized with caution. All this considered, it appears acceptable to propose that the 3D path of the CoM during the stride is a promising summary index of the maturation of gait control.

4. Experimental study: the curvature peaks of the trajectory of the body centre of mass during walking: a new index of dynamic balance[63]

The motion of the body CoM has been studied mostly in the sagittal plane. Ergometric (i.e., work-related) aspects of its pendular motion have already been described in detail. However, the motion of the CoM is inevitably deployed along a 3D path, comprehensive of lateral excursions.

Chapter 3 has recalled that if the average forward velocity is offset, this trajectory resembles an elegantly curved figure-of-eight, dubbed the bow tie, with an overall perimeter of about 18 cm. Both in adults and children, the bow tie's shape and perimeter significantly change as a function of the walking velocity and (unpublished results) in response to the various pathological alterations of walking. In particular, it is likely that excessively approaching the "no-return" point of the lateral trajectory leads to an increased risk of falling. From the perspective of balance, it seems essential to study the 3D trajectory of the body CoM, not only the energetic cost of its forward translation.

During walking, falling is most likely to occur during the single stance, towards the side of the supporting lower limb[59]. A timely lateral redirection of the CoM preceding the no-return position is necessary for balance. An index of the capacity to realize this challenging task may be useful in clinical practice and sports sciences.

In the present study, the curvature peaks (the inverse of the radius of curvature) of the 3D path of the CoM during the single stance were analyzed.

Introduction

A recent review examined the current literature on different methods for quantifying dynamic balance, and no consensus has been achieved concerning which measure is most suited [64]. A laboratory-based measure for evaluating balance performances during walking has been developed, referred to as the margin of stability (MOS) [65]. The MOS is defined as the distance between the horizontal position of the CoM times a factor reflecting the CoM velocity ('extrapolated centre of mass', XCoM) and the perimeter of the individual's base of support at any given instant of time [66–68]. This measure has been primarily used to assess balance during walking, undergoing the most various perturbations [68–73], at multiple ages [74,75], and in patients suffering from the most various motor impairments [76–78].

Previous studies suggested that lateral placement of the landing foot, generating the step width, creates the initial conditions to control lateral CoM motion, given the narrow width of the base of support during the single stance phase [60,69,79,80]. By contrast, little is known about the neuromotor mechanisms ensuring stability during the single stance. The lateral redirection of the CoM is necessary at each step [17]. This motion can be modeled as the oscillation of an inverted-pendulum on the frontal plane. The lateral redirection of the CoM must occur before the no-return point is reached, beyond which an irreversible fall sideways begins, unless sideways steps are performed. In principle, pivoting on a single leg might be passive, but the spontaneous period of oscillation of the CoM is incompatible with most of the velocity/cadence combinations adopted during walking [66]. Therefore, before the point of no-return is reached on the supporting leg, active corrections of the CoM trajectory are needed. These corrections are the topic of the present article. It is proposed that an index of the "motor skill" underlying the lateral CoM redirection may be represented by the curvature peak (the inverse of the radius) of the 3D path of the CoM during the single stance. This parameter is analyzed during walking at different velocities.

Specific methods

Participants

Twelve healthy volunteers were enrolled. The inclusion criteria were the ability to wittingly sign the informed consent form; the ability to understand the instructions and to complete the locomotor task; age between 18 and 60 years; absence of neurologic or orthopedic conditions affecting gait. Exclusion criteria were surgical orthopedic interventions on the lower limbs or the spine in the 18 months before the study, joint diseases (any forms of arthritis, joint laxity, joint replacement), symptomatic spine diseases, and walking experience on treadmills during the previous 6 months.

Experimental protocol

Participants were asked to walk at increasing velocities from 0.4 m s-1 up to 1.2 m s-1 in 0.2 m s-1 increments (one every 45 to 60 seconds). Participants were warned before each speed change, which took 5 s in a ramp-like fashion.

Analysis

The period of the step was defined as the time interval between the toe-off of the opposite foot (e.g., of the left foot for the right step) and the subsequent toe-off of the contralateral foot (e.g., of the right foot for the left step). This unusual criterion for defining the stride and step periods focused attention on the single stance phases, when the extreme lateral displacement of the CoM occurs, from the perspective of dynamic balance. For each subject, six subsequent strides were analyzed. Videos of the walking trials were off-line inspected to ascertain the absence of rough irregularities (e.g., stumbling).

The trajectory of the CoM path

The three-dimensional displacements of the CoM were computed via double integration of the GRF, as described in Chapter 2[4,12].

Instantaneous energy transfer and power in the CoM motion

The efficiency of the transfer between the kinetic and the potential energy of the CoM ("percent recovery", $R_{\%}$, see ch.1 Eq.1.1) has been usually measured along an entire step. In the present study, R was measured instantaneously in order to analyse in detail its relationships with the changes of external (muscular) power. It must be recalled that work and power subtending increments or decrements of E_{tot} are conventionally defined as positive or negative, respectively [14]. The instantaneous efficiency of the kinetic-potential energy transfer of the CoM was computed as the instantaneous recovery index, $R_{\%}$ (0% = no recovery, 100% = complete recovery, i.e. fully passive CoM translation). The formula, already given in Eq.1.1 in Chapter 1, is replicated here for better clarity [8,12,17]:

$$R_{\%} = \frac{|W_f| + |W_l| + |W_v| - |W_{tot}|}{|W_f| + |W_l| + |W_v|} * 100 \qquad [1.1]$$

It is of interest here that R can be lower than 100% both in case of "positive" and "negative" work values. For instance, during the "fall" phase of the single stance, when the CoM is lowered and accelerated forward, any "braking" action of the muscles turns into a negative W_{ext} value. In any case, a zero R indicates that no exchange is occurring between E_v and E_{kf} or E_{kl}, no matter if the observed changes represent increments or decrements of mechanical energy.

The curvature of the CoM path

The path curvature (inverse of the radius of curvature) of the CoM during one stride was computed from the 3D displacements of the CoM, according to the Frenet-Serret formula [18]. The analysis was conducted with a custom-made Matlab algorithm (version 8.0, MathWorks Inc., Natick, USA), and graphic representations were realized using SigmaPlot™ (version 14.0, Systat Software Inc., San Jose, USA).

Given a particle moving along a continuous, differentiable curve in three-dimensional Euclidean space, the Frenet–Serret formulas[81] describe its kinematic properties:

$$\frac{d\boldsymbol{T}}{d\boldsymbol{s}} = \boldsymbol{\kappa N}$$

$$\frac{d\boldsymbol{N}}{d\boldsymbol{s}} = -\boldsymbol{\kappa T} + \boldsymbol{\tau B}$$

$$\frac{d\boldsymbol{B}}{d\boldsymbol{s}} = -\boldsymbol{\tau N}$$

Where $\frac{d}{ds}$ is the derivative with respect to arclength, $\boldsymbol{\kappa}$ is the curvature, $\boldsymbol{\tau}$ is the torsion of the curve, **T** is the unit vector tangent to the curve, pointing in the direction of motion, and **N** is the normal unit vector, the derivative of **T** with respect to the arclength parameter of the curve, divided by its length, and **B** is the binormal unit vector, the cross product of **T** and **N**.

Maximum values of the path curvature in each walking phase (right single stance, right double stance, left single stance and left double stance) were computed and defined as curvature peaks.

Statistics

The normality of the distribution of the variables was checked using the Shapiro-Wilk test. Continuous variables were expressed as means (standard deviation, SD), medians, and 5th-95th percentile range, while categorical data were expressed as absolute frequency and percentage. The symmetry between right and left curvature peaks was assessed by calculating the logarithm of the ratio between the peaks (in order to cope with the non-linearity of proportions [15,19]), its SD, and the 95% tolerance and confidence limits. At variance with confidence limits, applied to estimated means, tolerance limits can be applied to individual observations [19] and are, therefore, wider [15,82]. The curvature peaks occurring during the single stance phases (ssA and ssC) and the double stance phases (dsB and dsC) and their log-ratios were analyzed using a non-parametric analysis of variance model (Friedman ANOVA) across walking velocities, phases (ss versus ds phases) and their

interaction. In case of the significant Friedman ANOVA model, Wilcoxon signed-rank post-hoc tests were run on contrasts between pairs of conditions. The Bonferroni correction (P-value set at 0.05 divided by the number of measures tested) was applied. The analysis was performed using StataSE™ (version 14.0; STATA Corp., College Station, USAResults.

Results

Subjects

Table 4.1 gives demographic and anthropometric information on the study participants.

gender (women: men)		6:6	
	Mean (SD)	**median**	**5^{th}-95^{th} percentile**
Age, years	25.1 (3.0)	25.5	21.0 – 28.9
Height, m	1.72 (0.12)	1.73	1.56 – 1.89
Weight, kg	67.7 (12.3)	64.0	53.3 – 88.2
Body Mass Index, kg m^{-2}	22.7 (2.1)	22.4	20.2 – 25.8

Table 4.1. Characteristics of study participants (n = 12). SD: standard deviation

The curvature peaks of the CoM trajectory

Figure 4.1 shows morphologic and dynamic data of the 3D path of the CoM during one stride, from one representative participant (woman, 26 years, 1.55 m tall) walking at 0.8 m s^{-1}. Panel B is "zooming" on some of the tracings in panel A.

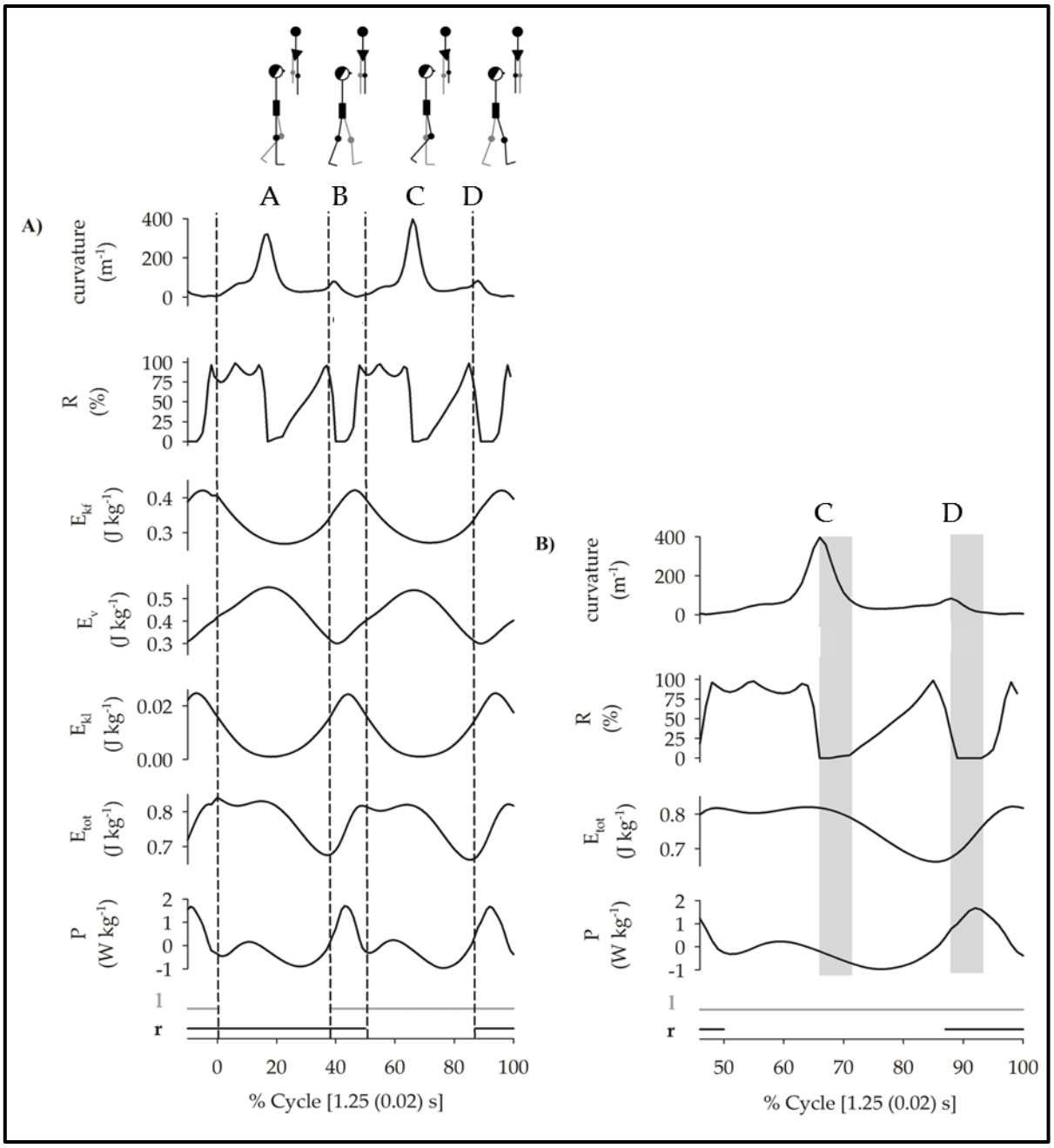

Figure 4.1. The tracings refer to the average over twenty subsequent strides performed by a representative participant (woman, 26 years, 1.55 m tall) walking on a force-sensorized treadmill at 0.8 m s^{-1}. In the left panel, the human outline forms on top of the graph help visualizing mechanical phenomena along the path of the CoM during the stride. From top to bottom, the curves refer to: the curvature of the CoM path, the instantaneous "percent recovery" of mechanical energy (R), the kinetic energy due to the forward velocity (E_{kf}), the kinetic energy due to the vertical displacement plus the gravitational potential energy (E_v), the kinetic energy due to the lateral velocity (E_{kl}), the total mechanical energy (E_{tot}), i.e., the sum of the above energies, and the external power (P) applied to the CoM, as a function of the normalized stride period. The stride begins with the toe-off of the left (l) lower limb (time 0 on the abscissa, initiation of single stance on the right, r, limb). The horizontal bars under the curves mark the single and double stance phases (black tract = right step period, grey tract = left step period). Peaks in the curvature values are labeled A to D along with the two subsequent steps. Panel B is "zooming" on the second step (actually encasing the last 5% of the previous step, see the abscissa) of panel B, but it omits

the kinetic and vertical energy curves. The grey bands encase the mechanical events occurring from the C and D peaks to the return to zero curvature. It can be seen that peaks occur during a phase of zero or near zero R (hence, of fully active muscular gait control). However, after the C peak, the CoM is actively braked (negative E_{tot} and power curves), whereas, after the D peak, the CoM is actively propelled (positive E_{tot} and power curves). See text for interpretation.

It must be recalled that the stride here begins at toe-off of the right rear limb (see above, Methods). The curvature of the CoM trajectory (top tracing) presents four visible peaks. These are labeled A and C, for the right and left steps, respectively, when they occur around the middle of the single stance phases, and are labeled B and D when they occur during the double stance phases (right and left foot behind, respectively). For simplicity, from now on, only the A to D labels will be adopted. The A and C peaks (single stance) are much higher than the B and D peaks (double stance). In both steps, all curvature peaks occur when the recovery of mechanical energy, R (second tracing from top), suddenly drops from 100 to 0, indicating that the passive pendulum-like mechanism of translation of the CoM is briskly substituted for by a muscle-driven mechanism. These findings replicate the results from a study by Tesio et al. [18].

At each step, the A and C curvature peaks, occurring during the single stance phases, are virtually synchronous with minima of both E_{kf} and E_{kl} and maxima of E_v (3^{rd} to 5^{th} tracings from the top, respectively), and with an approximately stable phase of the total mechanical energy of the CoM, E_{tot} (6^{th} tracing from top), hence of near-zero external power (7^{th} tracing from top). Figure 4.1B is zooming on the second step and omits the kinetic and potential energy curves. On closer inspection, it becomes evident that the C peak corresponds to a phase of braking of the motion of the CoM, highlighted by decrements of E_{tot} and by negative power values. The braking is fully muscle-driven (zero R values). By contrast, the D peak occurring at the beginning of the double stance corresponds to a phase of acceleration of the CoM in the vertical, sagittal, and lateral directions, highlighted by the increments of both E_{tot} and positive values of external power, P. Again, this propulsion is fully muscle-driven (zero R values). In short, the higher peaks (A, C) underlie the lateral U-turn of the CoM, requiring the braking action of active muscles. This braking action (highlighted by the negative power values) acts in opposite directions: it initially prevents the CoM from trespassing the no-return point, and then it slows down the fall towards the unsupported side until the front foot strikes the ground (in Figure 4.1A, see the coincidence of foot strike with the beginning of the push-off phase sustained by positive power). During the double stance (B, D), the lower peaks underlie the modest directional change towards the leading foot, occurring during the push-off. In this step

phase, most of the positive power required to keep the CoM in motion in the forward direction is provided [4].

Figure 4.2 helps to locate the curvature peaks within space, neglecting the time variable of the CoM displacements. The difference in curvature between the higher and sharper A and C peaks, occurring during single stance, and the lower and smoother B and D peaks, occurring during double stance, can be appreciated more intuitively.

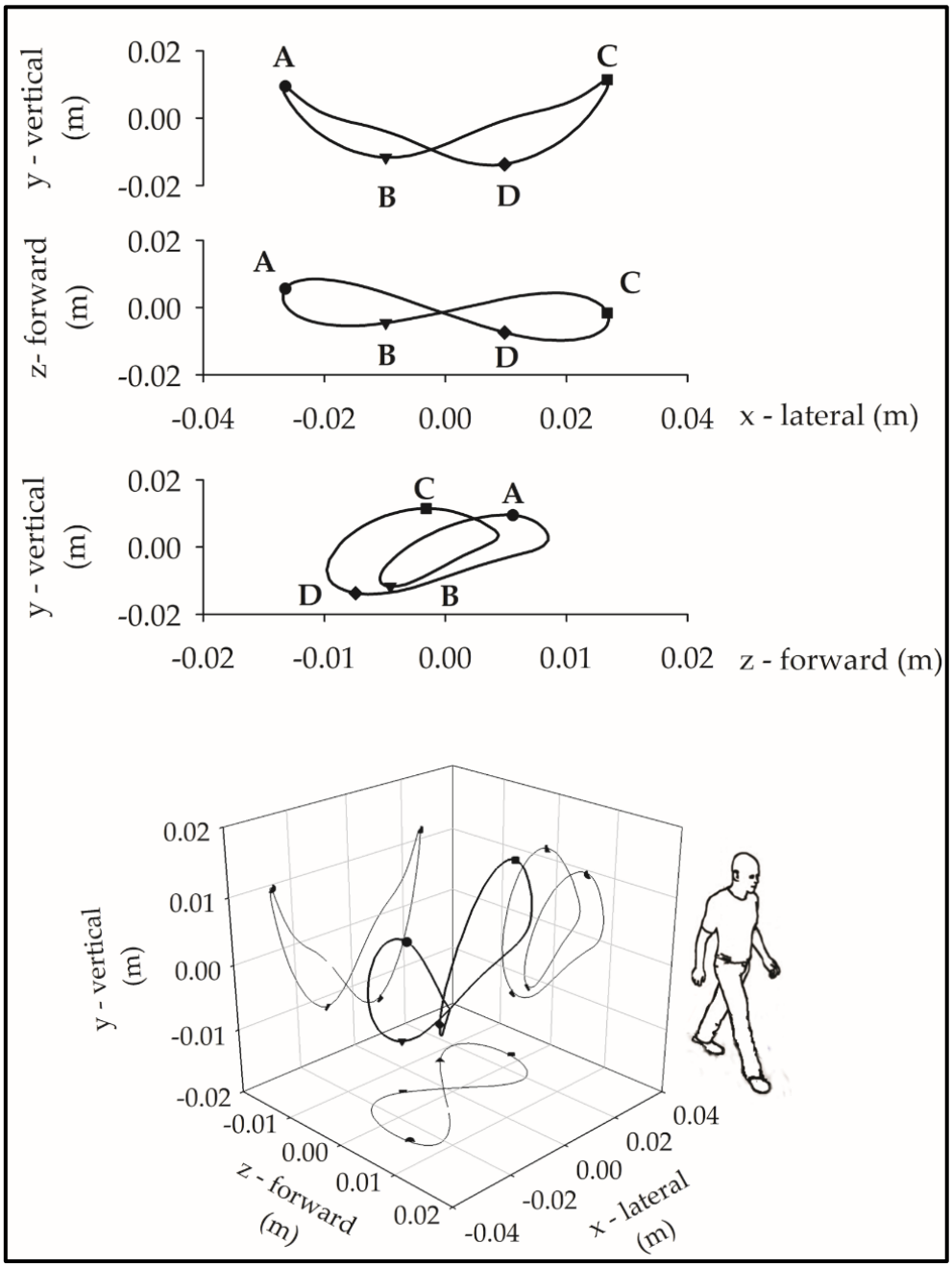

Figure 4.2. Curvature peaks along the CoM trajectory during one stride (mean of 20 strides in a representative subject; same data generating Figure 4.1B). From top to bottom, the upper three curves represent the y-x, z-x, and y-z planar projections of the CoM path, respectively (coordinates given in the bottom panel). The displacement due to the mean

forward velocity is subtracted. In the bottom graph, the black and grey curves refer to the 3D path of the CoM and its planar projections, respectively. Curvature peaks are labeled A to D, as in Figure 4.1, to facilitate the match among the curves given in Figures 4.1 and 4.2.

Curvature peaks as a potential clinical index of dynamic balance: reproducibility; dependence on stride duration

The reproducibility of the CoM curvature patterns can be appreciated in Figure 4.3. Curves from the 12 study participants (each curve is the mean across six strides) are superimposed on a shared x-axis giving the normalized stride period. Of note, the time course is very similar across the 12 subjects, although the peak values reveal two outliers - showing exceptionally high peaks. Besides, the changes in the curvatures look symmetric between the left and the right steps.

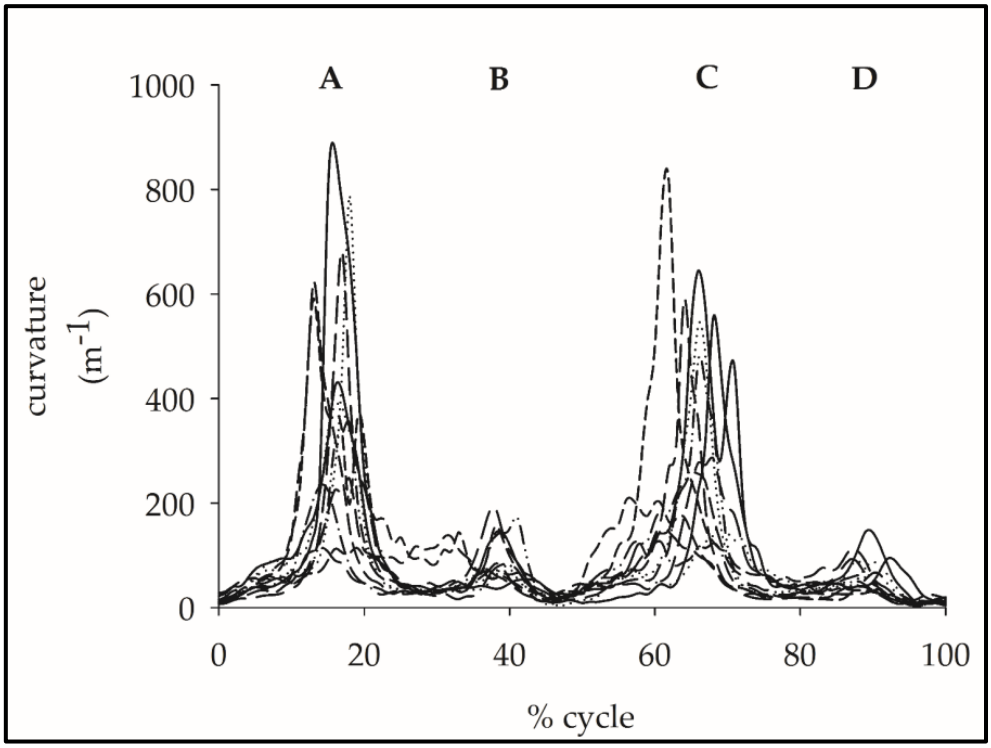

Figure 4.3. The curvature of the CoM path (m^{-1}, on the ordinate) during one stride on a force treadmill at 0.8 m s^{-1}, as a function of the normalized stride period (x-axis). The stride begins with the toe-off of the right foot. Curves (mean across six strides) from each of the 12 participants are superimposed and are marked by distinct tracts. Maxima of the curvature values are labeled A to D along the two subsequent right and left steps (see Figure 4.1).

Figure 4.4 shows that the CoM path's curvature maintains the same shape across increasing walking velocities, although peaks tend to be delayed with respect to the stride normalized cycles as the velocity increases.

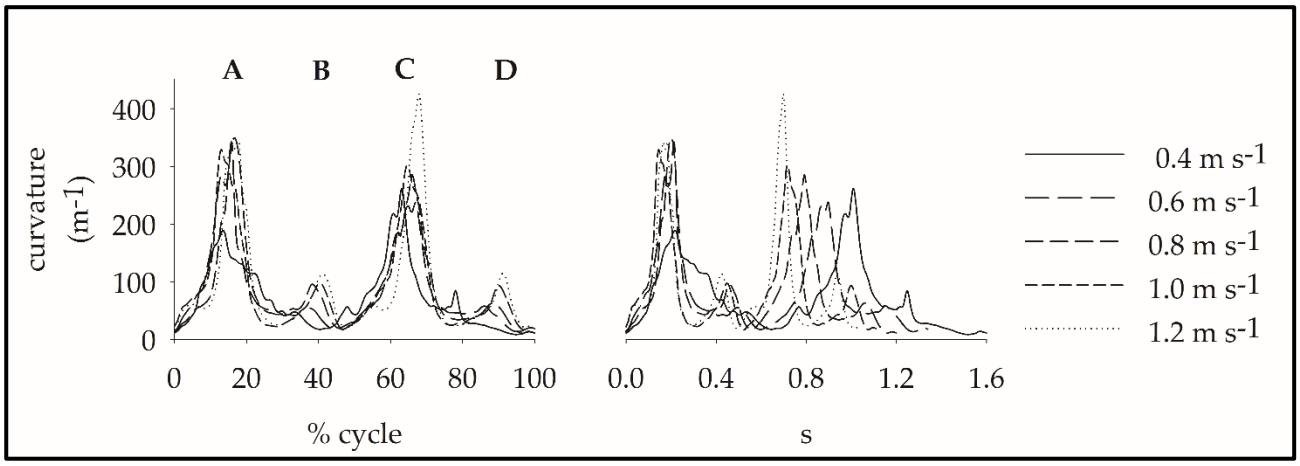

Figure 4.4. The curvature of the CoM path during one stride (mean across 72 observations, 12 subjects x 6 strides) at five different walking velocities (0.4 m s^{-1}, 0.6 m s^{-1}, 0.8 m s^{-1}, 1.0 m s^{-1}, and 1.2 m s^{-1}) as a function of the normalized stride period (x-axis) (left panel), and as a function of the absolute duration of the stride (right panel). Curves from the different walking velocities are marked by a different tract and superimposed. Peaks in the curvature values are labeled A to D along with the two subsequent steps (see Figure 4.1A for more details).

Figure 4.5A) to D) gives a graphic summary of the time delay of the curvature peaks with respect to the step initiation (onset of the single stance phase) at the different walking velocities tested. As expected, increasing walking velocities correspond to smaller step durations. All four peaks are progressively anticipated (and their time of occurrence becomes less variable) as the step period becomes shorter (A and B panels), but not enough to prevent a delay in terms of percentage of the step duration (C and D panels).

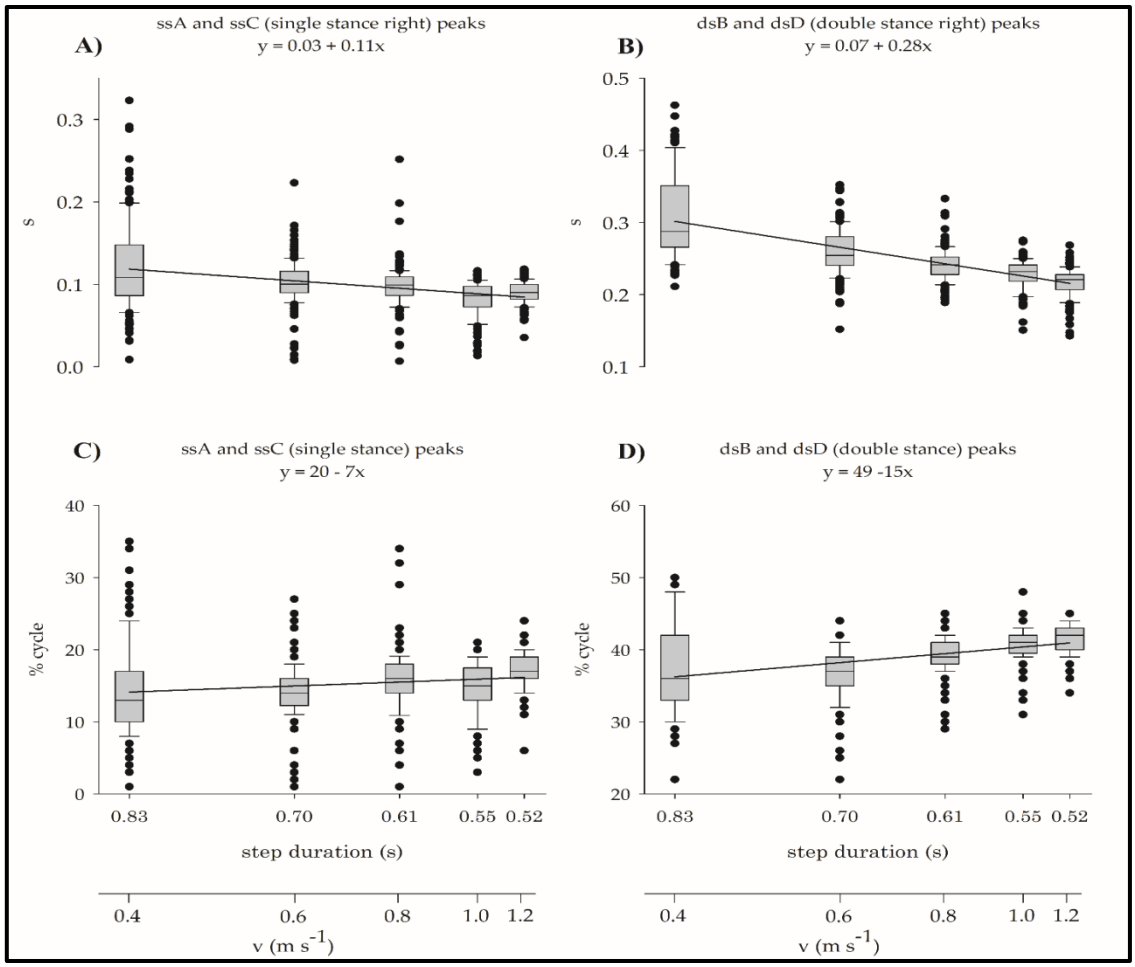

Figure 4.5. In panels A and B (upper row), the ordinate gives absolute time delay (s) of the peak curvature of the CoM with respect to step initiation (contralateral toe-off, or the initiation of single stance (see methods), both from left and right steps), whereas in panels C and D (lower row) the delay is given in percentage of the step duration. The upper and lower abscissa gives the step period (s) and the walking velocity (m s^{-1}), respectively. Each box plot refers to a distinct walking velocity and summarizes the results from 144 observations (12 subjects x 6 steps x 2 sides) at a given velocity. The horizontal segments under the boxes encase median values and 25^{th}-75^{th} percentiles; outliers are given as single black circles. Note that the step duration is lower, the higher the velocity. Left and right panels refer to single and double stance curvature peaks (ssA or ssC, and dsB or dsD), respectively. As a rough index of trend, a least square regression line is superimposed to boxes.

The symmetry between right and left curvature peaks (during both single and double stance) is analyzed in terms of right-left log-ratio of peak amplitudes in Figure 4.6. Results are given as a function of the mean amplitude of curvature peaks (Bland-Altman plot). This representation gives a graphic summary of the agreement between the single stance ssA (right) and ssC (left) peaks (panel A) and the double stance dsB (right) and dsD (left) peaks (panel B), also shown in Figures 4.3 and 4.4.

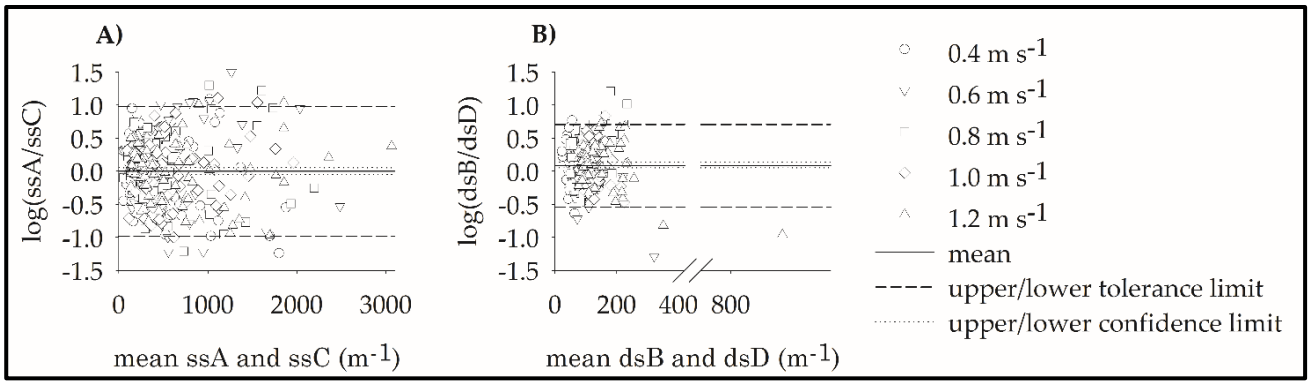

Figure 4.6. The plots show in the left panel (panel A) the logarithm of the ratio between the ssA and ssC curvature peaks amplitudes (y-axis) versus their mean (x-axis) and in the right panel (panel B) the logarithms of the ratio between the dsB and dsD curvature peaks amplitudes (y-axis) versus their mean (x-axis) (Bland-Altman plot). Solid lines report the mean of the $\log_{10}$ of the ratio between the curvature peaks amplitudes; dashed lines report the 95% tolerance limits, and dotted lines report the 95% confidence limits. Each symbol refers to the values recorded from six subsequent strides of each study participants (n = 12) at five walking velocities (0.4 m s^{-1}, 0.6 m s^{-1}, 0.8 m s^{-1}, 1.0 m s^{-1}, and 1.2 m s^{-1}). Distinct symbols represent the different walking velocities.

The figure highlights the substantial agreement between the ssA and ssC (left panel, panel A), and between the dsB to dsD (right panel, panel B) peaks. 19 out of 357 steps concerning the ssA and ssC peaks (expected by chance at $p<0.05$: 18 observations, panel A), and 11 out of 296 steps concerning the dsB and dsD peaks (expected by chance at $p<0.05$: 15 observations, panel B) trespass the tolerance limits. This suggests a substantial right-left symmetry.

Table 4.2 gives a numerical summary of the values represented in Figure 4.5 and 4.6.

	Curvature peaks (m^{-1}): mean (SD); medians (5^{th} ÷ 95^{th} percentiles)			
	Right step		Left step	
Gait velocities (m s^{-1})	ssA	dsB	ssC	dsD
0.4	365 (417); 227 (67 ÷ 1464)	132 (335); 53 (14 ÷ 890)	535 (671); 284 (59 ÷ 1895)	37 (24); 30 (9 ÷ 78)
0.6	548 (652); 326 (65 ÷ 1881)	82 (40); 70 (38 ÷ 143)	471 (627); 242 (78 ÷ 1594)	87 (78); 65 (38 ÷ 174)
0.8	551 (632); 344 (97 ÷ 1929)	125 (81); 93 (49 ÷ 301)	503 (605); 316 (85 ÷ 2117)	84 (47); 80 (30 ÷ 152)
1.0	593 (584); 386 (112 ÷ 2246)	124 (45); 114 (69 ÷ 215)	541 (451); 380 (101 ÷ 1670)	113 (50); 105 (50 ÷ 184)
1.2	659 (798); 324 (134 ÷ 2928)	150 (70); 126 (75 ÷ 308)	683 (684); 395 (93 ÷ 2221)	139 (187); 96 (54 ÷ 292)

Table 4.2. Curvature peaks occurring during the single (ss) and double (ds) stance phases on the right (ssA and dsB) and on the left (ssC and dsD) steps from 12 participants (6 strides each) walking at five different velocities: 0.4 m s^{-1}, 0.6 m s^{-1}, 0.8 m s^{-1}, 1.0 m s^{-1}, and 1.2 m s^{-1}, reported from top to bottom respectively). SD: standard deviation.

The large differences seen between means and medians on both steps (Table 4.2) were consistent with significant non-normality at the Shapiro-Wilk's tests, preventing parametric ANOVA modelling (not shown). The large differences seen between peaks occurring during the single and the double stance phases (Table 4.2) were significant after the Wilcoxon signed-rank test (Table 4.3). A non-parametric Friedman ANOVA model found significant differences in the curvature peaks between walking velocities. No significant differences were found in the interaction between the step phase (single vs double stance) and the walking velocity (Table 4.3). Interestingly, when contrasts between pairs of peaks were tested (Wilcoxon signed-rank test), no significant differences were found between peaks occurring during the right and left single stance phases (i.e., ssA vs ssC), while significant differences were found in all the other contrasts.

Wilcoxon signed-rank test	**p**			
Single *vs* double stance phase	0.00 w			
Friedman ANOVA model	**p**	**Kendall**		
Velocity	0.00 f	0.6137		
phase # velocity	0.06	0.1271		
Wilcoxon signed rank test	**p**			
Bonferroni corrected p-value	*0.005*			
	0.6 m s^{-1}	**0.8 m s^{-1}**	**1.0 m s^{-1}**	**1.2 m s^{-1}**
0.4 m s^{-1}	0.02 w	0.00 w	0.00 w	0.00 w
0.6 m s^{-1}		0.01 w	0.00 w	0.00 w
0.8 m s^{-1}			0.00 w	0.00 w
1.0 m s^{-1}				0.03 w
Bonferroni corrected p-value	*0.008*			
	B	**C**	**D**	
A	0.00 w	0.81	0.00 w	
B		0.00 w	0.00 w	
C			0.00 w	

Table 4.3. Results from the non-parametric Friedman ANOVA model on the curvature peaks occurring during the single and the double stance phases of the right and left step among the five different walking velocities. f : significant after Friedman ANOVA model; w: significant after Wilcoxon signed-rank test on contrasts between pairs of observations.

Discussion

The present study widens the observations made in a previous paper, which described for the first time the 3D trajectory of the CoM during walking [18]. That article highlighted the striking simultaneity of curvature peaks and transient annihilations of the pendulum-like mechanism during

the gait cycle, implying the sudden shift from passive oscillation to a fully active, muscle-driven control. The present article allows for some inferences on the underlying mechanics. The timing of the "external" power provided by muscles to keep the CoM in motion was already known for the sagittal plane [14]. The main injection of muscular power into the CoM motion takes place just before and during the first half of the double stance (when the CoM accelerates forward more than the concurrent fall allows), and it is mostly provided by the calf muscles of the rear limb. A 3-5 times lower injection of muscular power is required during single stance, again as a compensation for the incomplete exchange of mechanical energy (the CoM rises higher than what would be allowed by its former deceleration) [4]. The 3D trajectory of the CoM now allows a further interpretation of the CoM path from the standpoint of body balance, complementing the traditional "energetic" standpoint.

Motion on the frontal plane requires no more than 5% of the total external work spent during walking [12]. However, when balance is of concern, the relevance of CoM motion on the frontal plane emerges. During single stance, the lateral pendulum-like oscillation of the CoM towards the supporting side must be actively braked before the no-return position is reached, and then it must be actively braked while swinging back towards the suspended leg until the latter hits the ground. This refined mechanism implies a very precise dosage and sequencing between negative and/or positive work outputs from alternating muscles: for instance (just a matter of speculation), the hip adductors of the supporting limb and the contralateral paraspinal muscles might act as brakes on the CoM motion before the curvature peak is reached, and the hip abductors and the homolateral paraspinal muscles might be engaged as brakes after the peak is reached. This muscular sequence is imposing to an inverted pendulum, characterized by an arm more than 1 m long and a mass of several tenths of Kilograms, peak curvatures with radius in the order of 2 to 12 mm, within a limited time window of a few tenths of milliseconds. Precise mechanical modeling of this observation is far beyond the scope of the present article. Nevertheless, the U-turn of the CoM seems quite an impressive performance of neural control, hardly detectable by visual inspection. Consider that the shorter the step period, the faster the maneuver must be in the attempt to keep the U-turn event safely far from the no-return point (see Figure 4.5). During the double stance, minor curvatures are observed. On the other hand, there is no more need for a U-turn on a single limb, given that the opposite leg is also on the ground and ready to be loaded. By contrast, in this phase of the stride, strong positive power output is needed from the rear limb to accelerate forward and upward the CoM.

The "energetic" parameters of CoM motion (e.g., energy changes, external work and power, R) are known to be highly symmetric between the left and the right steps [8,15]. The same seems to hold, at a group level, for the CoM curvature at all the walking velocities here tested. However, the variability within and between the subjects both for curvature values and their right/left log-ratios (Table 4.2 and Figure 4.6, respectively) is higher than that observed for energetic parameters of the CoM motion in the sagittal plane (compare present data with data from [8,15]). The variance was much higher for the work done to move the CoM in the frontal plane compared to the sagittal plane (see Figure 4.3 in Ref [8]). One reason might be the intrinsic limits of precision of the method: measures of punctiform curvature peaks, based on angle derivatives, are inherently more noise-sensitive than energy estimates coming from double integration of forces.

Furthermore, this high variability might be intrinsic to the phenomenon. The size of both the allowed time windows and the required energy changes for the frontal redirection of the CoM is much smaller than those characterizing the CoM motion in the sagittal plane. Therefore, minor changes represent large relative variations. In other words, the precision of neuromotor control may impose a limit to the reproducibility of the peak curvatures within and between subjects.

In conclusion, the curvature peaks seen during the single stance (ssA and ssC peaks in Figures 4.1 to 4.4) seem a valid index of the mechanism underlying the xCoM, which is, in turn, a major determinant (together with the step width) of the maintenance of safe margins of stability (MOS) during the step. The xCoM and the MOS, however, describe the end result of joint mechanics and adaptive behaviors. By contrast, the curvature peaks shed light on the underlying neural control of the lateral oscillations of the CoM. In doing so, they seem to provide both some hints for deeper biomechanical and neurophysiologic studies and an index of dynamic balance complementing the existing ones.

5. Experimental study: limping on split-belt treadmills implies opposite kinematic and dynamic lower limb asymmetries[27]

Walking on a split-belt treadmill (each of the two belts running at different velocities) has been proposed as an experimental paradigm to investigate the flexibility of the neural control of gait and as a form of therapeutic exercise. However, the scarcity of dynamic investigations challenges the validity of the available findings. Therefore, the present study aimed at investigating the dynamic asymmetries of lower limbs of healthy adults during adaptation to walking on a split-belt treadmill. Ten healthy adults walked on a split-belt treadmill mounted on force sensors, with belts running either at the same speed ('tied' condition) or at different speeds ('split' condition, 0.4 vs 0.8 or 0.8 vs 1.2 m s^{-1}). The sagittal power and work provided by ankle, knee and hip joints, joint rotations, muscle lengthening, and surface electromyography were recorded simultaneously. Various tied/split walking sequences were requested.

Introduction

After a pioneering work by Dietz et al. [32], and thanks to an influential paper by Reisman et al. [33], the scientific literature paid growing attention to the effects of walking on a split-belt treadmill (hereafter 'split-gait'). The instrument consists of two independent belts able to rotate at different speeds. This imposes an asymmetrical gait, mimicking limping observed in various pathologic conditions. Healthy individuals and stroke [83], Parkinson's [84], and cerebellar [37] patients were studied. In stroke patients, split gait has been widely tested as a form of therapeutic exercise. The rationale is based on the observation that in hemiparetic patients, the paretic (as a rule: anterior) step is longer than the opposite one. In split gait, this asymmetry is emphasized by placing the paretic limb on the slower belt, although in various research protocols, the opposite arrangement was also tested [37,85–87]. When the belts are brought back to the same speed ("tied" condition) an after-effect occurs, entailing a more symmetric step length. In a unique paper, this was shown to last up to a month if repeated sessions are applied [36]. Some hypotheses were advanced on the differential control and storage of intra-limb and interlimb parameters, the potential cerebellar localization of the corresponding neural circuits [33,37,83,87], and the distorted perceptions of average single-limb speed during split gait [85,86,88,89].

Nevertheless, the absence of dynamic considerations challenges the validity of the above-cited neurologic speculations. In most unilateral impairments, kinematic symmetry is compatible with hidden dynamic asymmetries between the lower limbs and between the energy changes of the body CoM between subsequent steps [9,13,15,41].

Although split-belt walking has been claimed to be effective in decreasing step length asymmetry [90,91], to the authors' knowledge, only two research groups have reported that split gait is able to impose asymmetric production of work from the lower limbs [85,86,92]. In the present study, these preliminary observations were examined more systematically, and the differential effects of split gait on lower limb kinematics and dynamics were clarified.

Experimental methods

Participants

Ten healthy voluntary adults were enrolled. The inclusion criteria were: (i) ability to wittingly sign the informed consent form; (ii) ability to understand the instructions and to complete the locomotor task; (iii) age between 18 and 60 years; (iv) absence of neurologic or orthopedic conditions affecting walking. Patients were excluded if they had received surgical orthopedic interventions in the 18 months before the study and had joint diseases (any forms of arthritis, joint laxity, joint replacement), symptomatic spine diseases, and previous experience of walking on split-belt treadmills. Participants were tested for their foot dominance by means of the Waterloo footedness questionnaire-revised [39].

Participants' preparation

Participants were prepared according to the procedure described in Chapter 2. Moreover four sEMG probes (Free EMG; BTS Bioengineering Spa) were positioned, bilaterally, on the skin covering the bellies of Tibialis Anterior (TA), Gastrocnemius Lateralis (GaLat), Vastus Medialis (VaMed), and Semi-Membranosus (SM) as per the SENIAM guidelines[93]. Sample frequency was set at 1 kHz. The sEMG signals were off-line rectified (time constant: 0.08 s) and filtered (bandpass Hamming filter: 10-450 Hz).

Tagging walking patterns

Walking modality refers to walking on belts running either at the same speed (tied modality) or at different speeds (split modality). Walking condition indicates a specific combination of velocities of each belt. A four-number tag without decimals was assigned to each combination of walking speed and belt speed asymmetry. The first two numbers referred to the speed of the belt running under the non-dominant limb. The next two numbers referred to the speed of the other belt. For example, the tag 0408 labeled a walking trial where the belt under the non-dominant and the dominant lower limbs ran at 0.4 m s^{-1} and 0.8 m s^{-1}, respectively (split modality, 0408 condition).

Sequence and timing of gait conditions

The gait was analyzed using a split-belt force-sensorized treadmill embedded in the floor. Lower limb joint angles, power, muscle length, and sEMG were synchronously recorded. (see Chapter 2 for details). Table 5.1 shows the experimental timeline. During the baseline phase, participants were asked to walk in tied condition (belts running at the same speed) from 0.2 to 1.2 m s^{-1} at increasing speeds (in 0.2 m s^{-1} steps). Speed increments were applied every 30 s after a verbal warning. Changes in the average belt speed were completed gradually in 3–5 s. After a 2-min pause, the first adaptation test began. This included a tied condition, a split condition, and a post-split tied condition. Participants walked 30 s at 0404. Then, they had to walk for 3min at 0408, i.e. with the dominant lower limb on the faster belt, and again for 30 s at 0404. After another 2-minute pause, the second adaptation test began. The tied-split-tied sequence was repeated at higher speeds (0808, 0812, and 0808, respectively).

BASELINE		**ADAPTATION 1**				**ADAPTATION 2**		
		Tied 0404	Split 0408	Post-split tied 0404		Tied 0808	Split 0812	Post-split tied 0808
from 0.2 m s^{-1} to 1.2 m s^{-1} in 0.2 m s^{-1} increments every 30 s		0.4 m s^{-1}	0.4-0.8 m s^{-1}	0.4 m s^{-1}		0.8 m s^{-1}	0.8-1.2 m s^{-1}	0.8 m s^{-1}
180 s	120 s	30 s	180 s	30 s	120 s	30 s	180 s	30 s

Tab. 5.1. Experimental sequence and timing of walking conditions.

Data Analysis

The data were analyzed as previously described in Chapter 2. Moreover for each muscle, amplitudes were standardized as percentages of the maximum voltage recorded from that muscle across all of the recorded strides.

The length changes in GaLat, Rectus Femoris, and Semi-Membranosus were estimated from joint kinematics using an anthropometric model implemented in the SMART Software Suite (BTS Bioengineering Spa) and expressed as a percentage of the muscle length estimated at rest in the supine position.

Statistics

A sample size of 10 was considered sufficient for a reliable estimate of all the recorded parameters, given the very high reproducibility allowed within participants across subsequent steps [2,25,44]. Reproducibility is fostered by the known and constant average speed imposed by the treadmill, as confirmed by previous articles. The Shapiro–Wilk's test was used to assess the normality of the distribution of spatiotemporal, kinematic, and dynamic variables. Descriptive summaries were given as ranges (for age, only) and mean (SD). All variables were compared between the two sides using a paired Student's t-test or a non-parametric Wilcoxon signed-rank test in case of non-normality. The dominant/non-dominant side ratio (linearized through log-odd transformation [15]) was computed for the continuous variables. The faster/slower side ratios in the split modality with the dominant/non-dominant side ratio in the tied modality were compared using repeated analysis of variance (ANOVA) model (non-parametric Friedman ANOVA in case of non-normality). The contrasted tied modality was the one in which speed (a) matched either the faster or the slower speed between the split-belts, or (b) was the average between the two belt speeds. In the case of significant ANOVA models, Tukey's (or the Wilcoxon signed-rank test in case of non-normality) post-hoc tests were run on contrasts between pairs of conditions. The difference in side ratios was also tested between the two split conditions (i.e., 0408 vs 0812). Significance was set at $p < 0.05$. The Benjamini–Hochberg "false discovery rate" correction for multiplicity was adopted [42] whenever appropriate.

Results

Demographic and anthropometric information of the participants is presented in Table 5.2.

Gender, n (men/women)	5/5
Age, years (mean (SD))	26.10 (2.81)
Range	22 – 30
Height, m (mean (SD))	1.71 (0.12)
Weight, kg (mean (SD))	63.67 (11.13)
Dominant side (right/left), n	8/2

Table 5.2. Demographic and anthropometric parameters of the 10 participants.

Figure 5.1 graphically represents the mean values of the various spatiotemporal gait parameters as a function of the belt velocity combinations.

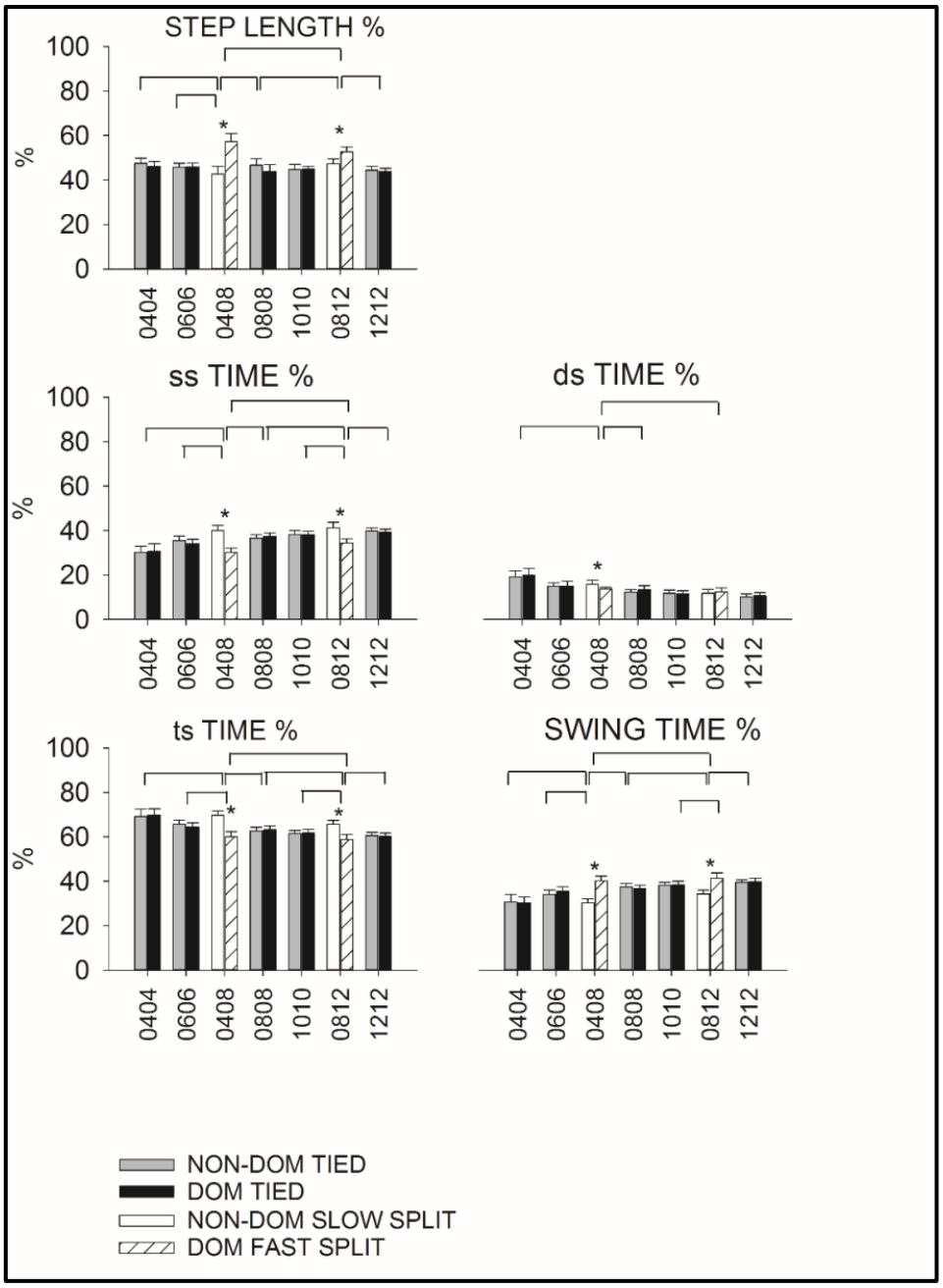

Figure 5.1. Spatiotemporal gait parameters. From top to bottom, the panels refer to spatiotemporal gait parameters indicated by the labels (ss TIME: single stance time, ds TIME: double stance time, ts TIME: total stance time).

Pairs of bars are provided for each combination of belt speeds given on the abscissa. The bars give the grand-mean (+ SD) across six subsequent strides performed by 10 subjects for each parameter. The grey and black bars refer to the non-dominant and the dominant side, respectively, in tied conditions. The white and the dashed bars refer to the same sides, becoming the slower and the faster sides in split conditions.

*: statistically significant (at $p<0.05$) pairwise comparisons between lower limb sides on the same gait condition.: statistically significant comparisons of faster/slower side ratios (linearized through log-odd transformation) in the split conditions with respect to the dominant/non-dominant side ratios in the tied conditions (i.e. 0408 vs 0404, 0606 and 0808; and 0812 vs 0808, 1010 and 1212), and between the two split conditions (i.e. 0408 vs 0812).

Numeric values [mean (SD)] are reported in Table 5.3.

Spatio temporal gait parameters	Step Length		Single Stance Time		Double Stance Time		Total Stance Time		Swing Time	
	slow (non-dom)	fast (dom)	slow (non-dom)	fast (dom)	slow (non-dom)	fast (dom)	slow (non-dom)	fast (dom)	slow (non-dom)	fast (dom)
0404	47.55 (2.29)	46.03 (2.24)	30.27 (2.75)	30.81 (3.26)	19.13 (2.81)	19.91 (3.17)	69.15 (3.31)	69.90 (2.60)	30.79 (3.29)	30.29 (2.77)
0606	45.73 (1.85)	45.90 (1.81)	35.51 (2.06)	34.20 (1.99)	15.07 (1.52)	15.14 (2.25)	65.66 (1.94)	64.39 (1.89)	34.24 (1.91)	35.47 (2.12)
0408	42.66 (3.61)	57.34 (3.61)	40.09 (2.26)	30.27 (1.98)	15.84 (1.88)	13.82 (0.78)	69.68 (1.94)	60.05 (2.34)	30.24 (1.98)	40.12 (2.19)
0808	46.65 (3.07)	43.73 (3.12)	36.64 (1.63)	37.45 (1.67)	12.33 (1.09)	13.48 (1.79)	62.64 (1.65)	63.16 (1.74)	37.43 (1.59)	36.66 (1.59)
1010	44.72 (2.27)	44.98 (1.25)	38.22 (1.77)	38.27 (1.36)	11.78 (1.55)	11.57 (1.35)	61.54 (1.32)	61.66 (1.61)	38.16 (1.43)	38.32 (1.72)
0812	47.29 (2.17)	52.71 (2.17)	41.28 (2.42)	34.44 (1.85)	11.81 (1.83)	12.42 (1.81)	65.64 (1.74)	58.70 (2.29)	34.39 (1.79)	41.35 (2.40)
1212	44.43 (1.81)	43.82 (1.34)	39.84 (1.49)	39.40 (1.35)	10.23 (1.26)	10.69 (1.44)	60.60 (1.44)	60.24 (1.44)	39.46 (1.25)	39.78 (1.53)

Table 5.3. Grand-mean (SD) of spatiotemporal gait parameters across six subsequent strides performed by 10 healthy subjects walking on the split-belt treadmill at different gait modalities and speed conditions. The dominant lower limb is labeled "fast (dom)" since it was placed on the faster belt during the split modality. The non-dominant lower limb is labeled "slow (non-dom)" since it was placed on the slower belt during the split modality.

In "tied" conditions, no significant mechanical differences emerged between steps on opposite sides. For all parameters, a difference between sides could be detected in both split conditions (i.e., 0408 and 0812), except for the double-stance time (side named after the posterior foot) in the 0812 split condition. The split conditions implied that, on the faster side, step length (side named after the posterior foot) and swing time were longer, whereas single-stance and double-stance (hence, total stance) time were shorter compared with the slower side. For all parameters, the faster/slower side ratios (log-transformed; see Methods) were statistically different between the two split conditions (i.e., 0408 vs 0812) as reported in Table 5.4.

The faster/slower side ratio of step length, single stance time, total stance time, and swing time showed significant differences in all the comparisons between gait conditions. Significance was missed only for the 0812/1010 comparison of step length (Tables 5.5 and 5.6).

Side ratios (log odds)	Step Length	Single Stance Time	Double Stance Time	Total Stance Time	Swing Time	Ankle		Knee		Hip	
						Peak Power	Work	Peak Power	Work	Peak Power	Work
R^2	0.81	0.83	0.85	0.77	0.83	0.80	0.87	0.91	0.94	0.80	0.78
p	0.00*	0.00*	0.00*	0.04*	0.00*	0.00*	0.00*	0.48	0.84	0.02*	0.07

Table 5.4. Results from repeated ANOVA model between faster/slower side ratios (linearized through log-odd transformation) in the two split conditions (i.e., 0408 vs 0812).

*: Significant after false discovery rate correction.

Side ratios (log odds)		Step Length	Single Stance Time	Double Stance Time	Total Stance Time	Swing Time	Ankle		Knee		Hip	
							Peak Power	Work	Peak Power	Work	Peak Power	Work
R^2		0.86	0.87	0.69	0.88	0.87	0.90	0.93	0.69	0.19	n.a.	0.68
p		0.00 [a]	0.00 [a]	0.00 [a]	0.00 [a]	0.00 [a]	0.00 [a]	0.00 [a]	0.25	0.65	0.02 [f]	0.03 [a]
Post-hoc test over (Gait modalities), *p* values												
0404	***vs***	0.91	0.42	0.90	0.31	0.48	0.97	0.98	n.a.	n.a.	0.78	0.83
0606												
0404	***vs***	0.93	0.89	0.85	0.96	0.90	0.85	1.00	n.a.	n.a.	0.77	0.95
0808												
0404	***vs***	0.00 [t]	0.00 [t]	0.02 [t]	0.00 [t]	0.00 [t]	0.00 [t]	0.00 [t]	n.a.	n.a.	0.86	0.21
0408												
0606	***vs***	0.59	0.14	0.46	0.15	0.18	0.98	0.95	n.a.	n.a.	0.78	0.54
0808												
0606	***vs***	0.00 [t]	0.00 [t]	0.14	0.00 [t]	0.00 [t]	0.00 [t]	0.00 [t]	n.a.	n.a.	0.16	0.71
0408												
0808	***vs***	0.00 [t]	0.00 [t]	0.00 [t]	0.00 [t]	0.00 [t]	0.00 [t]	0.00 [t]	n.a.	n.a.	0.28	0.07
0408												

Table 5.5. Results from repeated ANOVA model (Friedman ANOVA in case of non-normality) among faster/slower side ratios (linearized through log-odd transformation) in the 0408 split condition with dominant/non-dominant side ratios in the 0404, 0606 and 0808 tied conditions. False discovery rate correction was applied.

[a]: Significant after repeated ANOVA model; [f]: Significant after Friedman ANOVA model; [t]: Significant after Tukey's post-hoc test; [w]: Significant after Mann-Whitney U post-hoc test; n.a.: not applicable; ANOVA model p = non-significant

Side ratios (log odds)		Step Length	Single Stance Time	Double Stance Time	Total Stance Time	Swing Time	Ankle		Knee		Hip	
							Peak Power	Work	Peak Power	Work	Peak Power	Work
R^2		0.80	0.82	0.53	0.86	0.83	0.85	0.84	0.62	0.66	0.42	n.a.
P		0.00 [a]	0.00 [a]	0.49	0.00 [a]	0.00 [a]	0.00 [a]	0.00 [a]	0.96	0.37	0.77	0.03 [f]
Post-hoc test between walking modalities, p-values												
0808	***vs***	0.35	0.87	n.a.	1.00	0.77	0.99	1.00	n.a.	n.a.	n.a.	0.59
1010												
0808	***vs***	0.63	0.61	n.a.	0.96	0.67	0.87	1.00	n.a.	n.a.	n.a.	0.21
1212												
0808	***vs***	0.00 [t]	0.00 [t]	n.a.	0.00 [t]	0.00 [t]	0.22	0.00 [t]	n.a.	n.a.	n.a.	0.24
0812												
1010	***vs***	0.97	0.97	n.a.	0.96	1.00	0.96	0.99	n.a.	n.a.	n.a.	0.59
1212												
1010	***vs***	0.10	0.00 [t]	n.a.	0.00 [t]	0.00 [t]	0.15	0.00 [t]	n.a.	n.a.	n.a.	0.21
0812												
1212	***vs***	0.04 [t]	0.00 [t]	n.a.	0.00 [t]	0.00 [t]	0.06 [t]	0.00 [t]	n.a.	n.a.	n.a.	0.14
0812												

Table 5.6. Results from repeated ANOVA model (Friedman ANOVA in case of non-normality) among faster/slower side ratios (linearized through log-odd transformation) in the 0812 split condition with dominant/non-dominant side ratios in the 0808, 1010 and 1212 tied conditions. The false discovery rate correction for multiplicity was applied.

[a]: Significant after repeated ANOVA model; [f]: Significant after Friedman ANOVA model; [t]: Significant after Tukey's post-hoc test; [w]: Significant after Mann-Whitney U post-hoc test; n.a.: not applicable; ANOVA model p = non-significant

Figure 5.2 shows the kinematic, dynamic, and sEMG changes during a stride in the 0408 split condition and in tied conditions (0404, 0606, and 0808, respectively). Results show that the values of all parameters are barely distinguishable between the two sides in the tied conditions. Ankle plantar flexors provided most of the propulsive power required during the stride[25,44], as expected. This occurred just before and during the double stance of the corresponding step. A speed-dependent increase in kinematic and dynamic values and a decrease in ground contact time and relative phase duration were also evidenced.

The effect of split gait can be appreciated by comparing the split condition 0408 with the tied conditions. The shifting from the tied to the split condition induced a marked asymmetry between the parameters recorded from each of the two lower limbs, in particular from the ankle joint (Fig. 5.2, leftmost columns of each panel).

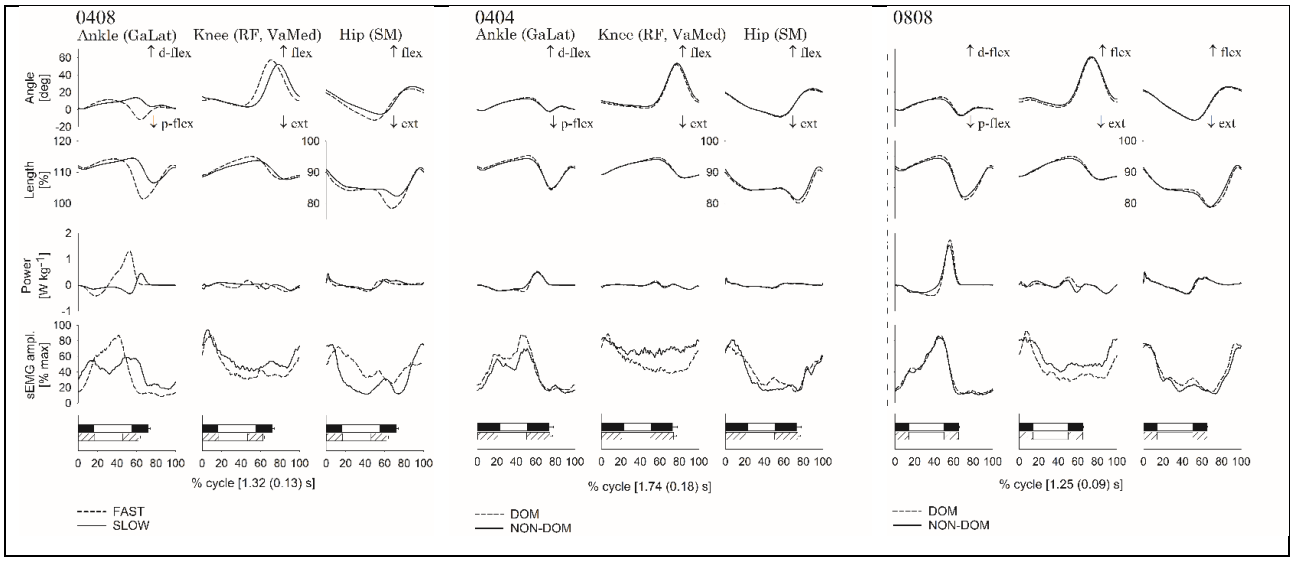

Fig 5.2. Kinematic, dynamic, and sEMG changes of joint parameters (on the ordinate) as a function of normalized stride time (on the abscissa, absolute mean duration within brackets) during walking on the force treadmill with belts running at 0.4 m s^{-1} and 0.8 m s^{-1} (0408 split condition, panel on the left), with both belts tied at 0.4 m s^{-1} (0404 tied condition, the panel in the middle), and at 0.8 m s^{-1} (0808 tied condition, the panel on the right). In each panel, the labels above the uppermost panel indicate the joint (ankle, knee, and hip from left to right, respectively) and the muscle (within brackets) analyzed in each column. From top to bottom, the rows show the sagittal joint rotations, the changes in muscle length, the joint sagittal power, and the sEMG signal. The curves show the grand-mean of data recorded from 6 subsequent strides performed by 10 healthy adults. The horizontal bottom bars show the single (dashed or filled background) and the double stance (white background) time. The "whiskers" give the total stance time SD. The dashed lines and bar segments refer to the dominant "dom" (fast in split gait) lower limb, the continuous lines and the filled bar segments refer to the non-dominant "non-dom"(slow in split gait) lower limb.

On the faster belt, the ankle rotation (negative values indicate plantar-flexed position) ranged from −12.7° to 11.8° versus 0.0° to 14.4° for the slower side. These ranges were superimposable to those found at the corresponding speeds in tied conditions: −8.2° to 14.6° and − 4.1° to 13.7° in 0808 and 0404 conditions, respectively.

On the slower side, by contrast, the ankle never reached a plantar-flexed position. Joint excursions were paralleled by changes in the GaLat muscle's elongation (second row from the top in each panel).

The ankle joint on the faster belt provided a much higher and earlier peak of plantar flexor power compared with the opposite joint and with an earlier onset. Ankle power was generated from 31 to 84% of the gait cycle on the faster belt versus 59 to 86% of the slower belt.

Interestingly, on both sides, the generation of power was preceded by a phase of power absorption. On the faster side, the negative power reached a higher peak, appeared earlier, and had a lower

duration compared with the slower side. This was paralleled by the larger lengthening–shortening cycle of the plantar flexor muscles and by a sEMG signal of higher duration. It is worth noting that the shape of sEMG during the split condition can be compared to the sEMG during the tied conditions at 0404 and 0808. At visual inspection, the shape of GaLat sEMG curve of the slow limb at 0408 is similar to 0404, while that of the fast limb recalls the one of 0808.

In Fig. 5.2, in each panel, the second and the third columns from left replicate the information given for the ankle with respect to the knee and hip joints, respectively. It can be noted that the split gait modality entailed much smaller asymmetries, compared with the ankle joint, for all the recorded parameters.

All of the above considerations also apply to 0812 and to its comparison with the tied conditions replicating the speed of either belt (0808 and 1212) or in their average speed (1010). For ankle joint rotation, (figure not-shown) the lower limb on the fast belt had a joint rotation range equal to 27.7° (5.7°), similar to that of the lower limbs moving with both belts tied at 1.2 m s^{-1} [24.8° (3.2°)], whereas the ankle joint on the slow belt had a rotation equal to 17.5° (2.7)°, resembling that of the lower limbs moving with both belts tied at slow speed [20.5° (3.4°)].

Peak power generated from the fast lower limb was greater than that from the slow lower limb [2.9 (0.3) vs 1.9 (0.6) W kg^{-1}]. Moreover, it was lower than that generated in 1212 [3.3 (0.5) W kg^{-1}], whereas it was more similar to that generated in 1010 [2.6 (0.3) W kg^{-1}]. In 0812, the ankle joint power generation lasted from 31 to 85% of the gait cycle of the fast lower limb and from 52 to 88% of the gait cycle of the slow lower limb.

It is worth noting that higher asymmetries were observed in 0408 compared with 0812. Analogous to the case of spatiotemporal parameters, the faster/slower speed ratio (here, 2:1 vs 1.5:1) between the two belts seemed more effective than speed difference in causing dynamic asymmetries.

In Fig. 5.3, a 3D representation of the ankle joint power as a function of the normalized stride time and of the walking conditions is reported.

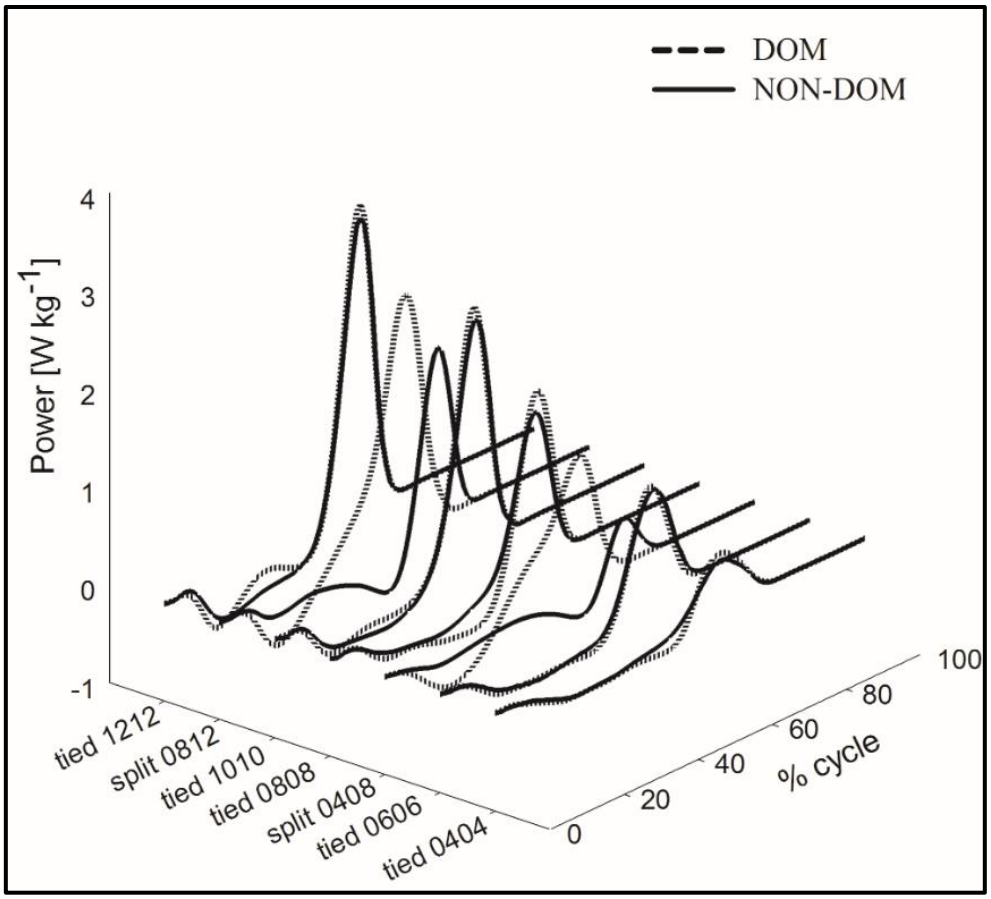

Fig. 5.3. Ankle power in the sagittal plane (ordinate) as a function of both the standardized stride time (right abscissa) and the belt speed combinations (walking conditions, left abscissa). The dashed and the continuous lines refer to the dominant and non-dominant side, respectively, becoming the faster and the slower side in the split gait modality, respectively.

This representation highlights that on the faster belt (dominant lower limb, dashed curves), power was generated in an earlier phase and for a longer relative duration compared with both the slower side and the tied conditions.

A summary of dynamic findings is shown in Fig. 5.4.

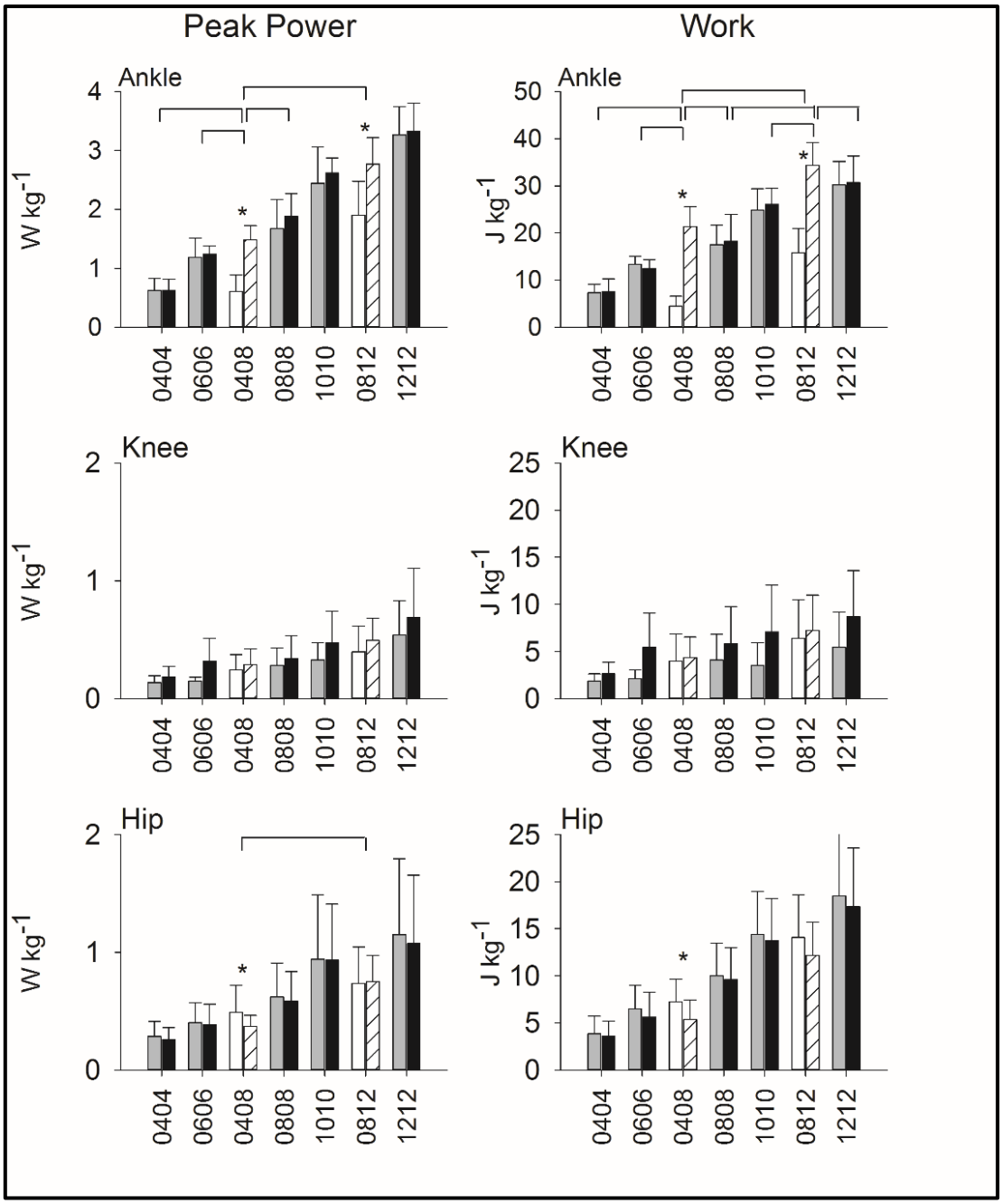

Fig.5.4. Dynamic gait parameters. From top to bottom, the panels refer to dynamic gait parameters of the ankle, knee and hip joints. The left and right columns refer to peak power and work, respectively. Note the different graphic scaling for the ankle, compared to both the knee and the hip. Other indications as in Figure 4.3.1.

Numeric values [mean (SD)] are shown in Table 5.7. The figure highlights and complements the pattern shown in Fig. 5.4, contributing quantitative evidence.

As expected, higher values of peak power were observed with increasing average speeds. The ankle provided a peak power 5.56 and 2.80 times higher compared with knee and hip, respectively, in tied conditions, in agreement with a previous study [25,44].

Both interlimb asymmetries and interaction with belt velocity combinations emerged.

Dynamic gait parameters	Ankle				Knee				Hip			
	Peak Power ($W\ kg^{-1}$)		Work ($J\ kg^{-1}$)		Peak Power ($W\ kg^{-1}$)		Work ($J\ kg^{-1}$)		Peak Power ($W\ kg^{-1}$)		Work ($J\ kg^{-1}$)	
	slow (non-dom)	fast (dom)	slow (non-dom)	fast (dom)	slow (non-dom)	fast (dom)	slow (non-dom)	fast (dom)	slow (non-dom)	fast (dom)	slow (non-dom)	fast (dom)
0404	0.62 (0.20)	0.62 (0.19)	7.30 (1.84)	7.49 (2.76)	0.14 (0.06)	0.19 (0.09)	1.86 (0.76)	2.63 (1.24)	0.29 (0.13)	0.26 (0.10)	3.85 (1.87)	3.59 (1.61)
0606	1.19 (0.32)	1.24 (0.14)	13.32 (1.73)	12.45 (1.91)	0.15 (0.03)	0.32 (0.19)	2.10 (0.95)	5.43 (3.67)	0.40 (0.17)	0.39 (0.17)	6.49 (2.49)	5.63 (2.61)
0408	0.60 (0.28)	1.49 (0.24)	4.43 (2.13)	21.34 (4.22)	0.24 (0.13)	0.29 (0.13)	3.99 (2.86)	4.33 (2.21)	0.49 (0.23)	0.37 (0.09)	7.23 (2.41)	5.36 (2.09)
0808	1.67 (0.50)	1.88 (0.38)	17.51 (4.12)	18.27 (5.68)	0.28 (0.15)	0.34 (0.19)	4.08 (2.74)	5.82 (3.95)	0.62 (0.29)	0.59 (0.25)	10.01 (3.44)	9.59 (3.39)
1010	2.45 (0.62)	2.62 (0.26)	24.83 (4.56)	26.06 (3.39)	0.33 (0.15)	0.47 (0.27)	3.55 (2.41)	7.07 (4.98)	0.94 (0.54)	0.93 (0.48)	14.41 (4.56)	13.75 (4.43)
0812	1.90 (0.58)	2.77 (0.45)	15.81 (5.08)	34.33 (4.85)	0.40 (0.22)	0.49 (0.19)	6.41 (4.08)	7.24 (3.75)	0.74 (0.31)	0.75 (0.22)	14.06 (4.56)	12.15 (3.55)
1212	3.26 (0.48)	3.33 (0.47)	30.23 (4.94)	30.69 (5.65)	0.54 (0.29)	0.69 (0.42)	5.46 (3.74)	8.69 (4.90)	1.15 (0.65)	1.07 (0.58)	18.48 (7.24)	17.32 (6.23)

Table 5.7. Grand-mean (SD) of dynamic gait parameters across six subsequent strides performed by 10 healthy subjects walking on the split-belt treadmill at different gait modalities and speed conditions. The dominant lower limb is labeled "fast (dom)" since it was placed on the faster belt during the split modality. The non-dominant lower limb is labeled "slow (non-dom)" since it was placed on the slower belt during the split modality.

Interlimb asymmetries

In the split conditions, higher peak power was provided at ankle and knee joints on the faster side compared with the slower side. Significance was missed for the knee (both 0408 and 0812). The split conditions implied a faster/slower side ratio of ankle peak power greater than the dominant/non-dominant ratios in tied conditions (Tables 5.5 and 5.6).

Only at the ankle, split walking entailed greater asymmetries for work than for power ($p=0.01$ for both split conditions; compare left and right upper panels of Fig. 5.4). This is consistent with the higher, anticipated, and prolonged power generation on the faster side (Figs 5.2).

Differences between walking modalities

Compared with the corresponding average tied speeds (i.e., 0606 vs 0408, and 1010 vs 0812), power and work were higher on the faster side and lower on the slower side (uppermost row histograms in Fig. 5.4, also see Fig. 5.2). Peak power was lower on the faster side (0408 vs 0808) and unchanged on the slower side (0408 vs 0404) with respect to the corresponding tied speeds. At variance with power, work was lower for the slower side and higher for the faster side.

Discussion

From the current study, split gait emerges as a unique paradigm of locomotion, not amenable to the familiar form of pathologic claudication known as escape limp. In a limping gait on firm ground, the affected leg 'escapes' from load, minimizing the stance time, whereas in split gait the faster leg 'escapes' from being dragged backwards with respect to the slower leg. This effort requires extra muscular work. In this effort, intrinsic muscle properties seem to be of some help. During human walking, elastic energy is stored in the calf muscle-tendon complex during ankle dorsal flexion and released during the subsequent shortening [94]. This mechanism is stronger, the faster the gait speed. The hypothesis of an effective elastic loading of the ankle on the faster side is consistent with the negative power phase, the muscle lengthening, and the sEMG tracings shown in Figs 5.2. In short, the split-belt treadmill induced mechanical asymmetries in healthy individuals between the subsequent steps that mimic the natural-pathologic escape limp only in its temporal step parameters, but neither for the spatial or for the dynamic ones, which are the focus of the present study.

The present results are consistent with published kinematic [33] and dynamic data [85,86,92]. However, the latter was limited to one belts' speed combination, to plantar flexor moments during post-adaptation (thus neglecting knee and hip dynamics) [85,86,92], or did not provide information on joint rotations and EMG signals [92]. As a key point, the present results suggest that a partial shift in perspective may help to clarify the potential of the split-belt paradigm as a research and rehabilitation tool. The aim of the adaptive behavior in split gait may be to keep the body system at an average forward speed lying between those of the two belts. The primary mechanism consists of the fine tuning of the main source of body propulsion, that is the plantar-flexion power and work. The pool of plantar flexor muscles is known to provide more than 65% of the power needed to keep

the body system in motion [94,95]. This power is provided by the posterior limb during push-off (largely overlapping with the double-stance phase) [13]. In split gait, however, there is more than a simple replication of the ankle power and work output provided on each side at the corresponding velocity in tied modality (e.g., when in 0408, the same power provided in 0404 and 0808). The time-course of power and work is tailored to the split modality, mostly on the faster side. The published inferences on the neural substrate of adaptation, possibly, should be simplified. All kinematic changes may be seen as the consequence of this necessary dynamic adaptation, not as a primary goal of the adaptive behavior. Dynamic symmetry implies a kinematic one, whereas the reverse is not necessarily true (see the extreme case of lower limb amputee's walking) [9,13,15,41]. Step length mostly arises from limb swing, whereas propulsive power is mostly generated during double stance when minor joint rotations occur. This may make the clinical assessment of dynamic walking asymmetries difficult on visual inspection alone. This notwithstanding, one should not ignore the fact that dynamic symmetry, reflecting an intrinsic, not an adaptive recovery, is a more relevant goal for rehabilitation. Split gait is a favorable form of rehabilitation exercise as long as it forces dynamic symmetry by assigning the faster belt to the affected or to the unaffected lower limb, depending on the search for adaptation or post-adaptation effects, respectively (a still open matter)[a]. In either case, however, it cannot be overemphasized that opposite changes occur on spatiotemporal and dynamic walking parameters.

Some limitations of this study must be highlighted. First, age was very homogenous across participants (it ranged from 22 to 30 years). Caution must be exercised when extrapolating results to either children or older patients. Quite surprisingly, data are missing for the age range 40–60 years [96]. The available literature suggests, in any case, that relevant dynamic differences are expected neither with respect to healthy children older than 5 years of age nor with respect to older adults, once the speed is adjusted for size in the former [15,41], and the same absolute velocity (not the preferred one) is compared across the latter [97]. Second, a velocity difference between the two belts greater than 0.4 m s^{-1} and a speed ratio greater than 2:1 have not been taken into consideration. Third, neither the whole time-course of adaptation nor the post-adaptation phases were analyzed. Step length tends to approach symmetry during late (e.g., > 10 min) adaptation [33], whereas in the present study, only the early phase (< 3 min) was considered. However, the dynamic perspective claimed for in this

[a] *A manuscript on the controversial duration and amplitude of post-adaptation to split walking is in preparation*

work predicts that plantar flexor power should remain asymmetric nonetheless to cope with the persisting asymmetry of belt speed.

These limitations seem to represent valuable targets for the next research agenda on the mechanics of split gait.

6. Experimental study: velocity of the body centre of mass during walking on split-belt treadmill[98]

Split walking is an artificial form of locomotion. As already stated in Chapter 5, the lower limb placed on the faster belt imitates the impaired limb of asymmetric patients from a temporal standpoint, which considerably differs from a dynamic standpoint. This notwithstanding, split walking is inspiring a growing number of researchers to study adaptation to this form of locomotion and its potential as a rehabilitation approach. An overlooked peculiarity of split walking is that the mean velocity adopted by the participant, considered as a whole system represented by the body CoM, can be different from the mean velocity of the two belts. This could lead to a wrong interpretation of kinematics and neurophysiological mechanisms of walking. Particularly important for the clinical perspective would be to interpret segmental motions in light of the CoM dynamics, requiring knowledge of its real mean velocity.

Twelve healthy participants (7 women) were recruited for the present study.

Introduction

All walking phenomena are velocity-dependent, including the mechanical and neural events characterizing the motion of the lower limbs. The mean velocity of the CoM may differ from the mean velocity of the treadmill belts: this is counterintuitive and is contrary to the assumptions in literature [99–101]. In this study, the same instrumental set adopted in previous studies was adopted (i.e., force-sensorized treadmill, optoelectronic kinematic registration of lower limb joint rotations, and sEMG from lower limb muscles). Details are provided in Chapter 2. The same algorithms to analyze the CoM motion were also adopted [4,6]. Of particular interest here, it must be recalled that the method allows to easily compute the point of application (POA), module, and three-dimensional orientation of the GRF from ground contact [2]. The idea subtending the present study is that the CoM can be considered as instantaneously accelerating or decelerating forward with respect to the forward velocity of the belt where the POA lies. The mean CoM velocity can thus be obtained by summating the velocities of the two belts, each weighted by the percentage of stride time the POA of the GRF originates from each belt.

Specific methods

Participants

Twelve healthy adults (7 women) with no history of neurological or orthopedic impairments were enrolled.

Testing procedure

The participants started the testing session walking in tied condition at 0.4 m s^{-1}. After 30 seconds, the velocity of the belt under the dominant lower limb[39] was increased to 1.2 m s^{-1}. The step initiation was marked by the vertical force exceeding 30 N [2]. Participants had to walk for 15 minutes on the treadmill in split condition. Two series of six subsequent strides were considered during the testing period, i.e., strides from the 7th to the 12th (tagged "initial") and the last (tagged "final") series.

Algorithms

GRFs resulting from forces recorded by sensors under both belts were computed. The belt over which the POA was located could easily be identified from the horizontal coordinate of the POA itself. During the whole stride, the mean velocity of the CoM was obtained from summating the velocities of the two belts, each weighted by the percentage of time during which the GRF originated from the corresponding belt.

The concept is formalized by Eq. 6.1. For each single gait cycle (stride):

$$\bar{V}CoM_{split} = \left[\bar{V}_{slow}\frac{t_{slow}}{t_{stride}}\right] + \left[\bar{V}_{fast}\frac{t_{fast}}{t_{stride}}\right] \qquad [6.1]$$

where

- $\bar{V}CoM_{split}$ [m s^{-1}] is the weighted mean forward velocity of the CoM during one stride in split-belt walking.
- V_{slow} and V_{fast} [m s^{-1}] are the (known and constant) forward velocities of the slower and faster treadmill belts, respectively.
- t_{slow} and t_{fast} [s] are the time intervals during which the POA originates from the slower or the faster belt, respectively, during a given stride.
- t_{stride} [s] is the whole stride duration (= t_{slow}+t_{fast}).

For the mean values of $\bar{V}CoM_{split}$ across six strides in a single participant, and across six strides per 12 participants (n=72), the notations $\bar{V}CoM_{split,6strides}$ and $\bar{V}CoM_{split,all}$ are adopted, respectively. When

medians, rather than means, are more appropriate as indexes of central tendency, the notations $\bar{V}^{MED}\text{CoM}_{\text{split,6strides}}$ and $\bar{V}^{MED}\text{CoM}_{\text{split,all}}$ are adopted.

Statistics

The normality of distributions was tested through Shapiro-Wilk's test. Statistics were based on means (SD) and 95% Confidence Intervals (C.I.) for normally distributed variables, and medians (25^{th}-75^{th} percentiles) otherwise. Inferential statistics on changes between time points were based on repeated analysis of variance (ANOVA) of data complying with the requirement of normal symmetric and homoscedastic distribution and Friedman ANOVA otherwise. In the case of significant ANOVA, a post-hoc test was applied. As an index of test-retest reliability, the intraclass correlation coefficients (ICCs) were computed[102]. The $ICC_{2,6}$ model was adopted ("6" stands for the six strides averaged by each participant). Where the ANOVA assumptions did not hold, Kendall's τ on ranks was computed. The significance level was set at p=0.05.

Results

Demographic information on the participants is given in Table 6.1.

Sex, female;male	7;5
Age, years (SD)	27.2 (4.4)
Height, cm (SD)	172.3 (7.3)
Weight, kg (SD)	66.7 (10.6)
Dominant lower limb, right;left	11;1

Table 6.1. Demographic data of participants (n=12)

Fig. 6.1 gives the velocity of the body's CoM (VCoM) during the strides 7^{th} to 12^{th} and the last six strides of the 15-minute walking trial. The CoM did not travel forward at exactly the median (equal to the mean) treadmill velocity, i.e., 0.8 m s^{-1}, in none of the participants. In nine out of 12 participants $\bar{V}\text{CoM}_{\text{split,6strides}}$ was lower than 0.8 m s^{-1}. A typical regression towards the mean[103] was observed between the two time points. Nevertheless, during the 15-minute trial, no participant "crossed" the median treadmill velocity, thus changing her/his early "choice" for a velocity lower or, respectively, higher than 0.8 m s^{-1}.

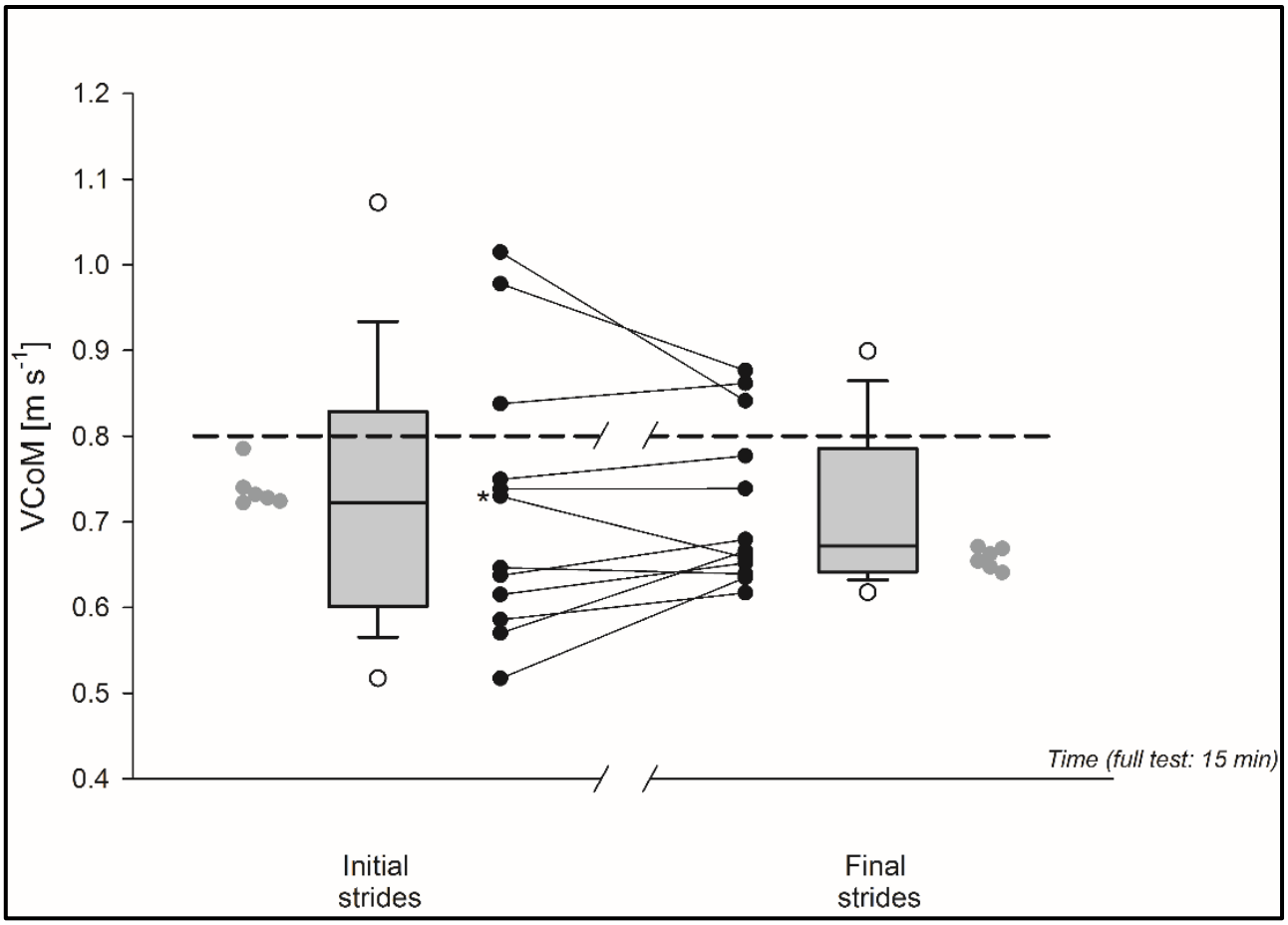

Fig.6.1. The ordinate gives the velocity of the centre of mass (VCoM) of the 12 participants (see Table 6.1) walking for 15 minutes (abscissa) on a force-sensorized split-belt treadmill with the two belts running at 0.4 and 1.2 m s-1. Grey circles give the values ($\bar{V}CoM_{split}$, see text) of the six early strides (leftmost cluster of symbols) and the six late strides (rightmost cluster of symbols) in a representative participant (male, 26 years, 1.76 m, 68 Kg). The box-plots summarize the distribution of $\bar{V}CoM_{split,all}$ of all observations (six strides per 12 participants, n=72) during the early and late series of strides (left and right boxes, respectively). Each box spans from the 25th to the 75th percentiles of the distribution. Whiskers extend from the 10th to the 90th percentiles. Outliers are presented as empty circles. The black circles give the median values across six strides ($\bar{V}^{MED}CoM_{split,6strides}$, see text) for each of the 12 participants during the initial (left) and final (right) series of six strides, respectively. The asterisk indicates the representative participant. Initial and final values for the same participant are connected through straight segments ("spaghetti graph") to give an overview of the test-retest stability of the measurements. The dashed horizontal line indicates the average velocity of the two belts (0.8 m s^{-1}), each running at 0.4 and 1.2 m s^{-1}, respectively. Numeric values are given in Table 6.2.

Table 6.2 provides a summary of the results and of the inferential statistics.

a)				
	n=72	Initial strides	Final strides	
$\bar{V}CoM_{split,all}$	Mean (SD)	0.723 (0.161)	0.721 (0.113)	
	C.I. 95%	0.685 - 0.760	0.694-0.747	
	Shapiro-Wilk's, *p*	0.000	0.000	
$\bar{V}^{MED}CoM_{split,all}$	Median (25^{th}-75^{th} percentiles)	0.722 (0.60-0.83)	0.672 (0.64-0.78)	
b)				
ICC$_{2,6}$		0.913	C.I. 95% = 0.698 - 0.975	*p* = 0.000
MRD (early vs late series of 6 strides); m s^{-1}		0.092		
c)				
Friedman ANOVA (n=72)		*p*-value		
	Time points ($\bar{V}$CoM$_{split}$)	0.000		
	Participants	0.256		
	Time*Participants	0.401		
d)				
Friedman ANOVA (n=12)		*p*-value	Kendall's τ	
	Time points ($\bar{V}^{MED}$CoM$_{split,6strides}$)	0.041	0.923	

Table 6.2. Numerical summary of results and inferential statistics. a) Overall means (standard deviation, SD) of $\bar{V}$CoM$_{split}$ values are given for both initial and final strides. The Shapiro-Wilk's test suggests a significant deviation from the normality of distributions; therefore, medians of $\bar{V}$CoM$_{split}$ values are also provided. b) Test-retest reliability assessment: Intraclass correlation coefficients (ICC model 2.6) and the related minimal real difference (MRD) estimated as per [102]. c) Friedman ANOVA on $\bar{V}$CoM$_{split,all}$ values. d) Friedman ANOVA and rank agreement (Kendall's τ) of individual $\bar{V}^{MED}$CoM$_{split,6strides}$ values.

At both time points, the confidence intervals of $\bar{V}$CoM$_{split}$ remained below the mean velocity between the two belts. The same held for the median CoM velocity of the sample. The mean velocity of the CoM was stable at the beginning and the end of the 15-minute walking trial. This consideration holds both for the sample mean and for individual values (see the high ICC and the low MRD values), provided a normal distribution is assumed. This assumption was a weak one. Non-parametric (Friedman) ANOVA shows that the group median decreased significantly between early and late measurements. The individual participants maintained their rank ordering between the two time points (see Kendall's τ).

Discussion

The results of this study provide evidence that the actual mean velocity of the body system on split-belt treadmills may not correspond to the mean velocity between the two belts, and that this velocity

can also change during the same walking trial. At a group level, the median CoM velocity is lower than the mean/median velocity between the two belts, and it tends to become even lower at the end of a 15-minute trial. However, care must be taken in aggregating data across strides and participants. The settings of the belts' velocities, in themselves invariant, may be associated with changes of $\bar{V}\mathrm{CoM}_{\mathrm{split}}$ from stride to stride and along with successive strides during the same walking trial. Moreover, different participants may show different $\bar{V}\mathrm{CoM}_{\mathrm{split,6strides}}$ values. It is not simply a matter of keeping the body midline right or left of the centre-line, but one of forces exerted against each belt.

Therefore, in split-gait studies, force-sensorized treadmills should always be adopted. The motion of the CoM can be analyzed through "indirect" methods based on kinematic analysis of the body segments (usually through optoelectronic "capturing" of retroreflective skin markers) as per anthropometric modeling[104]. During ground walking or traditional treadmill walking, this method has the advantage of locating the CoM with respect to the body segments; however, in split walking, the mean velocity of the CoM cannot be assumed to equate the mean velocities between the belts.

The behavior of participants seems time-dependent. Between-participant variance seems to decrease along with the trial. This may reflect something more than a simply chance-determined regression towards the mean [103]; instead, it might reflect a form of individual adaptation, mimicking random changes at a group level. For instance, overconfidence on the dominant limb might foster a higher velocity, whereas fear of falling or the tendency to save muscle power might foster a lower velocity, both behaviors being attenuated by practice. Therefore, the velocity of walking needs to be determined individually, preferably even stride by stride or, more realistically, every few subsequent strides.

The present study is based on a small sample. This notwithstanding, it seems sufficient to direct attention to the problem of the CoM velocity during split walking. This finding holds relevance from both research and clinical standpoints. As a hint to physiological research, when segmental motions and their adaptation to this unusual form of locomotion were studied, split-belt trials were often compared to baseline trials at velocities equal to the mean velocity between the two belts [27,99–101,105]. This approximation seems no longer acceptable. Also, the scope of research might now correctly extend beyond the kinematics and dynamics of the lower limbs. Research might now embrace metabolic and ergometric variables of the body system, thanks to estimates of kinetic energy based on CoM velocity. One should consider that errors in estimates of velocity generate squared errors in estimates of kinetic energy[6]. As a hint to rehabilitation research, it has been already highlighted that

an efficient translation of the CoM (across the whole stride, hence per unit distance) may coexist with different impairments [97,13]. This paradoxical efficiency may help decide if, and by how much, focal alterations represent an adaptation to, rather than a direct source of, walking abnormalities. In both cases, the high efficiency of the CoM transfer possibly prevents recovery, either spontaneous or based on rehabilitation. A sort of "acquired/learned non-use" seems to affect the impaired lower limb [4]. Increasing the dynamic requests of walking (i.e., by asking the patient to walk at a higher velocity or uphill) succeeds in obtaining a greater muscle work and power from both lower limbs, so that the acquired dynamic asymmetry, more than unilateral weakness itself, seems to be the invariant constraint of these gaits [27,4]. Split-belt walking paradigms allow a deeper investigation of this intriguing finding, as far as they allow experimental manipulation, not only observation, of the asymmetry. On the diagnostic side, the actual velocity of the CoM (for any given pair of belts' velocities) might become itself a primary measure of walking performance and an index of improvement after rehabilitation. The propulsive role of either lower limb can emerge from the simultaneous recording of joints' and CoM power changes. On the therapeutic side, the many divergent exercise paradigms on split-belt treadmills (e.g., impaired lower limb on the slower and/or on the faster belt [91]; different duration and scheduling of "split walking " sessions; imposed vs self-selected velocities of the belts) might be compared with respect to their capacity to restore the symmetry of the locomotor mechanism as a whole, not only to ameliorate focal joint kinematics and dynamics. The same holds for other potential treatments consistent with the hypothesis of "learned non-use" during asymmetric walking [4], such as lower limb forced-use exercises [106], non-invasive brain stimulation [107], and mirror training [108].

In these types of studies, walking on tied belts represents the control condition. Is the latter analogous to overground walking? Minor kinematic differences for the same average velocity have been outlined in adults [109,110]. These differences seem amenable to a step length shorter (hence to a cadence higher) by no more than 10% in treadmill compared to ground walking. Step shortening is perhaps caused by a higher cognitive effort [110] required to counteract the conflict between proprioception (signaling motion) and vision (signaling immobility). When height-adjusted, dynamic equivalent velocities (i.e., transformed into the same dimensionless Froude number) are compared, the same holds for children 5-13 years old [44]. Cadences above or below the "optimal" one entail a less efficient pendulum-like transfer of energy within the CoM motion (hence, a higher energy expenditure per unit distance), but with impact negligible for changes lower than 50% [111]. For this reason, results on split-belt treadmills can be considered as enlightening the

pathophysiology of “natural”, overground walking (for a Discussion on this topic, see page 525 in ref. [2]).

Although foreshadowed by the present study, all applications of split-belt treadmills require further research on the velocity of the CoM. For instance, open research questions are: which is the actual velocity of the CoM when various differences between the belts' velocities are imposed? What is the time course of changes in CoM velocity during a walking test? How strong is the after-effect in CoM velocity?

7. Experimental study: split walking in a patient with unilateral lower limb spastic paresis. A paradigmatic case report

This Chapter describes a clinical case that exemplifies the application of the analysis of the CoM motion to split walking in a person with unilateral motor impairment. Spatiotemporal and dynamic parameters of the ankle were analyzed. The real velocity of the body CoM (computed as specified in Chapter 6) was considered.

Introduction

Unilateral impairments can be the result of many neurological or musculoskeletal conditions. Patients with unilateral lower-limb impairments generally present with paresis (i.e., reduced voluntary force, work, and power in segmental or patterned movements). Paresis may originate from lesions in the central and peripheral nervous system, or in the musculoskeletal apparatus. Paresis may directly stem from muscle weakness or be the indirect result of various other impairments: spasticity, ataxia/incoordination, pain-related inhibition, and others. As a result, the impaired limb contributes less than the sound limb to the advancement of the body system. Much less muscle work and power are produced when the affected limb is in the rear position, during the push-off phase, compared to the subsequent push-off. Paradoxically, on average between two consecutive steps, work and power may keep within normal limits (see the previous Chapters). These phenomena were shown for post-stroke hemiparesis [112], hip replacement [113], knee rotationplasty (Van Nes-Borgreve operation)[114]. In case of higher dynamic demands (e.g., walking faster, uphill, or on the fast belt during split walking), the power from the impaired side can increase. This justifies the intriguing hypothesis [4] that, once a normal average efficiency is reached by the CoM motion, asymmetry, rather than weakness, is "learned and retained" by the brain even when the acute phase of the lesion faded away (so-called "learned non-use or "acquired non-use" phenomenon, ANU) [4,25,106,115]. The ANU model has provided a rationale to rehabilitation treatments based on "forced-use" exercises, mostly in the case of upper limb paresis [116–118]. In contrast, there are only sporadic proposals of diagnosis and treatment of ANU for lower limb, more precisely in Multiple Sclerosis [119] and in post-stroke hemiparesis [106,115].

Case study

In this study, a 35-year-old man (height 176.5 cm, body weight 79.8 kg) was enrolled for a walking trial on a split-belt treadmill, with belts running either at the same speed or at different speeds (see above, Chapter 3.3). The patient was affected by a chronic unilateral paresis of the right lower limb, persisting after surgical removal of a cavernous spinal angioma at D7 level, which occurred 19 years before the enrollment.

A typical (mild) Brown-Séquard syndrome[120] could be evidenced (below the lesion level, paresis and hypokinestesia on the homolesional side, pain-touch sensation deficit on the contralesional side). The physical examination revealed an escape limp on the right side and a severely reduced propulsion of the right lower limb (as deduced from the missed heel rise during stance). Nonetheless, walking was fully autonomous. A decent segmental control of the right lower limb movements was present, with difficulties in isolating the ankle and foot movements from flexor and extensor synergies. The clinical assessment also showed a moderate hypotrophy of the right lower limb without significant musculo-tendinous contractures. Osteo-tendinous hyperreflexia and a positive Babinsky sign were present on the affected lower limb. Sporadic clonus of the plantar flexor muscles and spasms of the limb extensors were reported. Lost vibration and position senses of the foot were observed, with preserved tactile sensitivity. On the contralateral lower limb, pain and touch sensation were moderately decreased. This case is presented here only as an example of the manipulation of dynamic asymmetries during split walking in a clinical assessment. Therefore, only the tests in which the impaired limb is placed on the faster belt are analyzed.

Specific methods

Testing procedure

The patient was asked to walk on the split-belt treadmill. The impaired limb was placed on the faster belt.

The phases of the experimental session were as follows:

- *Habituation phase:* the patient walked on a split-belt treadmill in tied condition with belts running at 0.2, 0.4, and 0.6 m s^{-1} (tagged 0202, 0404, 0606). Velocity increases were applied every 30 s after a verbal warning.

- *Adaptation phase*: after a 1-minute pause, the participant walked at 0202 for 10 seconds. Then, he walked at 0206 for 6 minutes with the impaired lower limb on the faster belt.
- *Post adaptation phase:* the belts returned at 0202 for 6 minutes.

The experimental sequence is shown in Figure 7.1:

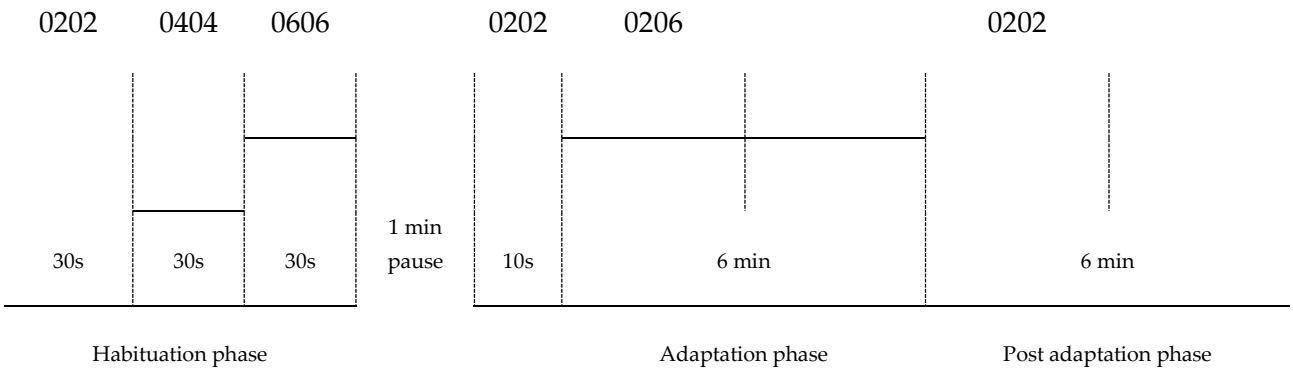

Fig. 7.1. The figure shows the protocol adopted in each of the two experimental sessions. The 0202, 0404, 0606 tags refer to the tied condition, while 0206 refers to the split condition. Continuous lines refer to belts' speed, while dashed lines separate the different conditions/phases.

Results

The Ankle Peak Power (APP), Ankle Work (AW), posterior Step Length (pSL), Single Stance Time (SST), and posterior Double Stance Time (pDST) were analyzed. Parameters were acquired in tied modality (0202, 0404, and 0606) during the habituation phase, and in four test modalities (strides from the 7^{th} to the 12^{th} in split walking at 0.2-0.6 m s^{-1} during the adaptation phase, 0206i; the last six consecutive strides in split walking at 0.2-0.6 m s^{-1} during the adaptation phase, 0206f; the first six consecutive strides in tied walking at 0.2 m s^{-1} during the post adaptation phase, 0202i; the last six consecutive strides in tied walking at 0.2 m s^{-1} during the post adaptation phase, 0202f). Figure 7.2 summarizes the parameters mentioned above (impaired lower limb on the faster belt).

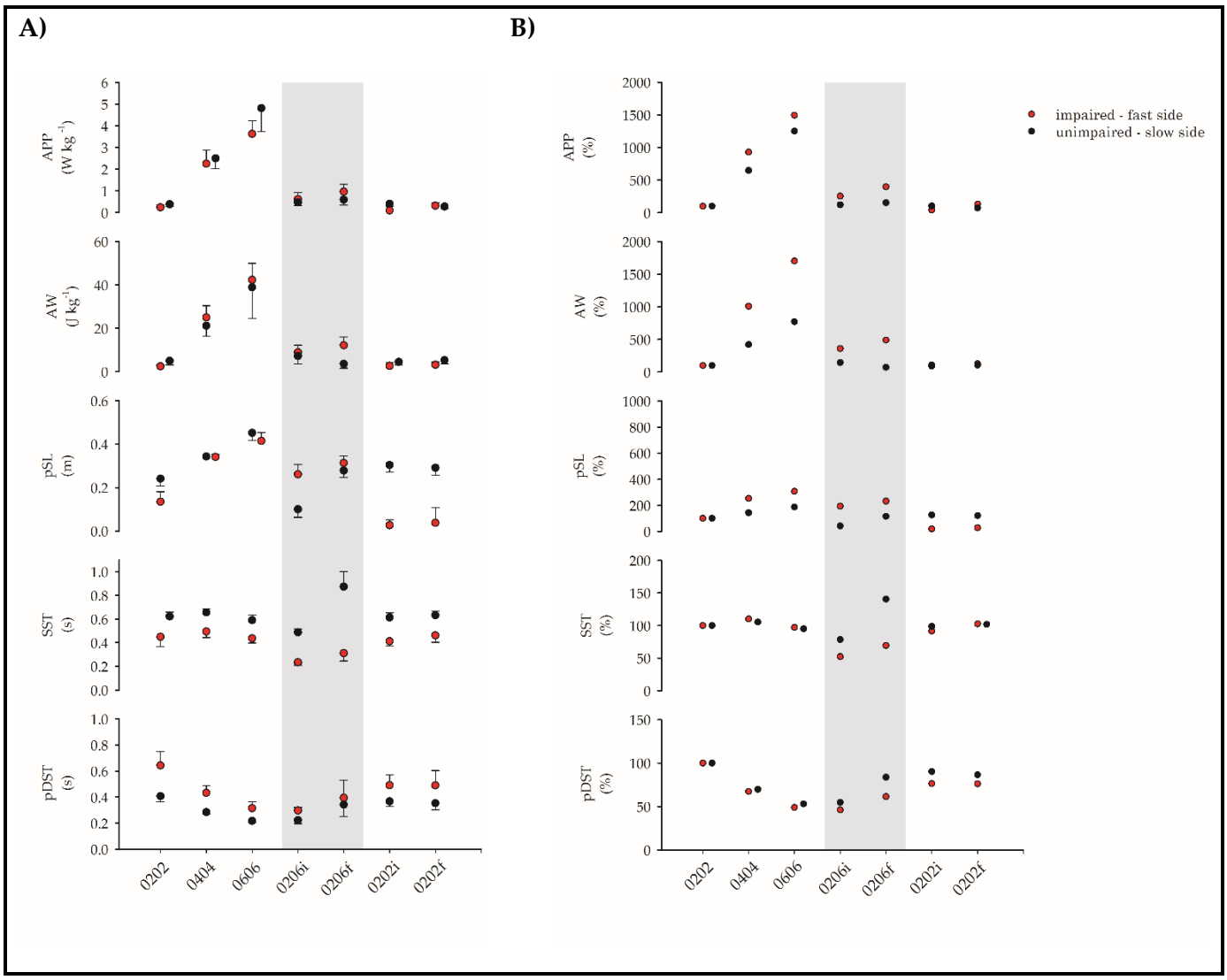

Fig.7.2. From top to bottom, the figure shows on the ordinate the Ankle Peak Power (APP), Ankle Work (AW), posterior Step Length (pSL), Single Stance Time (SST) and posterior Double Stance Time (pDST) in the different conditions/phases of the experimental protocol reported on the abscissa. Red dots refer to the impaired limb, while black dots refer to the unimpaired one. The parameters are reported both in A) absolute value and B) in percentage with respect to their value during the previous tied condition 0202. The real velocity of the CoM during split was 0.36 m s^{-1} and 0.33 m s^{-1} in the initial and final adaptation phases, respectively. For each combination of belts' velocities, symbols are horizontally scattered when needed for graphic clarity.

In the split phase, the real velocity of the CoM was initially 0.36 m s^{-1} and then declined to 0.33 m s^{-1} (see Chapter 3.4 for computation algorithms). Therefore, a fair comparison can be made between split condition and tied condition at 0.4 m s^{-1}.

- *Dynamic parameters.*

In tied conditions, the APP and AW of both limbs increase at increasing speed (0202, 0404, 0606), although the increase is higher on the unimpaired side. A difference of about 10-17% in velocity remains between the closest baseline velocity (0.4 m s^{-1}) and the split-real CoM velocities during the adaptation phase. This discrepancy may explain why the dynamic parameters were, on average, lower during the split, compared to the baseline, phase. Looking at the between-limb asymmetry, it can be seen that both in absolute and, more evidently, in relative terms, the impaired side is forced to provide more power and work, compared to unimpaired side (red symbols, upper two rows of panels).

- *Spatial and temporal parameters.*

The pSL shifts from superimposable values on the two sides during 0202 to higher values on the impaired limb during 0206 compared to the unimpaired one. The SST does not show reversals of asymmetries (it remains shorter on the paretic side), whereas the pDST (push-off, impaired side behind) shortens remarkably, approaching the duration of the contralateral one. In the final adaptation phase, the pSL returns to symmetry, whereas the SST of the unimpaired limb gets much longer than the contralateral one. Some short-lasting after-effect can be observed on the return to the tied condition. The pSLbecomes shorter on the paretic side, much more than at baseline. At the end of the 6-minute post-adaptation phase, all of the baseline conditions were restored.

The numeric results are reported in Table 7.1.

A)

		APP		AW		pSL		SST		pDST	
limb	**condition**	**W kg $^{-1}$**	***SD***	**J kg^{-1}**	***SD***	**m**	***SD***	**s**	***SD***	**s**	***SD***
	0202	0.24	*0.10*	2.48	*0.74*	0.13	*0.05*	0.45	*0.08*	0.64	*0.11*
	0404	2.25	*0.62*	25.02	*5.39*	0.34	*0.01*	0.50	*0.05*	0.43	*0.06*
	0606	3.62	*0.60*	42.30	*7.68*	0.41	*0.04*	0.44	*0.04*	0.32	*0.05*
Impaired	**0206i**	0.62	*0.31*	8.93	*3.27*	0.26	*0.05*	0.24	*0.03*	0.30	*0.02*
	0206f	0.97	*0.33*	12.16	*3.86*	0.31	*0.03*	0.31	*0.07*	0.39	*0.14*
	0202i	0.10	*0.05*	2.73	*1.50*	0.03	*0.03*	0.41	*0.04*	0.49	*0.08*
	0202f	0.32	*0.15*	3.19	*1.29*	0.04	*0.07*	0.46	*0.06*	0.49	*0.11*
	0202	0.38	*0.11*	2.48	*0.74*	0.24	*0.03*	0.62	*0.04*	0.41	*0.04*
	0404	2.50	*0.47*	5.03	*1.91*	0.34	*0.01*	0.66	*0.03*	0.28	*0.01*
	0606	4.81	*1.08*	21.20	*4.82*	0.45	*0.04*	0.59	*0.05*	0.22	*0.01*
Unimpaired	**0206i**	0.47	*0.15*	38.90	*14.30*	0.10	*0.04*	0.49	*0.03*	0.22	*0.03*
	0206f	0.59	*0.25*	7.27	*3.68*	0.28	*0.03*	0.87	*0.13*	0.34	*0.09*
	0202i	0.40	*0.13*	3.64	*2.07*	0.30	*0.03*	0.61	*0.04*	0.37	*0.04*
	0202f	0.28	*0.09*	4.56	*1.45*	0.29	*0.03*	0.63	*0.03*	0.35	*0.05*

B)

		APP	AW	pSL	SST	pDST
Lower limb	**condition**	**%**	**%**	**%**	**%**	**%**
	0202	100.00	100.00	100.00	100.00	100.00
	0404	930.00	1008.08	253.01	110.00	67.36
	0606	1495.45	1704.16	307.90	97.04	48.96
Impaired	**0206i**	254.80	359.67	193.59	52.22	46.11
	0206f	398.37	490.02	231.97	69.26	61.40
	0202i	41.10	110.00	18.96	91.48	76.43
	0202f	131.10	128.53	27.48	102.59	76.17
	0202	100.00	100.00	100.00	100.00	100.00
Unimpaired	**0404**	648.92	421.20	142.55	105.36	69.80

0606	1250.63	773.00	187.57	94.91	53.06
0206_i	121.09	144.53	41.43	78.55	54.69
0206_f	154.18	72.27	115.41	140.48	83.67
0202_i	104.93	90.51	126.40	98.66	90.21
0202_f	72.94	105.03	120.63	101.61	86.53

Table 7.1. Dynamic and spatiotemporal parameters across six subsequent strides during walking at the different walking conditions (tags as in Figure 7.2). Ankle Peak Power (APP), Ankle Work (AW), posterior Step Length (pSL), Single Stance Time (SST) and posterior Double Stance Time (pDST) are reported both as (A) mean and standard deviations (SD) in absolute values and as (B) percentage values with respect to the value recorded during the previous tied condition 0202.

Discussion

The results showed that shifting from tied to split implied remarkable changes in both the dynamic and the kinematic parameters of walking. The tested velocities were quite low, so that moderate differences could be observed in the tied modalities (most important, a lower work and peak power from the impaired lower limb). This asymmetry could be reversed by forcing the impaired limb to work on the faster belt. The same held for the posterior step length. The spatial aspect of walking became more symmetric. By contrast, the "escape" limp was enhanced (an even shorter single stance time was observed on the impaired side, as expected). Changes do occur during the 6-minute adaptation. Dynamic and temporal asymmetries increase, while the spatial asymmetry (posterior step length) decreases. During the 6-minute post-adaptation phase, no relevant after-effects could be observed on power and work, while spatial asymmetry (posterior step length) reverted to the baseline pattern (posterior step shorter on the impaired side, perhaps to a greater extent compared to baseline). Certainly, the most visible manipulation of walking parameters, caused by the split-belt paradigm, concerned the step length (which most of the literature was focused on).

The clinical case presented is purely anecdotal, yet, it fosters three clinical considerations. First, it is important to compare the real velocity of the CoM ("split-CoM velocity") with a "tied belts" velocity as close as possible to the split one. This is a hard experimental challenge. A solution would be to adjust the baseline "tied" velocities values to match at least the initial CoM velocity in split conditions. However, this would require a double adaptation phase: one for calibration and the other after the ideal baseline velocity has been tested, for further split walking, with no warranty that the tied and the real split CoM velocities will continue to match during the whole testing period.

Alternatively, a meticulous and long-baseline test should be conducted, in which various velocities are progressively tested, in increments as small as possible. After the trial, some of the tested baseline velocities might reasonably match the real split CoM velocities during various time-windows of the test. A further alternative might be represented by the on-line computation of the real split CoM velocity, generating a feed-back controlled adaptation of the belts' velocities. This arrangement would be the ideal one to keep known and constant the average CoM velocity during the test in order to investigate the effect of different asymmetries between the belts' velocities for that given CoM velocity.

Second, no dramatic after-effect seems to be generated by split walking. The dynamic after-effect is virtually nil: some after-effect seems to apply to the spatial asymmetry, in agreement with previous literature findings. The results from the literature suggest that the paretic limb should be placed on the slower belt in order to obtain, after adaptation, a greater posterior step and perhaps a higher power output. This arrangement, however, is at risk for implying an even shorter stance time, thus enhancing the limping aspect of gait (increase "escape" from the paretic limb loading). More research is needed to test the effect of either arrangement (paretic limb on the faster or the slower belt) and the duration of the after-effect, whichever it might be.

Third, the questions raised above might be (at least partially) answered by the synchronous analysis of lower limb and CoM mechanics. The capacity of any after-effect to be retained possibly depends on the overall efficiency achieved by the pendulum-like motion of the CoM. Focal symmetries (or asymmetries) elicited as after-effects but causing mechanical inefficiency at the body-system level look unlikely to be "learned" and retained by the central nervous system.

Again, this is only an anecdotal case study, which, in addition, is illustrated here only partially. A clinical trial is presently in progress, which will hopefully shed some light on the new domain of research open by the analysis of the CoM motion during split walking.

8. Conclusion: a narrative summary and interpretation of the rationale and results of the Ph.D. program.

Human walking is usually studied from the segmental standpoint. Her, it has been presented from the perspective of the motion of the body system as a whole, summarized by its CoM. The reasons for such a unique perspective have been summarized in the Preface. Here below, as per the promise made in the Preface, the attempt will be made to highlight the guiding thread underlying the many apparently independent experiments while, at the same time, providing an overview of research and clinical scenarios sparked. In order to better fulfil this task, a narrative style will be adopted.

Section 1: Physiology of the CoM motion.

Results from this section pave the way for studies in children and inaugurate the study of the 3D CoM motion in balance impairments.

Chapter 3. **Three-dimensional path of the body centre of mass (CoM) during walking in children: an index of neural maturation.**

The results reported in this study suggest that the CoM path shape changes as a function of speed. Changes are most prominent in the lateral displacement of the CoM path in children 5–13 years of age. In particular, a lateral shrinking of the CoM path is demonstrated, with increasing age, accounting for the effects of height and absolute forward speed. In the literature, several age-related changes of walking mechanics have been described [56,57]: the results of the present study now add tiles to the puzzle of the CoM/segments relationship.

Chapter 4. **The curvature peaks of the trajectory of the body centre of mass during walking: a new index of dynamic balance.**

The present study follows the observations of Tesio et al.[18] regarding the description of the 3D trajectory of the CoM during a stride. Tesio et al. demonstrated the simultaneity of curvature peaks and transient annihilations of the pendulum-like mechanism during the gait cycle, implying the sudden shift from passive oscillation to a fully active, muscle-driven control [4]. The 3D trajectory of the CoM now allows a wider interpretation of the CoM path from the balance standpoint.

Section 2: Understanding split-walking.

This section gives experimental evidence that the dynamics of split walking are far from the dynamics expected in pathologic claudication and (unfortunately) assumed in most of the clinical literature. A transient "therapeutic" after-effect (a lower asymmetry) may follow after split walking with the impaired limb placed on the faster belt if the temporal symmetry is aimed at, or with the same limb placed on the slower belt if dynamic symmetry is aimed at. Future experimentation will have to solve this puzzle. Clinical decisions will have to be taken on the therapeutic target while considering this paradox. Also, the velocity of the CoM is not the mean velocity between the belts, as it was (perhaps ingenuously) assumed in the literature, but the one of a virtual belt rotating at a velocity depending on how long the resulting ground reaction vector originates from either belt. Therefore, the split-belt adaptation was shown to represent primarily a matter of CoM mechanics and secondarily of limb mechanics: a critical hint for the design of future experiments.

Chapter 5. Limping on split-belt treadmill implies opposite kinematic and dynamic lower limb asymmetries.

Split walking can be considered a unique paradigm of locomotion, different from "natural" pathologic claudication. While in overground limping gait the impaired limb 'escapes' from load, minimizing its stance time, in split gait the faster limb 'escapes' from being dragged backwards with respect to the slower leg, therefore requiring extra muscular work.

The split gait can induce mechanical asymmetry in healthy subjects similar to pathologic claudication, only from the temporal standpoint. However, neither the spatial nor the dynamic parameters induced by split walking can be compared with pathologic claudication.

The experiments seemed to demonstrate that the primary adaptive mechanism consists of fine tuning the plantar-flexion power and work, representing the main source of body propulsion.

Possibly, the published inferences on the neural substrate of adaptation should be simplified. All kinematic changes may be considered as the consequence of this necessary dynamic adaptation, not as a primary goal of the adaptive behavior. A dynamic symmetry implies a kinematic one, whereas the reverse is not necessarily true. In the Authors (and the candidate's) opinion, dynamic symmetry, which reflects an intrinsic and not adaptive recovery, is a more relevant goal for rehabilitation compared to spatiotemporal symmetry. Split gait might be considered an effective form of rehabilitation exercise only as long as it may cause persistent dynamic symmetry. The unresolved

clinical dilemma is the choice between assigning the faster belt to the affected or to the unaffected lower limb, depending on the search for adaptation or post-adaptation effects.

Chapter 6. **Study of the velocity of the CoM during split-gait.**

The results of the present study provide evidence that the actual mean velocity of the body system on split-belt treadmills may not correspond to the mean velocity between the two belts. Moreover, it can change during the same walking trial.

This finding looks relevant from both research and clinical standpoints. As a hint to physiological research, when segmental motions and their adaptation to this unusual form of locomotion were studied, split-belt trials were often compared to baseline trials at velocities equal to the mean velocity between the two belts[27,99–101,105].

It has been already outlined that in asymmetric walking the (paradoxical) high efficiency of the CoM transfer may work against recovery, either spontaneous or based on rehabilitation. A sort of "acquired/learned non-use" seems to affect the impaired lower limb [4]. Increasing the dynamic requests of walking succeeds in obtaining greater muscle work and power from both lower limbs, so that the acquired dynamic asymmetry seems to be the invariant constraint of these pathologic gaits [27,4]. Split-belt walking paradigms allow a deeper investigation of this finding.

Section 3: foreshadowing clinical applications of the analysis of the CoM motion

Chapter 7. **A paradigmatic clinical case report.**

In this anecdotal case (a patient with paresis of the right lower limb due to a thoracic spinal lesion), various parameters were analyzed during adaptation to split walking and post-adaptation. Results showed that symmetry (or asymmetry) of the dynamic, spatial, and temporal parameters of walking could indeed be manipulated by forcing adaptation to split walking. However, opposite effects could be induced in dynamic and temporal parameters, and the after-effect was remarkable only for the spatial asymmetry (i.e., step length). Knowledge of the response of the CoM motion to the split experimental manipulation would provide cues to the interpretation of the clinical meaning of the observed changes. In short, this case does not allow sound conclusions but supports the idea that a clinical trial is worth (actually, it is in progress), exploiting the potential of a synchronous analysis of segmental and CoM motions during the puzzling split walking.

9. References

(Authors of the articles published during the research project are highlighted in bold)

1. Fenn WO. Work against gravity and work due to velocity changes in running. *Am J Physiol*. 1930;92:583-611.

2. Tesio L, Rota V. Gait analysis on split-belt force treadmills: validation of an instrument. *Am J Phys Med Rehabil*. 2008;87(7):515-526. doi:10.1097/PHM.0b013e31816f17e1

3. Benedetti MG, Beghi E, De Tanti A, et al. SIAMOC position paper on gait analysis in clinical practice: General requirements, methods and appropriateness. Results of an Italian consensus conference. *Gait Posture*. 2017;58:252-260. doi:10.1016/j.gaitpost.2017.08.003

4. Tesio L, Rota V. The motion of the body center of mass during walking: a review oriented to clinical applications. *Front Neurol*. 2019;10(999). doi:10.3389/fneur.2019.00999

5. Tesio L. Il movimento del sistema corporeo in toto nell'analisi clinica del cammino. Published online 1991.

6. Cavagna GA. Force platforms as ergometers. *J Appl Physiol*. 1975;39(1):174-179. doi:10.1093/icb/40.1.101

7. Tesio L, Civaschi P, Tessari L. Motion of the center of gravity of the body in clinical evaluation of gait. *Am J Phys Med*. 1985;64(2):57-70.

8. Tesio L, Lanzi D, Detrembleur C. The 3-D motion of the centre of gravity of the human body during level walking. I. Normal subjects at low and intermediate walking speeds. *Clin Biomech*. 1998;13(2):77-82. doi:10.1016/S0268-0033(97)00080-6

9. Rota V, Benedetti MG, Okita Y, Manfrini M, Tesio L. Knee rotationplasty: motion of the body centre of mass during walking. *Int J Rehabil Res*. 2016;39(4):346-353. doi:10.1097/MRR.0000000000000195

10. Saunders Jbd, Inman V, Eberhart H. The major determinants in normal and pathological gait. *J Bone Jt Surg - Am Vol*. 1953;35-A(3):543-558.

11. Cavagna GA. *Muscolo e Locomozione*. (RaffaelloCortina, ed.).; 1997.

12. Cavagna GA. Force platforms as ergometers. *J Appl Physiol*. 1975;39(1):174-179. doi:10.1152/jappl.1975.39.1.174

13. Tesio L, Lanzi D, Detrembleur C. The 3-D motion of the centre of gravity of the human body during level walking. II. Lower limb amputees. *Clin Biomech*. 1998;13(2):83-90. doi:10.1016/S0268-0033(97)00081-8

14. Cavagna GA, Thys H, Zamboni A. The sources of external work in level walking and running. *J Physiol*. 1976;262(3):639-657.

15. Cavagna GA, Tesio L, Fuchimoto T, Heglund NC. Ergometric evaluation of pathological gait. *J Appl Physiol*. 1983;55(2):607-613. doi:10.1152/jappl.1983.55.2.606

16. Cavagna GA, Thys H, Zamboni A. The sources of external work in level walking and running. *J Pysiol*. 1976;262:639-657.

17. Cavagna GA, Willems PA, Legramandi MA, Heglund NC. Pendular energy transduction within the step in human walking. *J Exp Biol*. 2002;205(Pt 21):3413-3422.

18. Tesio L, Rota V, Perucca L. The 3D trajectory of the body centre of mass during adult human walking: Evidence for a speed-curvature power law. *J Biomech*. 2011;44(4):732-740. doi:10.1016/j.jbiomech.2010.10.035

19. Tesio L, Rota V, Chessa C, Perucca L. The 3D path of body centre of mass during adult human walking on force treadmill. *J Biomech*. 2010;43(5):938-944. doi:10.1016/j.jbiomech.2009.10.049

20. Neptune RR, Zajac FE, Kautz SA. Muscle mechanical work requirements during normal walking: The energetic cost of raising the body's center-of-mass is significant. *J Biomech*. 2004;37(6):817-825. doi:10.1016/j.jbiomech.2003.11.001

21. Murray M, Spurr G, Sepic S, Gradner G, Mollinger JA. Treadmill vs. floor walking:kinematics, electromyogram, and heart rate. *J Appl Physiol*. 1985;59(1):87-91. doi:10.1152/jappl.1985.59.1.87

22. Wootten ME, Kadaba MP, Cochran GVB. Dynamic electromyography. II. Normal patterns during gait. *J Orthop Res*. 1990;8(2):259-265. doi:10.1002/jor.1100080215

23. Agostini V, Nascimbeni A, Gaffuri A, Imazio P, Benedetti MG, Knaflitz M. Normative EMG activation patterns of school-age children during gait. *Gait Posture*. 2010;32(3):285-289. doi:10.1016/j.gaitpost.2010.06.024

24. Kirtley C. *Clinical Gait Analyisis.Theory and Practice.* Elsevier-Churchill Livingstone; 2006.

25. Tesio L, Rota V, Malloggi C, Brugliera L, Catino L. Crouch gait can be an effective form of forced-use/no constraint exercise for the paretic lower limb in stroke. *Int J Rehabil Res*. 2017;40(3):254-267. doi:10.1097/MRR.0000000000000236

26. Kuo AD. Energetics of actively powered locomotion using the simplest walking model. *J Biomech Eng*. 2002;124(1):113-120.

27. Tesio L, Malloggi C, Malfitano C, Coccetta CA, Catino L, Rota V. Limping on split-belt treadmills implies opposite kinematic and dynamic lower limb asymmetries. *Int J Rehabil Res*. 2018;41:304-315. doi:10.1097/MRR.0000000000000320

28. Honeine JL, Schieppati M, Gagey O, Do MC. The functional role of the triceps surae muscle during human locomotion. *PLoS One*. 2013;8(1). doi:10.1371/journal.pone.0052943

29. Sutherland D. The development of mature gait. *Gait Posture*. 1997;6(2):163-170. doi:10.1016/S0966-6362(97)00029-5

30. Francis CA, Lenz AL, Lenhart RL, Thelen DG. The modulation of forward propulsion, vertical support, and center of pressure by the plantarflexors during human walking. *Gait Posture*. 2013;38(4):993-997. doi:10.1016/j.gaitpost.2013.05.009

31. Helm EE, Reisman DS. The split-belt walking paradigm: exploring motor learning and spatiotemporal asymmetry poststroke. *Phys Med Rehabil Clin N Am*. 2015;26(4):703-713. doi:10.1016/j.pmr.2015.06.010

32. Dietz V, Zijlstra W, Duysens J. Human neuronal interlimb coordination during split-belt locomotion. *Exp brain Res*. 1994;101(3):513-520.

33. Reisman DS, Block HJ, Bastian AJ. Interlimb coordination during locomotion: what can be adapted and stored? *J Neurophysiol*. 2005;94(4):2403-2415. doi:10.1152/jn.00089.2005

34. Reisman DS, Wityk R, Silver K, Bastian AJ. Locomotor adaptation on a split-belt treadmill can improve walking symmetry post-stroke. *Brain*. 2007;130(7):1861-1872. doi:10.1093/brain/awm035

35. Reisman DS, Bastian AJ, Morton SM. Neurophysiologic and rehabilitation insights from the split-belt and other locomotor adaptation paradigms. *Phys Ther*. 2010;90(2):187-195. doi:10.2522/ptj.20090073

36. Reisman DS, Wityk R, Silver K, Bastian AJ. Split-belt treadmill adaptation transfers to overground walking in persons poststroke. *Neurorehabil Neural Repair*. 2009;23(7):735-744. doi:10.1177/1545968309332880

37. Morton SM, Bastian AJ. Cerebellar Contributions to Locomotor Adaptations during Splitbelt Treadmill Walking. *J Neurosci*. 2006;26(36):9107-9116.

38. Martin TA, Keating JG, Goodkin HP, Bastian AJ, Thach WT. Throwing while looking through prisms I. Focal olivocerebellar lesions impair adaptation. *Brain*. 1996;119(4):1183-1198. doi:10.1093/brain/119.4.1183

39. Elias LJ, Bryden MP, Bulman-Fleming MB. Footedness is a better predictor than is handedness of emotional lateralization. *Neuropsychologia*. 1998;36(1):37-43. doi:10.1016/S0028-3932(97)00107-3

40. Davis RB, Õunpuu S, Tyburski D, Gage JR. A gait analysis data collection and reduction technique. *Hum Mov Sci*. 1991;10(5):575-587. doi:10.1016/0167-9457(91)90046-Z

41. Cavagna GA, Franzetti P, Fuchimoto T. The mechanics of walking in children. *J Physiol*. 1983;343:323-339. doi:10.1113/jphysiol.1983.sp014895

42. Benjamini Y, Hochberg Y. Controlling the false discovery rate: a practical and powerful approach to multiple testing. *J R Stat Soc Ser B*. 1995;57(1):289-300.

43. Malloggi C, Rota V, Catino L, et al. Three-dimensional path of the body centre of mass during walking in children: an index of neural maturation. *Int J Rehabil Res*. 2019;42(2):112-119. doi:10.1097/MRR.0000000000000345

44. Tesio L, Malloggi C, Portinaro NM, Catino L, Lovecchio N, Rota V. Gait analysis on force treadmill in children: comparison with results from ground-based force platforms. *Int J Rehabil Res*. 2017;40(4):315-324. doi:10.1097/MRR.0000000000000243

45. Cavagna GA. *Physiological Aspects of Legged Terrestrial Locomotion: The Motor and the Machine*. Springer Int Publisher AG; 2017.

46. Bennett BC, Abel MF, Wolovick A, Franklin T, Allaire PE, Kerrigan DC. Center of mass movement and energy transfer during walking in children with cerebral palsy. *Arch Phys Med Rehabil*. 2005;86(11):2189-2194. doi:10.1016/j.apmr.2005.05.012

47. Dierick F, Lefebvre C, Van Den Hecke A, Detrembleur C. Development of displacement of centre of mass during independent walking in children. *Dev Med Child Neurol*. 2004;46(8):533-539. doi:10.1111/j.1469-8749.2004.tb01011.x

48. Jensen RK. Changes in segment inertia proportions between 4 and 20 years. *J Biomech*. 1989;22(6-7):529-536. doi:10.1016/0021-9290(89)90004-3

49. Sutherland D, Olshen R, Cooper L, Woo S-Y. The development of mature gait. *J Bone Jt Surg*. 1980;62(3):336-353.

50. Cupp T, Oeffinger D, Tylkowski D, Gage J. Age-related kinetic changes in normal pediatrics. *J Pediatr Orthop*. 1999;19(4):475-478.

51. Alexander RM. *Principles of Animal Locomotion*. Princeton University Press; 2003.

52. Moser EB. Repeated Measures Modeling With PROC MIXED. In: *SUGI 29*. ; 2004:188-217.

53. Royston P, Ambler G, Sauerbrei W. The use of fractional polynomials to model continuous risk variables in epidemiology. *Int J Epidemiol*. 1999;28(5):964-974. doi:10.1093/ije/28.5.964

54. Burnham KP, Anderson DR. *Model Selection and Multimodel Inference*. 2nd ed. Springer New York; 2004. doi:10.1007/b97636

55. Orendurff MS, Segal AD, Klute GK, Berge JS, Rohr ES, Kadel NJ. The effect of walking speed on center of mass displacement. *J Rehabil Res Dev*. 2004;41(6):829-834. doi:10.1682/JRRD.2003.10.0150

56. Forssberg H. Ontogeny of human locomotor control. I. Infant stepping, supported locomotion and transition to independent locomotion. *Exp brain Res*. 1985;57(3):480-493. doi:10.1007/BF00237835

57. Ledebt A. Changes in arm posture during the early acquisition of walking. *Infant Behav Dev*. 2000;23(1):79-89. doi:10.1016/S0163-6383(00)00027-8

58. Donelan JM, Shipman DW, Kram R, Kuo AD. Mechanical and metabolic requirements for active lateral stabilization in human walking. *J Biomech*. 2004;37(6):827-835. doi:10.1016/j.jbiomech.2003.06.002

59. Smeesters C, Hayes WC, McMahon TA. Disturbance type and gait speed affect fall direction and impact location. *J Biomech*. 2001;34(3):309-317. doi:10.1016/S0021-9290(00)00200-1

60. MacKinnon CD, Winter DA. Control of whole body balance in the frontal plane during human walking. *J Biomech*. 1993;26(6):633-644. doi:10.1016/0021-9290(93)90027-C

61. Thevenon A, Gabrielli F, Lepvrier J, et al. Collection of normative data for spatial and temporal gait parameters in a sample of French children aged between 6 and 12. *Ann Phys Rehabil Med*. 2015;58(3):139-144. doi:10.1016/j.rehab.2015.04.001

62. Hallemans A, Verbecque E, Dumas R, Cheze L, Van Hamme A, Robert T. Developmental changes in spatial margin of stability in typically developing children relate to the mechanics of gait. *Gait Posture*. 2018;63:33-38. doi:10.1016/j.gaitpost.2018.04.019

63. Malloggi C, Scarano S, Cerina V, Catino L, Rota V, Tesio L. The curvature peaks of the trajectory of the body centre of mass during walking: a new index of dynamic balance. *J Biomech*. 2020;Under revi.

64. Siragy T, Nantel J. Quantifying dynamic balance in young, elderly and Parkinson's individuals: a systematic review. *Front Aging Neurosci*. 2018;10:387. doi:10.3389/fnagi.2018.00387

65. Hof AL, Gazendam MGJ, Sinke WE. The condition for dynamic stability. *J Biomech*. 2005;38:1-8. doi:10.1016/j.jbiomech.2004.03.025

66. Hof AL. The 'extrapolated center of mass' concept suggests a simple control of balance in walking. *Hum Mov Sci*. 2008;27:112-125. doi:10.1016/j.humov.2007.08.003

67. Hof AL. The equations of motion for a standing human reveal three mechanisms for balance. *J Biomech*. 2007;40(2):451-457. doi:10.1016/j.jbiomech.2005.12.016

68. Hof AL, van Bockel RM, Schoppen T, Postema K. Control of lateral balance in walking Experimental findings in normal subjects and above-knee amputees. *Gait Posture*. 2007;25:250-258. doi:10.1016/j.gaitpost.2006.04.013

69. Hurt CP, Rosenblatt NJ, Grabiner MD. Form of the compensatory stepping response to repeated laterally directed postural disturbances. *Exp Brain Res*. 2011;214(4):557-566. doi:10.1007/s00221-011-2854-1

70. Okubo Y, Brodie M, Sturnieks D, et al. Exposure to unpredictable trips and slips while walking can improve balance recovery responses with minimum predictive gait alterations. *PLoS One*. 2018;13(9):e0202913. doi:10.1371/ journal.pone.0202913

71. Mc Andrew Young PM, Wilken JM, Dingwell JB. Dynamic margins of stability during human walking in destabilizing environments. *J Biomech*. 2012;45(6):1053-1059. doi:doi.org/10.1016/j.jbiomech.2011.12.027

72. Rogers M, Hedman L, Johnson M, Cain T, Hanke T. Lateral stability during forward-induced stepping for dynamic balance recovery in young and older adults. *J Gerontol A Biol Sci Med Sci*. 2001;56A(9):M589-594. doi:10.1093/gerona/56.9.m589

73. Gates DH, Scott SJ, Wilken JM, Dingwell JB. Frontal plane dynamic margins of stability in individuals with and without transtibial amputation walking on a loose rock surface. *Gait Posture*. 2013;38(4):570-575. doi:10.1016/J.GAITPOST.2013.01.024

74. Bierbaum S, Peper A, Karamanidis K, Arampatzis A. Adaptational responses in dynamic stability during disturbed walking in the elderly. *J Biomech*. 2010;43(12):2362-2368. doi:10.1016/j.jbiomech.2010.04.025

75. Hurt CP, Grabiner MD. Age-related differences in the maintenance of frontal plane dynamic stability while stepping to targets. *J Biomech*. 2015;48(4):592-597. doi:10.1016/J.JBIOMECH.2015.01.003

76. Vistamehr A, Kautz SA, Bowden MG, Neptune RR. Correlations between measures of dynamic balance in individuals with post-stroke hemiparesis. *J Biomech*. 2016;49(3):396-400. doi:10.1016/j.jbiomech.2015.12.047

77. Kao P-C, Dingwell JB, Higginson JS, Binder-Macleod S. Dynamic instability during post-stroke hemiparetic walking. *Gait Posture*. 2014;40(3):457-463. doi:10.1016/J.GAITPOST.2014.05.014

78. Hak L, Houdijk H, van der Wurff P, et al. Stepping strategies used by post-stroke individuals to maintain margins of stability during walking. *Clin Biomech*. 2013;28(9-10):1041-1048. doi:10.1016/J.CLINBIOMECH.2013.10.010

79. Bauby CE, Kuo AD. Active control of lateral balance in human walking. *J Biomech*. 2000;33(11):1433-1440. doi:10.1016/S0021-9290(00)00101-9

80. Rosenblatt NJ, Grabiner MD. Measures of frontal plane stability during treadmill and overground walking. *Gait Posture*. 2010;31(3):380-384. doi:10.1016/j.gaitpost.2010.01.002

81. Rovenski V, Rovenski V. Curvature and Torsion of Curves. In: *Geometry of Curves and Surfaces with MAPLE*. Birkhäuser Boston; 2000:125-132. doi:10.1007/978-1-4612-2128-9_13

82. Altman DG, Bland JM. Measurement in medicine: the analysis of method comparison studies. *Stat*. 1983;32(3):307-311.

83. Malone LA, Bastian AJ. Spatial and temporal asymmetries in gait predict split-belt adaptation behavior in stroke. *Neurorehabil Neural Repair*. 2014;28(3):230-240. doi:10.1177/1545968313505912

84. Fasano A, Schlenstedt C, Herzog J, et al. Split-belt locomotion in Parkinson's disease links asymmetry, dyscoordination and sequence effect. *Gait Posture*. 2016;48:6-12. doi:10.1016/j.gaitpost.2016.04.020

85. Lauzière S, Mièville C, Betschart M, Duclos C, Aissaoui R, Nadeau S. Plantarflexion moment is a contributor to step length after-effect following walking on a split-belt treadmill in individuals with stroke and healthy individuals. *J Rehabil Med*. 2014;46(9):849-857. doi:10.2340/16501977-1845

86. Lauzière S, Miéville C, Duclos C, Aissaoui R, Nadeau S. Perception threshold of locomotor symmetry while walking on a split-belt treadmill in healthy elderly individuals. *Percept Mot Skills*. 2014;118(2):475-490. doi:10.2466/25.15.PMS.118k17w6

87. Hoogkamer W, Bruijn SM, Sunaert S, Swinnen SP, Van Calenbergh F, Duysens J. Adaptation and aftereffects of split-belt walking in cerebellar lesion patients. *J Neurophysiol*. 2015;114:1693-1704.

88. Malone LA, Bastian AJ. Thinking about walking: effects of conscious correction versus distraction on locomotor adaptation. *J Neurophysiol*. 2010;103(4):1954-1962. doi:10.1152/jn.00832.2009

89. Hoogkamer W, O'Brien MK. Sensorimotor recalibration during split-belt walking: task-specific and multisensory? *J Neurophysiol*. 2016;116(4):1539-1541.

90. Reisman DS, McLean H, Bastian AJ. Split-belt treadmill training poststroke: a case study. *J Neurol Phys Ther*. 2010;34(4):202-207. doi:10.1097/NPT.0b013e3181fd5eab

91. Reisman DS, McLean H, Keller J, Danks KA, Bastian AJ. Repeated split-belt treadmill training improves poststroke step length asymmetry. *Neurorehabil Neural Repair*. 2013;27(5):460-468. doi:10.1177/1545968312474118

92. Roemmich RT, Stegemöller EL, Hass CJ. Lower extremity sagittal joint moment production during split-belt treadmill walking. *J Biomech*. 2012;45(16):2817-2821. doi:10.1016/j.jbiomech.2012.08.036

93. Hermens HJ, Freriks B, Merletti R, et al. *European Recommendations for Surface ElectroMyoGraphy*.; 1999.

94. Zelik KE, Huang TWP, Adamczyk PG, Kuo AD. The role of series ankle elasticity in bipedal walking. *J Theor Biol*. 2014;346:75-85. doi:10.1016/j.jtbi.2013.12.014

95. Meinders M, Gitter A, Czerniecki JM. The role of ankle plantar flexor muscle work during walking. *Scand J Rehabil Med*. 1998;30(1):39-46.

96. Herssens N, Verbecque E, Hallemans A, Vereeck L, Van Rompaey V, Saeys W. Do spatiotemporal parameters and gait variability differ across the lifespan of healthy adults? A systematic review. *Gait Posture*. 2018;64(November 2017):181-190. doi:10.1016/j.gaitpost.2018.06.012

97. Tesio L, Roi GS, Möller F. Pathological gaits: inefficiency is not a rule. *Clin Biomech*. 1991;6(1):47-50. doi:10.1016/0268-0033(91)90041-N

98. Tesio L, Scarano S, Cerina V, Malloggi V, Catino L. Velocity of the body center of mass during walking on split-belt treadmill. *Am J Phys Med Rehabil*. Published online 2021. doi:10.1097/PHM.0000000000001674

99. Sánchez N, Simha SN, Donelan JM, James M, Finley JM. Taking advantage of external mechanical work to reduce metabolic cost: the mechanics and energetics of split-belt treadmill walking. *J Physiol*. 2019;597(15):4053-4068. doi:10.1113/JP277725

100. Sánchez N, Park S, Finley JM. Evidence of energetic optimization during adaptation differs for metabolic, mechanical, and perceptual estimates of energetic cost. *Sci Rep*. 2017;7(7682). doi:10.1038/s41598-017-08147-y

101. Sombric CJ, Torres-Oviedo G. Augmenting propulsion demands during split-belt walking increases locomotor adaptation of asymmetric step lengths. *J Neuroeng Rehabil*. 2020;17(69). doi:10.1186/s12984-020-00698-y

102. Tesio L. Outcome measurement in behavioural sciences: a view on how to shift attention from means to individuals and why. *Int J Rehabil Res*. 2012;35(1):1-12. doi:10.1097/MRR.0b013e32834fbe89

103. Stigler SM. Regression towards the mean, historically considered. *Stat Methods Med Res*. 1997;6(2):103-114. doi:10.1177/096228029700600202

104. Cappozzo A, Della Croce U, Leardini A, Chiari L. Human movement analysis using

stereophotogrammetry: Part 1: theoretical background. *Gait Posture*. 2005;21(2):186-196. doi:10.1016/j.gaitpost.2004.01.010

105. Catino L, Malloggi C, Tesio L. Combined study of segmental movements and motion of the Centre of Mass during adaptation on a split-belt treadmill. In: *ISPGR World Congress*. ; 2019. https://ispgr.org/wp-content/uploads/2019/07/ISPGR-Abstract-Book.pdf

106. Tesio L. Learned-non use affects the paretic lower limb in stroke: "occlusive" exercises may force the use. *Eura Medicophys*. 2001;37(1):51-56.

107. Tung Y, Lai C, Liao C, Huang S, Liou T, Chen H. Repetitive transcranial magnetic stimulation of lower limb motor function in patients with stroke: a systematic review and meta-analysis of randomized controlled trials. *Clin Rehabil*. 2019;33(7):1102-1112. doi:10.1177/0269215519835889

108. Li Y, Wei Q, Gou W, He C. Effects of mirror therapy on walking ability, balance and lower limb motor recovery after stroke: a systematic review and meta-analysis of randomized controlled trials. *Clin Rehabilation*. 2018;32(8):1007-1021. doi:10.1177/0269215518766642

109. Parvataneni K, Ploeg L, Olney SJ, Brouwer B. Kinematic, kinetic and metabolic parameters of treadmill versus overground walking in healthy older adults. *Clin Biomech (Bristol, Avon)*. 2009;24(1):95-100. doi:10.1016/j.clinbiomech.2008.07.002

110. Zanetti C, Schieppati M. Quiet stance control is affected by prior treadmill but not overground locomotion. *Eur J Appl Physiol*. 2007;100(3):331-339. doi:10.1007/s00421-007-0434-7

111. Cavagna GA, Franzetti P. The determinants of the step frequency in walking in humans. *J Physiol*. 1986;373(1):235-242. doi:10.1113/jphysiol.1986.sp016044

112. Olney SJ, Griffin MP, McBride ID. Temporal, kinematic, and kinetic variables related to gait speed in subjects with hemiplegia: a regression approach. *Phys Ther*. 1994;74(9):872-885.

113. Moyer R, Lanting B, Marsh J, et al. Postoperative Gait Mechanics After Total Hip Arthroplasty: A Systematic Review and Meta-Analysis. *JBJS Rev*. 2018;6(11):e1. doi:10.2106/JBJS.RVW.17.00133

114. Catani F, Capanna R, Benedetti MG, et al. Gait analysis in patients after Van Nes rotationplasty. *Clin Orthop Relat Res*. 1993;(296):270-277.

115. Tesio L. From neuroplastic potential to actual recovery after stroke: a call for cooperation between drugs and exercise. *Aging (Albany NY)*. 1991;3(1):97-98.

116. Taub E, Uswatte G, Pidikiti R. Constraint-induced movement therapy: a new family of techniques with broad application to physical rehabilitation --a clinical review. *J Rehabil Res Dev*. 1999;36(3):237-251.

117. Miltner WHR, Bauder H, Sommer M, Dettmers C, Taub E. Effects of constraint-induced movement therapy on patients with chronic motor deficits after stroke: A replication. *Stroke*. 1999;30(3):586-592. doi:10.1161/01.STR.30.3.586

118. Kwakkel G, Veerbeek JM, van Wegen EEH, Wolf SL. Constraint-induced movement therapy

after stroke. *Lancet Neurol*. 2015;14(2):224-234. doi:10.1016/S1474-4422(14)70160-7

119. Mark VW, Taub E, Uswatte G, et al. Constraint-Induced Movement Therapy for the Lower Extremities in Multiple Sclerosis: Case Series With 4-Year Follow-Up. *Arch Phys Med Rehabil*. 2013;94(4):753-760. doi:10.1016/j.apmr.2012.09.032

120. Shams S, Arain A. *Brown Sequard Syndrome*. StatPearls Publishing; 2019.

121. Aristotle. *Parts of Animals. Movement of Animals. Progression of Animals*. Loeb Classical Library 323; 1937.

122. Baker R. The history of gait analysis before the advent of modern computers. *Gait Posture*. 2007;26(3):331-342. doi:10.1016/j.gaitpost.2006.10.014

123. Borelli GA. *De Motu Animalium*. Pieter Vander, Leiden; 1710.

124. Richards J, Levine D, Whittle M. *Whittle's Gait Analysis*. 5th Ed. Elsevier; 2012.

125. Weber W, Weber E, Maquet P, Furlong R. *Mechanics of the Human Walking Apparatus:* Springer Verlag; 1992.

126. Marey E-J. *La Machine Animale: Locomotion Terrestre et Aeriénne*. Germer Baillière et C.; 1873.

127. Muybridge E. *The Male and Female Figure in Motion: 60 Classic Photographic Sequences*. Dover; 1984.

128. Sutherland DH. The evolution of clinical gait analysis: Part II kinematics. *Gait Posture*. 2002;16(2):159-179. doi:10.1016/S0966-6362(02)00004-8

129. Carlet G. *Essai Expérimental Sur La Locomotion Humaine: Etude de La Marche*. Impr. E. Martinet; 1872.

130. Elftman H. The measurement of the external force in walking. *Science (80-)*. 1938;88(2276):152-153. doi:10.1126/science.88.2276.152

131. Whittle MW. Clinical gait analysis: A review. *Hum Mov Sci*. 1996;15(3):369-387. doi:10.1016/0167-9457(96)00006-1

132. Sutherland DH. The evolution of clinical gait analysis part III - Kinetics and energy assessment. *Gait Posture*. 2005;21(4):447-461. doi:10.1016/j.gaitpost.2004.07.008

133. Cavagna GA, Kaneko M. Mechanical work and efficiency in level walking and running. *J Physiol*. 1977;268:467-481.

134. Willems PA, Cavagna GA, Heglund NC. External, internal and total work in human locomotion. *J Exp Biol*. 1995;198(2):379-393.

APPENDIX 1

Historical Background of gait analysis

The scientific interest in human walking goes back to Aristotle (384-322 B.C.). He wrote: "If a man walked on the ground next to a wall with a cane dipped in ink attached to his head, the line traced by the cane would not be straight but at zigzag, because it would go down when [the man] goes down too and up when he lifted" [121].

The initial descriptive studies of human walking, as well-defined in the review of Richard Baker [122], dated back to Renaissance. However, the first modern scientific study of gait analysis is due to an eclectic scientist, disciple of Galileo Galilei (1564-1642), Giovanni Alfonso Borelli (1608-1679). In 1682 he published "De Motu Animalium". He deduced the presence of medio-lateral movements of the head during walking, estimated the position of the body centre of gravity, and described how the balance could be maintained by the continuous forward displacement of the support area provided by the feet [123,124]. Then, Herman Boerhaave (1668-1738) applied physical laws, elaborated by Isaac Newton (1642-1727), to human motion [122].

Until the end of the XVIII century, there was not an advancement of knowledge in this field. This was attributed either to the absence of experiments based on preceding theories or to a purely passive view of the phenomenon: those with a physiologic education stated that walking was entirely due to muscular activity; those with a physical background identified the predominant engine in the gravitational and inertial forces [122].

Only with Wilhelm Eduard Weber (1804-1891) and Eduard Friedrich Weber (1806-1871), the two visions were integrated, thus leading to a significant contribution to the knowledge of walking. Thanks to experiments made with a chronometer, a belt with known length, and a telescope, they gave the first clear description of the gait cycle, demonstrating how the length and cadence changed as a function of velocity [125]. Moreover, they were the first ones to depict the position of limbs in 14 different instants of walking.

In 1870, from a purely descriptive study of walking, they switched to the first works on kinematics, a branch of physics that describes the geometry of motion in terms of displacements, velocities, and

accelerations [124]. Pioneers of this discipline were Eadward Muybridge (1830-1904) and Jules Etienne Marey (1830-1904) (Fig. A1.1)

Fig. A1.1. Runner equipped with tools used to record body accelerations during locomotion (from Marey JE, [126])

Eadweard Muybridge was an American photographer who became famous for his photographs of a trotting horse, realized in rapid succession. He won the prize paid by an eccentric American millionaire to anyone being able to show whether the trotting horse always had at least one hoof in contact with the ground, as envisaged by the rules of the race, or if there were short instants of flight. Using 24 aligned cameras and activated in a repeated sequence, Muybridge captured the instant in which all the four horse's legs were simultaneously lifted from the ground. Muybridge also showed interest in human and animal motion, included human locomotion, studied with his particular photographic method, based on many different cameras in series and foreshadowing the birth of cinema [127] (Fig. A1.2).

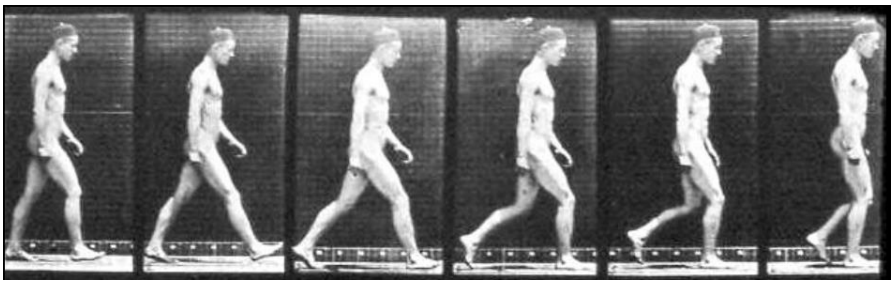

Fig. A1.2. E Muybridge, Walking [127].

Jules Etienne Marey (1830-1904) believed that the technique used by Muybridge could be improved. Muybridge's method inevitably implied that the photographs had different angles with respect to the subject, preventing valid measures on records. For this reason, he invented the chronophotography, i.e. a shutter able to acquire consecutive photographs and to overlap them on the same photographic plate [122,124]. The subjects wore black clothes with reflecting wipes superimposed to the limbs (Fig. A1.3).

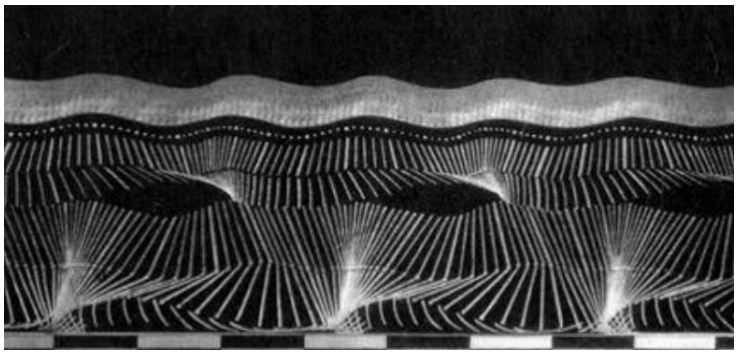

Fig. A1.3. E Marey, Joinville Soldier Walking, 1883.

At the end of the XIX century, Wilhelm Braune (1831-1892) and Otto Fischer (1861-1917) performed, for the first time, a 3D analysis of walking [122,124,128].

For a long time, photography remained the only instrument for analyzing the kinematic walking parameters. Nonetheless, in the '80s of the XX century, the development of tools as cameras directly connected to a computer allowed to calculate a significant number of data in a short time [124,128].

The first studies of walking from a dynamic standpoint, i.e. a branch of classical mechanics that concerns the effect of forces and torques on the motion of bodies having mass, are attributed to Marey and his two disciples, Gaston Carlet (1849-1892) and Georges Demeny (1850-1918). Marey

developed a shoe with three pressure transducers and a pneumatic platform, which were able to register the vertical component of GRF continuously during the foot contact [129]. The force components in the three dimensions were obtained by Jules Amar (1879-1935), who created a suitable mechanical platform, again with pneumatic transmission [122].

Further development of this instrument is due to the American researchers Wallace Fenn (1893-1971) and Herbert Elftman (1902-1988), who produced the first modern force platforms in the '30s of the XX century [1,130].

Today, many different gait laboratories utilize systems able to integrate kinematic and dynamic analysis. This allows obtaining much further information as measurements of torques and joint powers [131,132]. As a rule, surface electromyographic signals from different muscles are also registered.

APPENDIX 2

External and Internal Work

a) External work

The advancement of the body system during walking requires some muscular work. In the literature, this is called "external" work (W_{ext}) and permits the CoM displacement with respect to the ground against gravity and ground friction (neglecting air and internal friction), given that the efficiency of the pendulum-like mechanism is not perfect [5,11]. It must be specified that with W_{ext} the "positive" work is commonly intended, i.e. the one subtending E_{tot} increments. In a gait cycle (double step or *stride*) in stationary conditions, as E_{tot} returns to its initial level, positive and negative work are of the same amount. "Negative" work will not be treated in the present Thesis, although it is of crucial relevance, for instance, with respect to the neural control of balance during walking [4,63].

b) Internal work

Legged animals need an unavoidable cyclic reset of lower limbs with respect to the CoM. These motions look theoretically ineffective for the mere purpose of the CoM displacement, and they require an "internal" work (W_{int}). W_{int} has been calculated for the first time by Cavagna [133], using cinematography: once the mass of body segments and the location of their CoM is known, the analysis of the displacements of body segments can lead to the analysis of the whole body CoM. Anatomic tables and anthropometric modelling are required (hence the indirectness of the method). Following the initial studies by Cavagna, Patrick Willems investigated in detail the contribution of W_{int} to the total (external+internal) muscular work during walking [134]. In general, at intermediate and low walking velocities (e.g. lower than 0.8 m s^{-1}), W_{int} is a modest fraction of the total Work (no more than 10%). There is still a debate on how much W_{ext} comes from W_{int} [14]. Some studies demonstrated that spontaneous velocity and step cadence in physiologic gait are very close to those minimizing the sum of internal and external Work [16]. Of course, all issues related to W_{int} are relevant for the physiology of walking but will not be considered in this Thesis.

APPENDIX 3. Candidate's contribution to the research project

The aim of the present Thesis is the clinical translation of GAFT and split-GAFT. The entire project recalls a research line set up by Prof Luigi Tesio, but it has its roots in the '30s with the work of Prof. Rodolfo Margaria and then Prof. Giovanni A. Cavagna.
The author entirely wrote and conceptualized the present Thesis under the supervision of Prof. Luigi Tesio. However, other collaborators took part in the experiments, analysis and writing of the different studies discussed from Chapter 3 to 7. Therefore, a list of the authors contributing to the realization of the studies is reported below.
The authors' contribution is defined according to the following criteria:

- Conceptualization.
- Planning.
- Experimentation.
- Analysis.
- Writing.
- Revision for important intellectual content.
- Supervision.

Chapter 3. Three-dimensional path of the body centre of mass during walking in children: an index of neural maturation

The first goal relates to a study on the extension of data on the 3D motion of the body CoM during walking. The aim of the study was to describe the 3D path of the CoM in children during walking, in order to disentangle the effect of age from that of absolute forward speed and body size and to define preliminary pediatric normative values.
The study was published in the International Journal of Rehabilitation Research in 2019.

Authors: Chiara Malloggi, Viviana Rota, Luigi Catino, Calogero Malfitano, Stefano Scarano, Davide Soranna, Antonella Zambon, and Luigi Tesio.

The authors' contribution is summarized below.

- Conceptualization: Luigi Tesio.
- Planning. Viviana Rota, Chiara Malloggi and Luigi Catino.
- Experimentation: Viviana Rota, Chiara Malloggi and Luigi Catino.
- Analysis: Viviana Rota, Chiara Malloggi and Luigi Catino.
- Writing: Chiara Malloggi, Luigi Tesio, Luigi Catino and Davide Soranna.
- Revision for important intellectual content: Luigi Tesio, Chiara Malloggi, Antonella Zambon.
- Supervision: Luigi Tesio.

Chapter 4. The curvature peaks of the trajectory of the body centre of mass during walking: a new index of dynamic balance

In this investigation, the curvature peaks of the trajectory of the body CoM as an index of dynamic balance were studied. The rationale was based on the fact that during walking, falling is most likely to occur during the single stance towards the side of the supporting lower limb. The timely lateral redirection of the CoM, preceding the no-return position, is necessary for balance.
The manuscript has been submitted to the Journal of Biomechanics in 2020.

Authors: Chiara Malloggi, Stefano Scarano, Valeria Cerina, Luigi Catino, Viviana Rota and Luigi Tesio.

- Conceptualization: Luigi Tesio
- Planning: Chiara Malloggi, Luigi Catino and Viviana Rota
- Experimentation: Luigi Catino, Chiara Malloggi, Valeria Cerina and Stefano Scarano
- Analysis: Chiara Malloggi, Valeria Cerina, and Luigi Catino
- Writing: Chiara Malloggi, Stefano Scarano and Luigi Catino
- Revision for important intellectual content: Luigi Tesio, Chiara Malloggi and Stefano Scarano
- Supervision: Luigi Tesio

Chapter 5. Limping on split-belt treadmills implies opposite kinematic and dynamic lower limb asymmetries

In this study, the effects of split gait have been described. Walking on a split-belt treadmill has been proposed as an experimental paradigm to investigate the flexibility of the neural control of gait and

as a form of therapeutic exercise. However, the scarcity of dynamic investigations challenges the validity of the available findings. Here, the dynamic lower limbs' asymmetries of healthy adults were investigated during adaptation to gait on a split-belt treadmill.
The study was published in the International Journal of Rehabilitation Research in 2018.

Authors: Luigi Tesio, Chiara Malloggi, Calogero Malfitano, Carlo A. Coccetta, Luigi Catino, and Viviana Rota. Their contribution is reported below.

- Conceptualization: Luigi Tesio.
- Planning: Chiara Malloggi, Viviana Rota, Calogero Malfitano and Carlo A. Coccetta.
- Experimentation: Chiara Malloggi, Viviana Rota and Luigi Catino.
- Analysis: Chiara Malloggi, Viviana Rota and Luigi Catino.
- Writing: Luigi Tesio, Chiara Malloggi, and Luigi Catino.
- Revision for important intellectual content: Luigi Tesio, Chiara Malloggi, Calogero Malfitano and Carlo A. Coccetta.
- Supervision: Luigi Tesio.

Chapter 6. Velocity of the body centre of mass during walking on split-belt treadmill

In this study, the velocity of the CoM during split gait has been computed. Walking on a split-belt treadmill has inspired a growing number of researchers to study gait adaptation and rehabilitation. An overlooked peculiarity of this form of gait is that the mean velocity adopted by the participant, considered as a whole system, can be different from the mean velocity of the two belts.

A manuscript is in press in the American Journal of Physical Medicine and Rehabilitation.

Authors: Luigi Tesio, Stefano Scarano, Valeria Cerina, Chiara Malloggi, Luigi Catino.

- Conceptualization: Luigi Tesio and Stefano Scarano.
- Planning: Stefano Scarano, Chiara Malloggi, Valeria Cerina and Luigi Catino.
- Experimentation: Chiara Malloggi, Valeria Cerina and Luigi Catino.
- Analysis: Chiara Malloggi, Luigi Catino and Valeria Cerina.
- Writing: Luigi Tesio, Stefano Scarano and Luigi Catino.

- Revision for important intellectual content: Luigi Tesio, Stefano Scarano, Luigi Catino and Chiara Malloggi.
- Supervision: Luigi Tesio and Stefano Scarano.

Chapter 7. A paradigmatic clinical case

The last part of the present Thesis refers to a clinical trial in which the split gait-paradigm has been applied to asymmetric patients. In this chapter, a paradigmatic case is presented.
This research is currently in progress and the Project has been inserted at ClinicalTrial.Gov (protocol identifier number: NCT04635436).

- Conceptualization: Luigi Tesio.
- Planning: Chiara Malloggi, Luigi Catino, Stefano Scarano and Valeria Cerina.
- Experimentation: Chiara Malloggi, Valeria Cerina, Luigi Catino and Stefano Scarano.
- Analysis: Luigi Catino, Chiara Malloggi.
- Writing: Luigi Catino.
- Revision for important intellectual content: Luigi Catino, Stefano Scarano and Luigi Tesio.
- Supervision: Luigi Tesio.